USE OF A HIGH RESOLUTION

PHOTOGRAPHIC TECHNIQUE FOR

STUDYING COAGULATION/FLOCCULATION

IN WATER TREATMENT

A Thesis Submitted to the College of

Graduate Studies and Research

in Partial Fulfillment of the Requirements

for the Degree of Master of Science

in the Department of Civil and Geological

Engineering

University of Saskatchewan

Saskatoon

By

Yan Jin

PERMISSION TO USE

In presenting this thesis in partial fulfillment of the requirements for a Postgraduate degree from the University of Saskatchewan, I agree that the Libraries of this University may make it freely available for inspection. I further agree that permission for copying of this thesis in any manner, in whole or in part, for scholarly purposes may be granted by the professor who supervised my thesis work or, in his absence, by the Head of the Department or the Dean of the College in which my thesis work was done. It is understood that any copying, publication, or use of this thesis or parts thereof for financial gain shall not be allowed without my written permission. It is also understood that due recognition shall be given to me and to the University of Saskatchewan in any scholarly use which may be made of any material in my thesis.

Requests for permission to copy or to make other use of material in this thesis in whole or part should be addressed to:

Head of the Department of Civil and Geological Engineering

University of Saskatchewan

Saskatoon, Saskatchewan

Canada S7N 5A9

i

ABSTRACT

The coagulation/flocculation process is an important part of surface water treatment. It has direct impact on the reliability of plant operations and final water qualities together with cost control. Low water temperature has a significant impact on the operation of drinking water treatment plants, especially on coagulation/flocculation processes.

A microscopic image technique has been used to study the coagulation and flocculation process in recent years, but it requires sample handling that disturbs the floc characteristics during measurement. A high resolution photographic technique was applied to evaluate flocculation processes in the present work. With this technique, the images of the flocs were obtained directly while the flocculation process was taking place. In combination with camera control software and particle size analysis software, this procedure provided a convenient means of gathering data to calculate size distribution. Once the size distribution was calculated, the floc growth and floc size change in the aggregation process could be analyzed. Results show that low water temperature had a detrimental impact on aggregation processes. A water temperature of 0 °C resulted in a slow floc growth and small floc size. Although the floc growth rates at 4 °C and 1 °C were less than those at 22 °C, they were higher than at 0 °C. To improve aggregation processes at low water temperature, adding the coagulant aid of anionic copolymer of acrylamide into the water was found to be effective when the temperature was not less than 1 °C. However, it made only a slight impact on aggregation when the temperature approached 0 °C. At water temperatures of 22 °C, 4

°C and 1 °C, the polymer caused the formation of large floc (larger than 0.5 mm^2 in projected area). The polymer significantly shortened the required time of flocculation and sedimentation. Three minutes of flocculation and 20 minutes of sedimentation were sufficient for the polymer to achieve good treatment performance, while the flocculation time and sedimentation time had to be 20 and 60 minutes, respectively, without using the polymer. On the other hand, when the temperature was close to 0 °C, the polymer did not cause the formation of the large floc, nor did it shorten the time of flocculation and sedimentation.

The experimental results in this research agree with the model for flocculation kinetics given by Argaman and Kaufman (1970). With decreasing water temperature, the aggregation constant (K_A) decreased and breakup constant (K_B) increased. K_A and K_B with aluminum sulfate was close to those with ferric sulfate, respectively.

In treating the South Saskatchewan River water, an aluminum sulfate or ferric sulfate dosage greater than 50 mg/L resulted in marginal gains in treatment efficiency. Decreasing dosages of aluminum sulfate or ferric sulfate caused lower floc growth rates and smaller floc sizes. Extremely low dosages (5 mg/L or less) resulted in poor floc formation and extremely small sizes.

ACKNOWLEDGEMENTS

TABLE OF CONTENTS

LIST OF TABLES

LIST OF FIGURES

LIST OF ABBREVIATIONS

A	Paddle-blade area at right angle to the direction of movement
α	Collision efficiency
β	Collision frequency between particles
$^\circ C$	Degrees Celsius
C_D	Coefficient of drag
D	Dielectric constant of the liquid
D_i	Impeller diameter
d_p	Particle diameter
E_a	Activation energy, constant for a given reaction
ε	Rate of energy dissipation
$^\circ F$	Degrees Fahrenheit
F_D	Drag force of the paddle
G	Velocity gradient
g, g_c	Gravitational constant
ΔH^o	Change in enthalpy
k	Boltzmann's constant
K_A	Aggregation constant
K_B	Breakup constant
K_L	Impeller constant for laminar flow
K_{sp}	Solubility product constant
K_T	Impeller constant for turbulent flow
K_{w1}, K_{w2}	Equilibrium constants at T_1 and T_2 respectively
mg/L	Milligrams per liter
N_{ij}	Number of collisions
n_i, n_j	Particle count for particles of size i and j, respectively
NTU	Nephelometry turbidity units
φ	Volume fraction of the dispersed phase
P	Power input
$PACl$	Ploylaluminium chloride
ρ_p	Particle density
ρ_w	Water density

δ	Floc breakup rate exponent
rpm	Rotational speed, revolution per minute
rps	Rotational speed, revolution per second
R	Ideal gas constant, 1.987cal K^{-1} mol^{-1}
S	Floc projected area
t	Time
T	Temperature
μm	Micrometers
μ	Viscosity
ψ	Electrophoretic velocity
v	Settling velocity
V	Volume
λ	Kolmogorow microscale
Z_p	Zeta potential, millivolts

Chapter 1 – Introduction

1.1 Background

Water is one of the most important substances on the Earth. People can only survive seven or less days without water (SaskH$_2$O 2003). There are two principal sources of water for municipal supply: surface water and ground water. Surface water is found in rivers, lakes or other surface impoundments. This water usually does not contain much mineral content. Surface water may contain many kinds of contaminants, such as animal wastes, insecticides, industrial wastes, algae and many other organic materials (Vesilind et al. 1988). Even surface water in a primitive mountain stream possibly contains coliform bacteria from the feces of wild animals, and it must be disinfected or boiled prior to drinking.

Groundwater is water trapped beneath the surface of the earth. For instance, rivers that disappear beneath the earth and rain that soaks into the ground are a few of the ground water sources. Due to the many sources of recharge, groundwater may contain any or all of the contaminants found in surface water. It may also include dissolved minerals, which it picks up during its long stay underground (Speight and Lee 2000). Usually groundwater contains dissolved minerals. Its hardness, which is the sum of the concentrations of multivalent ions, principally calcium and magnesium, is higher than surface water. High hardness can form the deposition of scale in plumbing fixtures and soap scum in sinks and tubs (AWWA 1984). The characteristic of groundwater is

relatively consistent throughout the year, while surface water quality can be highly variable.

Actually the drinking water sources are limited on Earth. Of the 326 million cubic miles of water on earth, freshwater lakes, rivers and underground aquifers hold only 2.5% of the world's water (SaskH$_2$O 2003). By comparison, saltwater oceans and seas contain 97.5% of the world's water supply. Of the total world's freshwater supply, about one third is found underground (SaskH$_2$O 2003).

With a growing world population and industrial development, as well as the attendant discharge of wastes and chemicals, most of the water, particularly surface water, cannot be drunk directly without treatment. Water treatment is a process of cleaning raw water and making it safe for people to drink. Generally speaking, there are five main steps in the operation of surface drinking water treatment plants: Coagulation, Flocculation, Sedimentation, Filtration and Disinfection (Vesilind et al. 1988).

The coagulation/flocculation process is an important part of surface water treatment. It has a direct impact on the reliability of plant operations and final water quality together with cost control (Hooge 2000).

There are numerous factors that influence coagulation/flocculation processes, such as raw water quality including physical, chemical and bacteriological parameters, treatment device structures, as well as coagulant types and dosages. Water temperature change has a significant impact on the operation of drinking water treatment plants,

especially on coagulation/flocculation processes (Mpofu et al. 2004, Lin and Jin 2003, Borstnik et al. 2000). Health Canada (1996) indicated that low water temperature decreased the efficiency of water treatment processes and could thus have a deleterious effect on drinking water quality.

The effect of water temperature, especially cold water (i.e., 1-5 °C), on the various water treatment processes has been reported in the literature. Studies have been conducted to investigate temperature effects on conventional metal ion coagulation (Morris and Knocke 1984, Kang et al. 1995, and Hooge 2000) and flocculation loading rates (Schultz et al. 1984, Shea et al. 1971, and Adhin et al. 1974). The studies by Morris and Knocke (1984) showed that a decrease in water temperature was accompanied by a decrease in turbidity removal. Xie (2000) demonstrated that raw water in winter generally had low turbidities and the aggregation/flocculation process in winter was less effective than that in other seasons. Mothadi and Rao (1973) found that decreasing water temperature required an increase in alum dosage to achieve the same degree of flocculation.

Driscoll and Letterman (1988) indicated that the rates of coagulation/deposition of $Al(OH)_3$ on the surface of particulates significantly reduced with decreasing temperature, and a lot of species such as $Al(OH)_2^+$ might remain in the solution. Similarly, from the study of coagulation using alum, ferric chloride, or polymeric metal coagulants, O'Melia et al. (1989) suggested that slowing the hydrolysis and precipitation reactions of metal coagulants in cold water was beneficial to some

conditions, perhaps by permitting hydrolysis species to react more extensively with turbidity and with humic substances. This research conflicted somewhat with the research by Morris and Knocke (1984) who concluded that low water temperature did not significantly reduce the rate of aluminum (III) or iron (III) precipitation, and that the impact of low temperature on turbidity removal efficiency was not related to the reduced metal hydroxide precipitation rates. They ascribed the reduced turbidity removal at low temperature to variations in the floc characteristics, alkalinity levels, turbidity levels and dissolved organic levels. The contradictory research indicates the lack of a definitive understanding of water temperature effects on water treatment.

While various studies have examined the effect of temperature on flocculation efficiency, little work has been performed using flocculation kinetics as a tool to study the temperature effect due to the limitation of measurement technologies. Thus the evolution and structures of flocculation are still not clear.

In recent years, the microscopic image technique has been used to study the coagulation and flocculation process (Spicer and Pratsinis 1996, Kang et al. 1995, and Wang et al. 2002), but it requires sample handling that disturbs the floc characteristics during measurement. So the method may not represent the practical situation. An advanced high resolution photographic technique was developed in the present work. With this technique, the images were obtained directly while the flocculation process was still taking place.

In this research, the effect of cold water conditions and coagulating agents on coagulation/flocculation processes was investigated, and a better understanding of coagulation/flocculation processes was attained.

1.2 Research Goals and Methodology

The goal of this research was to apply a new measurement method that would capture the images of particle/floc variation throughout the aggregation process and then develop a method of evaluating the aggregation process. With particle size analysis software, each particle/floc size distribution at different aggregation time could be recorded. The aggregation processes were studied by analyzing floc growth with increasing time and floc size change with different temperature or coagulant dosage under the same time conditions.

The specific objectives of this research were:

1) To investigate aggregation processes under different temperature and coagulant conditions;

2) To review current technologies in the area of measuring aggregation processes;

3) To apply a measurement method of observing aggregation processes;

4) To develop a new method of evaluating aggregation processes, including image analysis, image observation and the analysis of flocculation kinetics.

1.3 Organization of Thesis

In this chapter, the importance of water treatment, the difficulties of small water treatment systems and the reason for the present research are described. Research goals are then stated. Chapter two reviews general water treatment methods and coagulation/flocculation processes and mechanisms. A review of temperature effects on coagulation/flocculation is also included. Chapter three describes the experimental methods and procedures, including bench-scale tests and image-processing tests.

The test run conditions, test results and discussion are described in Chapter four. The coagulation/flocculation processes with different temperatures, different types and dosages of coagulants, as well as different reaction time are discussed. A systematic method based on a bench-scale test, floc size analysis and image observation was formed to evaluate the aggregation processes.

Finally, Chapter five provides a summary of this research program. The conclusions derived from this study and some recommendations for future work are also presented.

Chapter 2 - Literature Review

2.1 General

The primary function of water treatment is to provide a continuous supply of safe and palatable drinking water. Safe water is free of contaminants which can be harmful to a consumer; and palatable water is practically free of unpleasant characteristics such as color, taste and odour.

This chapter reviews the theories of water treatment methods, coagulation/flocculation mechanisms and temperature impacts on water properties and water treatment processes. It also presents a summary of previous research on the temperature effect on coagulation/flocculation.

2.2　Water Treatment Methods

There are various water treatment methods for making water safe. Common water treatment processes are summarized in Table 2.1. However, the types and arrangements of processes in water treatment plants vary from community to community, depending on the specific characteristics of the raw water.

- Preliminary treatment consists of screening, chemical pretreatment, presedimentation, and microstraining (AWWA 1984).

Table 2.1. Complete water treatment processes (AWWA 1984)

Process	Purpose
Preliminary Treatment	
Screening	Removes large debris that can foul or damage plant equipment
Chemical Pretreatment	Conditions the water for the eventual removal of algae and other aquatic nuisances that cause taste, odor and color
Presedimentation	Removes gravel, sand, silt, and other gritty material that can foul or damage plant equipment
Microstraining	Removes algae, aquatic plants, and small debris that can clog or foul other processes.
Main Treatment	
Aeration	Removes odors and dissolved gases, adds oxygen to improve taste
Coagulation/flocculation	Converts nonsettleable particles to settleable particles
Sedimentation	Removes settleable particles
Softening	Removes hardness-causing chemicals from water
Filtration	Removes fine particles, suspended flocs and most microorganisms
Adsorption	Removes organics and color
Fluoridation	Adds fluoride in order to harden tooth enamel
Disinfection	Kills or inactivates disease-causing organisms

Screening, presedimentation and microstraining are used to remove materials that can damage or clog plant equipment or foul the major treatment processes.

Chemical pretreatment is to add chemicals to remove some of undesirable materials, such as adding copper sulfate to control the growth of algae and adding potassium permanganate or chlorine dioxide to oxidize organic matter to remove taste and odor.

- Main treatment consists of aeration, coagulation/flocculation, sedimentation, softening, filtration, adsorption, fluoridation and disinfection (AWWA 1984).

Aeration, the mixing of air into water, is to remove certain dissolved gases in the water and increase the dissolved oxygen content of the water. It is the first step to remove iron and manganese.

Coagulation/flocculation is to destabilize the colloidal particles and then agglomerate small nonsettleable particles into larger and heavier particles by adding and mixing coagulants into water. Sedimentation is to settle out large and heavy particles in water by gravity.

Some water has high hardness. High hardness can result in scale buildups in hot water pipes and cause the formation of soap scum in sinks and tubs. Hardness can be removed through the softening processes.

Filtration always follows the sedimentation process to remove the remaining small particles. It removes some harmful microorganisms to reduce the load on the disinfection process, increasing disinfection efficiency.

Adsorption is to remove certain dissolved organic materials that can influence health and cause taste and odor problems.

Fluoridation is to add small quantities of fluoride to the water in order to strengthen tooth enamel and help prevent tooth decay.

Disinfection is the process to kill or inactivate biological contaminants present in a water supply. Chlorination, ozone, and ultraviolet light are the three major technologies used to disinfect water.

2.3   Coagulation/flocculation Processes and Mechanisms

2.3.1 Solids Composition in Water

Solids are present in water in three main forms: suspended particles, colloids, and dissolved molecules. Suspended particles, such as sand, vegetable matter and silts, range in size from very large particles down to particles with a typical dimension of 10 μm. Colloids are very fine particles, typically ranging from 10 nm to 10 μm. Dissolved molecules are present as individual molecules or as ions (Binnie et al. 2002). Figure 2.1 illustrates the size ranges of solids in water.

Typical diameter in metres

| 1E-10 | 1E-08 | 1E-06 | 1E-04 | 1E-02 |

1 nm

1 um

1 mm

Molecules

Colloids

Suspended Particles

Viruses

Pathogenic
Protozoa

Bacteria

Algae
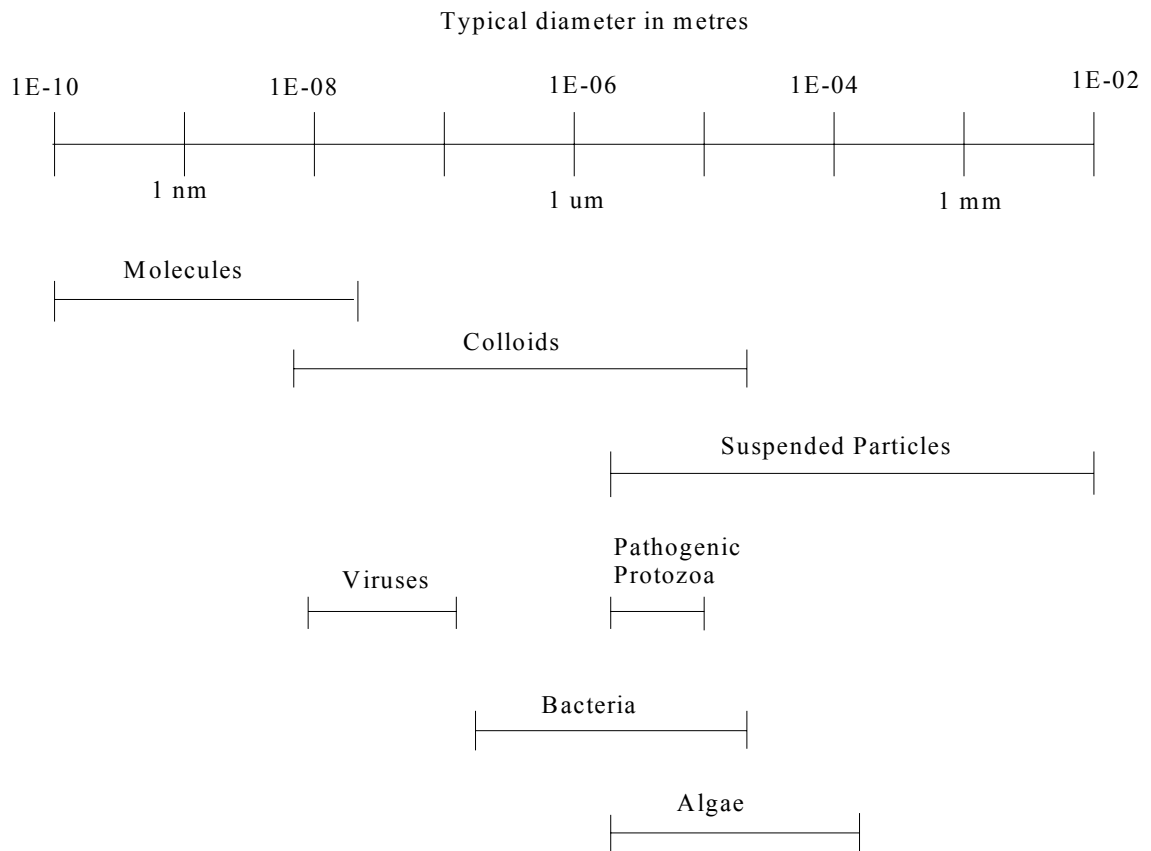
Figure 2.1. Size range of particles of concern in water treatment (Binnie et al. 2002)

In general, suspended particles are simply removed by conventional physical treatment like sedimentation and filtration. Dissolved molecules cannot be removed by conventional physical treatment. Thus, the removal of colloids is the main objective and the most difficult aspect in conventional water treatment (Binnie et al. 2002).

There are two types of colloids: hydrophilic colloids and hydrophobic colloids. Hydrophobic colloids, including clay and non-hydrated metal oxides, are unstable. The colloids are easily destabilized. Hydrophilic colloids like soap are stable. When these

colloids are mixed with water, they form colloidal solutions that are not easily destabilized. Since the particles have similar negative electrical charges and electrical forces to keep the individual particles separate, the colloids stay in suspension as small particles (Binnie et al. 2002).

The magnitude of the zeta potential (Z_p) is usually used to indicate colloidal particle stability. Z_p is described with the double-layer model shown in Figure 2.2 (Reynolds and Richards 1996). A negative colloidal particle attracts to its surface ions of the opposite charge. A compact layer on the colloid surface is called the fixed layer. The remaining counterions extend into the bulk of the solution, and constitute the diffused layer. The two layers represent the region surrounding the particle where there is an electrostatic potential. The shear plane or shear surface surrounding the particle contains the volume of water which moves together with the particle. Z_p is the electrostatic potential at the shear surface. The equation for Z_p is (Reynolds and Richards 1996)

$$[2.1] \qquad Z_p = \frac{4\pi\psi\mu}{D}$$

where:

Z_p = zeta potential (millivolts)

μ = absolute viscosity of the solution (N-s/m^2)

ψ = electrophoretic velocity (cm/s)

D = dielectric constant of the solution
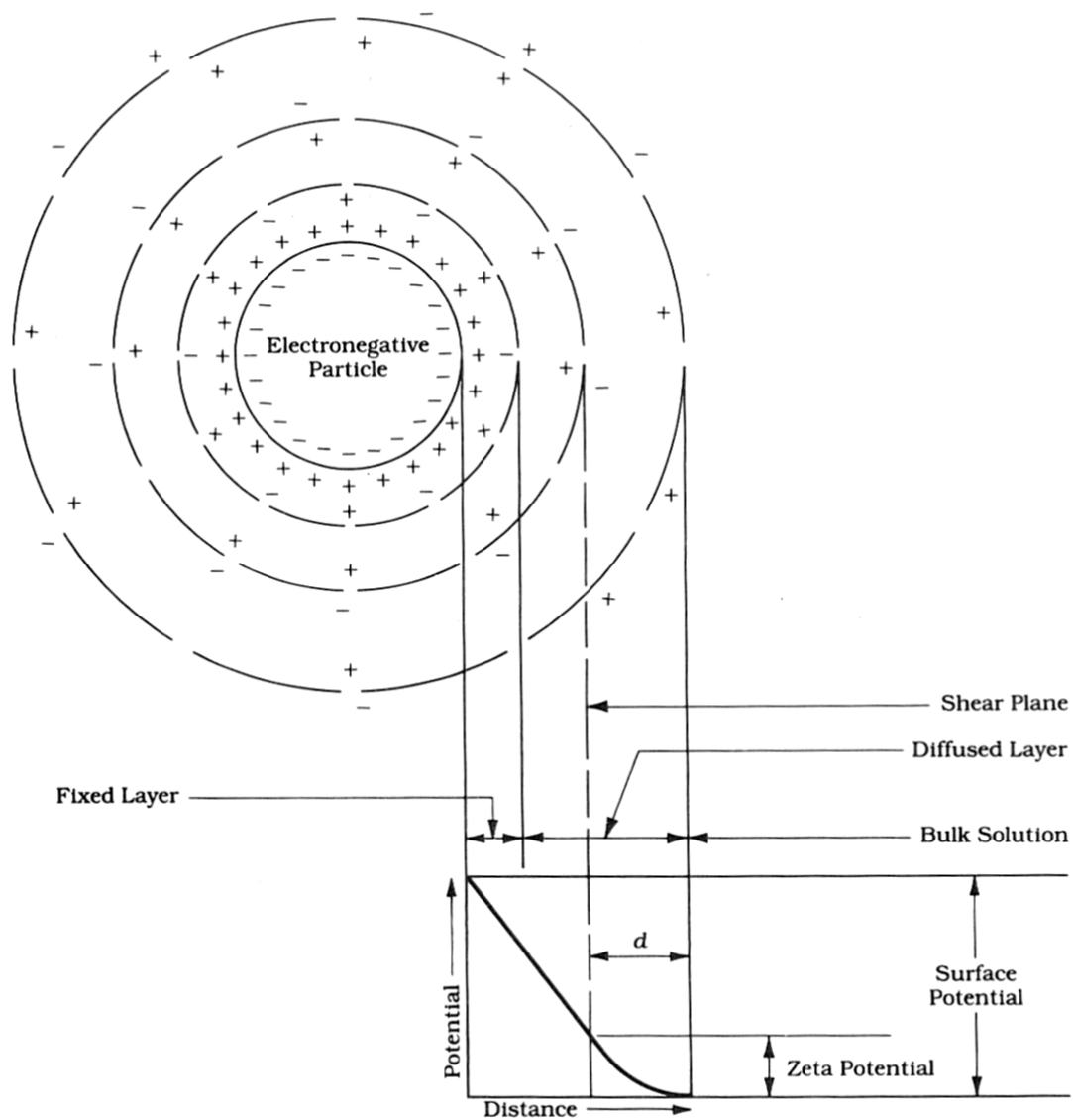
Figure 2.2. A negative colloid particle with its electrostatic field
(Reynolds and Richards 1996)

The higher the zeta potential, the greater are the repulsion forces between the colloidal particles and, therefore, the more stable is the colloidal suspension. A high Z_p represents strong forces of separation (via electrostatic repulsion) and a stable system, i.e. particles tend to suspend. Low Z_p indicates relatively unstable systems, i.e. particles tend to aggregate (Reynolds and Richards 1996).

To remove colloids, small particles have to be destabilized first, and then they will form larger and heavier flocs which can be removed by conventional physical treatment. This process can be described by coagulation/flocculation mechanisms. Coagulation combined with flocculation is a two-step, physico-chemical process that forms an essential component of accepted water treatment processes.

2.3.2 Coagulation

Coagulation is the destabilization of colloidal particles brought about by the addition of a chemical reagent (coagulant). The purpose of destabilization is to lessen the repelling character of the particles and allow them to be attached to other particles so that they may be removed in subsequent sedimentation processes (AWWA 1984). The particulates in raw water, which contribute to color and turbidity, are mainly clays, silts, viruses, bacteria, humic acids, minerals (including asbestos, silicates, silica, and radioactive particles), and organic particulates. At pH levels above 4.0, such particles or molecules are generally negatively charged (ASCE and AWWA 1998).

Coagulation can be accomplished through any of four different mechanisms. The following section details these various mechanisms.

1) Double-layer compression

The mechanism of double-layer compression relies on compressing the diffuse layer surrounding a colloid. This is accomplished by increasing the ionic strength of the solution through the addition of an indifferent electrolyte. The added electrolyte increases the charge density in the diffuse layer. The diffuse layer is 'compressed' toward the particle surface, reducing the thickness of the layer. Therefore, the zeta potential, Z_p, is significantly decreased (Reynolds and Richards 1996).

2) Adsorption and charge neutralization

Adding coagulants with a charge opposite to that on the colloidal particles can cause adsorption of the ions on to the colloidal particles and neutralize surface charge (Bagwell et al. 2001). This leads to easier aggregation. However, the coagulant dosage should be proportional to the quantity of colloids present. If overdose is applied, charge reversal on the colloids occurs and the colloids are not destabilized.

Al(III) and Fe(III) are most frequently used as coagulants in water treatment. When added to water, Al(III) and Fe(III) salts dissociate to their respective trivalent ions, Al^{3+} and Fe^{3+}, and then react with water (hydrolyze) to form hydroxy complexes, $Al(H_2O)_6^{3+}$ and $Fe(H_2O)_6^{3+}$. These complexes then react with water by replacing the H_2O molecules in the aquometal complex with OH^- ions. These subsequent reactions

are called hydrolytic reactions. There are many different species such as the following (Sanks 1979 and O'Melia 1978):

[2.2] $\qquad Fe^{3+} + H_2O = Fe(OH)^{2+} + H^+$

[2.3] $\qquad Al^{3+} + H_2O = Al(OH)^{2+} + H^+$

[2.4] $\qquad 7Al^{3+} + 17H_2O = Al_7(OH)_{17}{}^{4+} + 17H^+$

[2.5] $\qquad Fe(OH)^{2+} + H_2O = Fe(OH)_2{}^+ + H^+$

[2.6] $\qquad 2Fe^{3+} + 2H_2O = Fe_2(OH)_2{}^{4+} + 2H^+$
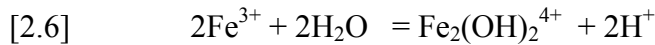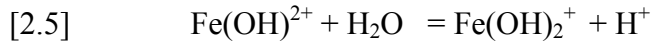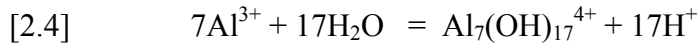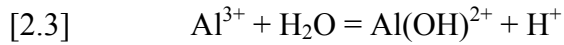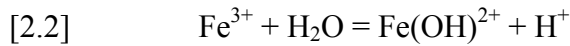
There are several soluble species formed, such as $Al_6(OH)_{15}{}^{3+}$, $Al_7(OH)_{17}{}^{4+}$, $Al_8(OH)_{20}{}^{4+}$, $Al_{13}(OH)_{34}{}^{5+}$, $Fe_2(OH)_2{}^{4+}$, $Fe_3(OH)_2{}^{4+}$. These complexes possess high positive charges and are adsorbed onto the surface of the negative colloids. This leads to a reduction of Z_p to a level where the colloids are destabilized. The aforementioned hydrolytic reactions cause the increase of H^+ concentration. If sufficient alkalinity is present in water, it would absorb hydrogen ions to avoid severe pH depression during the coagulation process. Alkalinity greater than 50 mg $CaCO_3$/L yields a pH drop less than 0.6 pH units.

3) Enmeshment by a precipitate (Sweep-floc coagulation)

Chemical compounds such as aluminum sulfate ($Al_2(SO_4)_3$), ferric chloride ($FeCl_3$), and lime (CaO or $Ca(OH)_2$) are frequently used as coagulants to form the precipitates of $Al(OH)_3$, $Fe(OH)_3$ and $CaCO_3$. These precipitates physically entrap the suspended colloidal particles as they settle, especially during subsequent flocculation.

When the colloidal particles themselves serve as nuclei for the formation of the precipitate, the flocs are formed around colloidal particles and the sweep-floc coagulation process can be enhanced. Thus, the rate of precipitation increases with increasing concentration of colloidal particles (turbidity) in the solution (Binnie et al. 2002).

The speciation of metal complexes or hydroxides depends on the amount of Al(III) or Fe(III) salts added. Bagwell et al. (2001) indicated that the hydrolysis products will form and will be adsorbed onto the colloidal particles when the amount of Al(III) or Fe(III) added to water is less than the solubility limit of the hydroxide. Adsorption of the hydrolysis products will result in destabilization by charge neutralization. When the amount of Al(III) or Fe(III) added to the water exceeds the solubility limit of the hydroxide, the hydrolysis products will form as kinetic intermediates in the eventual precipitation of metal hydroxides.

Figure 2.3 demonstrates how alum functions as a coagulant to treat a high turbidity water (greater than 100 NTU). There is no reduction in turbidity while alum doses are low, for there is insufficient hydroaluminum (III) species to provide effective destabilization. With increasing alum dose, turbidities decrease to a minimum value, as complete destabilization occurs. This stage is dominated by adsorption and charge neutralization mechanism. The optimum dosage often (but not always) corresponds to a Z_p which is near zero. A further increase in alum dose will cause restabilization of the particles due to charge reversal on the colloids occurring. The further addition of alum

to very high doses results in the formation of a precipitate of $Al(OH)_{3(S)}$ because the amount of Al(III) added to the water exceeds the solubility limit of the hydroxide. This bulky precipitate enmeshes particles and settles rapidly to form the 'sweep-floc' region of coagulation (Sanks 1979).

For a low turbidity water (less than 10 NTU), removal by adsorption and neutralization of alum polymers is not possible for insufficient contact opportunities are available. Removal is dominated by sweep-floc coagulation (Sanks 1979).
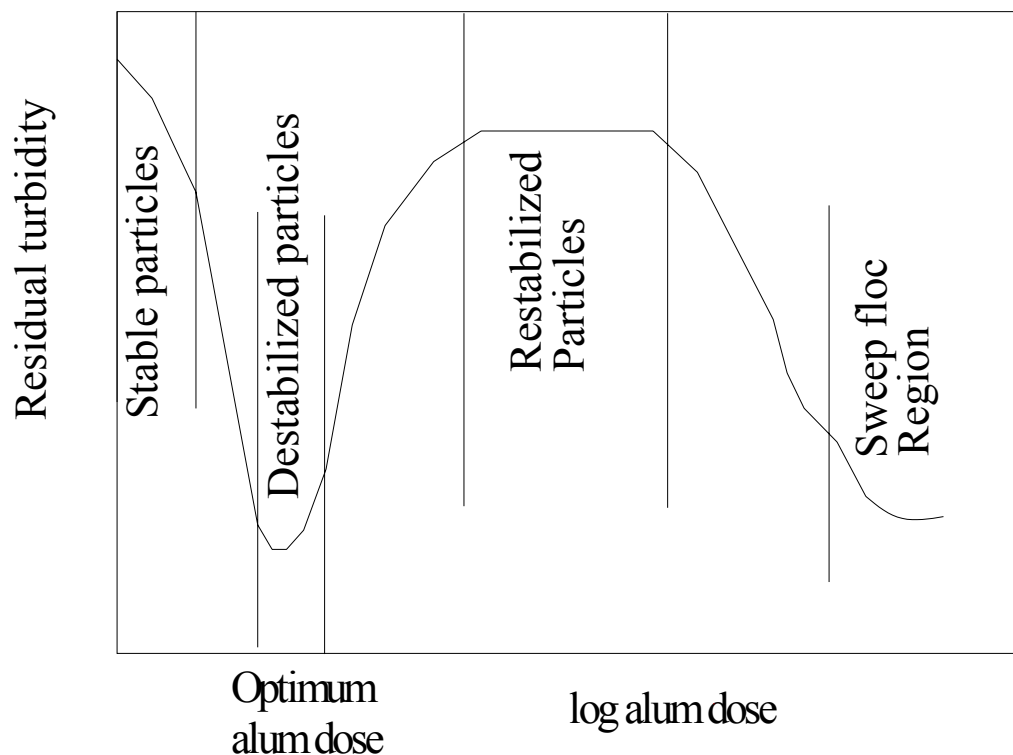
Figure 2.3. Alum dose versus residual turbidity for water coagulation/flocculation (Snoeyink and Jenkins 1980)

18

4) Interparticle bridging

Since synthetic polymeric compounds have large molecular sizes and multiple electrical charges along a molecular chain of carbon atoms, they are effective for the destabilization of colloids in water.

The interparticle bridging process was summarized by Bagwell et al. (2001) as follows. Figure 2.4a shows the simplest form of bridging, a polymer molecule will attach to a colloidal particle at one or more sites. Colloidal attachment is caused by coulombic attraction if the charges are of opposite charge or from ion exchange, hydrogen bonding, or van der Waal's forces.

Figure 2.4b shows the second reaction, in which the remaining length of the polymer molecule from the colloidal particle in the first reaction extends out into the solution. Attachment can occur to form a bridge if a second particle having some vacant adsorption sites contacts the extended polymer molecule. Thus, the polymer serves as the bridge. However, if the extended polymer molecule does not contact another particle, it can fold back on itself and adsorb on the surface of itself, as shown in Figure 2.4c. The original particle is restabilized.

If the quantity of polymer is overdosed, polymer segment may saturate the colloidal surfaces, thus no sites on the surfaces are available for interparticle bridging. This reaction (Figure 2.4d) causes restabilization of the particles. Intense agitation in solution

can cause restabilization because polymer-surface bonds or bridges formed are destroyed. These reactions are shown in Figure 2.4e and 2.5f.
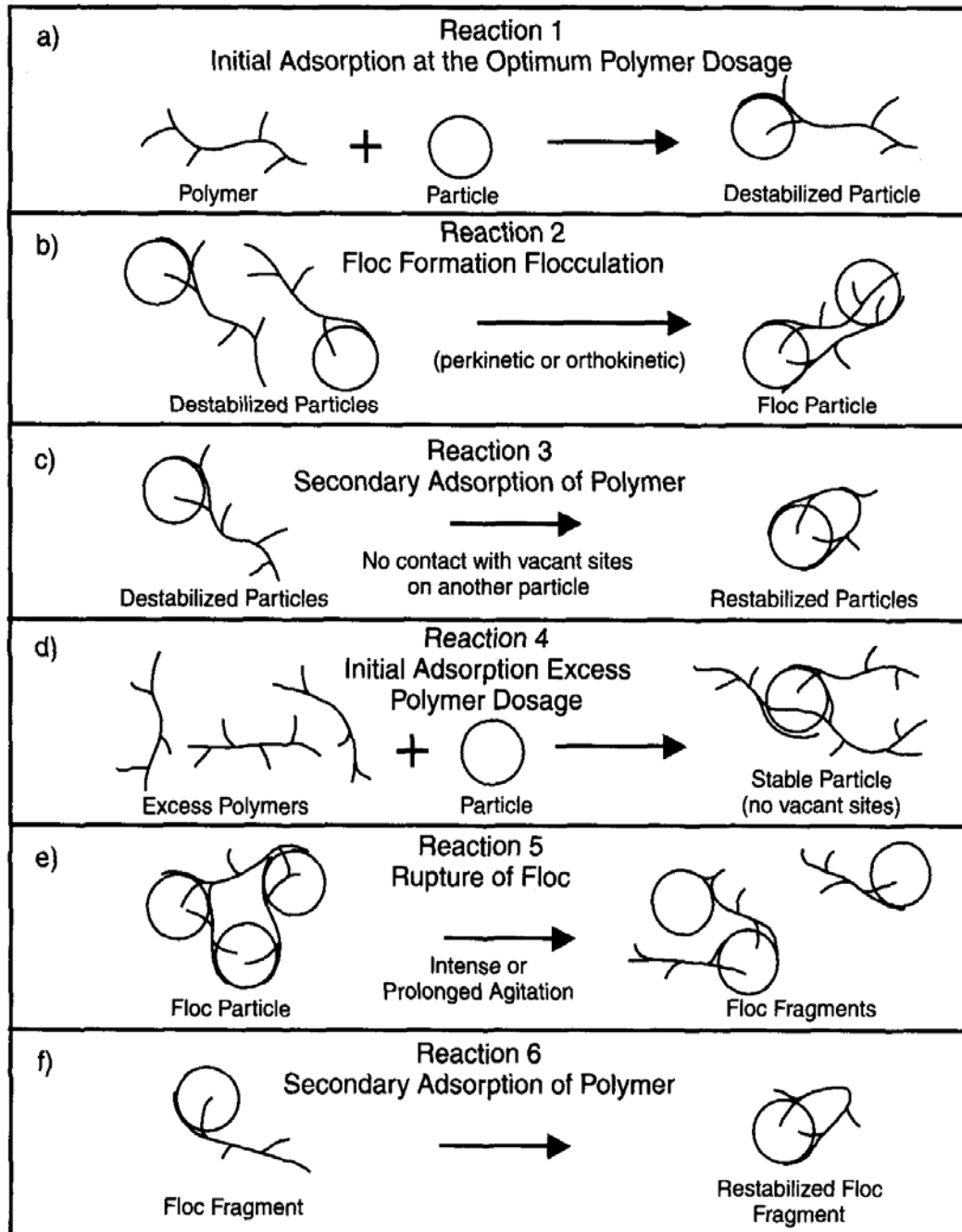
Figure 2.4. Schematic representation of bridging model for destabilization of colloids by polymers (Bagwell et al. 2001)

WSSA (1992) demonstrated that cationic polymers can be effective in coagulating negatively charged clay particles; they do not require a large molecular weight to be effective in destabilization. Electrostatic forces or ion exchange is the process by which the polymers become attached to the clay particles. In general, cationic polymers assist in particle destabilization by charge neutralization and therefore assist in colour and turbidity removal.

Anionic polymers of large molecular weight or size are able to bridge the energy barrier between two negatively charged particles, thereby effectively enhancing the coagulation efficiency. Generally speaking, anionic polymers can only assist in the physical process of flocculation. They reduce turbidity by inter-particle bridging but do not affect the removal of colour (WSSA 1992). The use of polymers offers a number of benefits. For instance, polymers increase the rate of flocculation, produce larger, denser floc that settles faster and strengthen the floc which helps improve filtration. They enable a greater volume of water to be treated in a given plant size.

2.3.3 Flocculation

Flocculation is the agglomeration of destabilized particles into microfloc and then into bulky floccules which can be called floc. While the coagulation process destabilizes particles through chemical reactions between the coagulant and the suspended colloids, flocculation is the transport step that causes the necessary collisions between the destabilized particles and subsequent floc aggregations or floc breakup (Binnie et al. 2002).

The following equation describes the rate of successful collisions between particles of size i and j (Thomas et al. 1999). When particles of size i successfully collide with particles of size j, particles of size k are formed.

[2.7] $N_{ij} = \alpha\beta(i, j)n_i n_j$

where:

N_{ij} = the number of collisions between particles of size i and j (count / m^3-sec)

α = collision efficiency

$\beta(i, j)$ = collision frequency between particles of size i and j (m^3/sec)

n_i, n_j = particle count for particles of size i and j, respectively (ct/m^3)

Almost all flocculation models are derived from Equation 2.7. Assuming no particle breakup, the general model for flocculation was given as (Swift and Friedlander, 1964)

[2.8] $$\frac{dn_k}{dt} = \frac{1}{2}\sum_{i+j=k}\beta(i, j)n_i n_j - \sum_{i=1}^{\infty}\beta(i, k)n_i n_k$$

In Equation 2.8, dn_k/dt is the rate of change in the count of particles of size k (ct/m^3-sec). The first term on the right hand side is the increase in particles of size k by flocculation of particles of size i and j (ct/m^3-sec). The second term on the right hand side is the loss of particles of size k by virtue of their aggregation with other particle sizes (ct/m^3-sec).

This equation with appropriate β values can be used to predict the aggregation rate of particles in suspension while a flocculation process occurs. β is a function of the flocculation transport mechanisms.

There are three major mechanisms of flocculation transport as described below:

1) Perikinetic flocculation is the aggregation of particles caused by random thermal motion (Brownian diffusion). The driving force for particle movement is the thermal energy of the fluid. It most likely occurs when at least one of the particles is quite small, which is less than approximately 1 μm in diameter (Han and Lawler 1992), so it is normally not a major factor in the transport associated with flocculation in water treatment (Bagwell et al. 2001).

The collision frequency, β, for Brownian transport is given by Smoluchowski (1917)

[2.9]
$$\beta_{Br} = \frac{8}{3} \alpha \frac{kT}{\mu}$$

where:

k = Boltzmann's constant (m^3/K-sec^2)

T = absolute temperature (K)

Equation 2.9 was based on the following assumptions:

- α is unity for all collisions

- the particles are monodispersed (i.e. all of the same size)

- collision involves only two particles

- all particles and flocs are spherical

- fluid motion undergoes laminar shear

- no breakage of flocs occurs

The aggregation rate of particles is derived from the combination of Equations 2.8 and 2.9:

[2.10] $$\frac{dN_t}{dt} = -\frac{4}{3}\alpha\frac{kT}{\mu}N_t^2$$

where:

N_t – total particle count at time t, $N_t = \sum n_k$ (ct)

2) Orthokinetic flocculation is the aggregation of particles caused by induced energy in the fluid. The destabilized particles follow the streamlines and eventually result in interparticle contacts (Binnie et al. 2002). Han and Lawler (1992) indicated that orthokinetic flocculation most likely occurs when both particles are greater than approximately 1 μm in diameter and fairly similar in size (within a factor of 10 in size ratio).

The fluid flow varies with different intensity of mechanical mixing. There are laminar flow, turbulent flow and the flow between laminar and turbulent flow. When the fluid moves in layers or laminas, and one layer gliding smoothly over an adjacent layer with only molecular interchange of momentum, the flow is laminar flow. However, turbulent flow has very erratic motion of fluid particles, with a violent transverse interchange of momentum (Thomas et al. 1999).

For laminar flow, the relative velocity between two points in suspension can be decomposed into two components of rotation and shear. The rotational component does not contribute to the rate of collisions for the particles remain at the same distance apart. In contrast, the shear component causes collisions between particles due to shear stress. The shear stress in a fluid is proportional to velocity gradient (du/dy), which is different velocity between two points (Thomas et al. 1999).

Camp and Stein (1943) defined the root-mean-square velocity gradient, G:

[2.11] $$G = \left[\frac{\varepsilon}{\mu} \right]^{1/2}$$

where:

G – velocity gradient (sec^{-1})

For mechanical mixing, the following equation for value of G was developed:

[2.12] $$G = \left[\frac{P}{\mu V} \right]^{1/2}$$

where:

P = power input to the water (N-m/s)

V = volume of reactor (m^3)

The collision frequency function is proportional to the velocity gradient. The relationship between β and du/dy is as follows (Swift and Friendlander, 1964):

[2.13] $$\beta_{Sh} = \frac{8}{\pi} \frac{du}{dy} V_i$$

where:

V_i – volume of i particles of size d_i (m^3)

Combining Equations 2.8 and 2.11 and neglecting floc breakup, the aggregation rate of particles is

[2.14]
$$\frac{dN_t}{dt} = \frac{4}{\pi}\frac{du}{dy}\alpha\varphi N_t$$

where:

φ – volume fraction of the dispersed phase

For turbulent flow, the isotropic model (Thomas et al. 1999) has been widely accepted although turbulence phenomenon remains poorly understood. Turbulences are considered a cascade of eddies of diminishing size. During mixing, induced energy is primarily used for the formation of large eddies. These large eddies carry out most of the momentum transport and energy is transferred via a series of eddies of decreasing size until a certain size of eddy is formed where all the energy is dissipated by viscous forces. The length scale of the eddy where energy is dissipated is called the Kolmogorow microscale (λ). λ is defined as

[2.15]
$$\lambda = \left[\frac{\mu^3}{\varepsilon}\right]^{1/4}$$

where:

ε – rate of energy dissipation (N-m/S-m^3)

The more energy put into the water in a reactor, the smaller λ is (Hanson and Cleasby 1990).

Under the turbulent flow conditions, floc breakup is an important factor and cannot be neglected (Zhang and Li 2003). Thus, G is not sufficient in itself to categorize the flocculation process because floc breakup phenomenon is not considered. The rate of disappearance of primary particles (dn_t/dt) should include both the rate of particle aggregation and the rate of particle breakup. The dn_t/dt is described as follows (Montgomery, 1985)

[2.16]
$$\frac{dn_t}{dt} = -K_A G n_t + K_B G^\delta$$

Where:

K_A – aggregation constant

K_B – breakup constant (sec)

δ – floc breakup rate exponent ($\delta=2$ for viscous dissipation subrange)

K_A depends on the chemical properties of the suspension, hydrodynamic characteristics of the turbulence field, and the size of particulates. K_B is dependent on the floc internal binding forces or the floc strength of the aggregate (Agraman and Kaufman 1970). K_A and K_B can be determined in the laboratory or pilot-scale tests. Some of reported data are shown in Table 2.2.

Table 2.2. Flocculation Kinetic Parameters

System	K_A	K_B (sec)	Reference
Kaolin-alum	$4.5 * 10^{-5}$	$1.0 * 10^{-7}$	Argaman (1970)
Kaolin-alum	$2.5 * 10^{-4}$	$4.5 * 10^{-7}$	Bratby (1977)
Natural particulates-alum	$1.8 * 10^{-5}$	$0.8 * 10^{-7}$	Argaman (1971)
Alum-phosphate precipitate	$2.8 * 10^{-4}$	$3.4 * 10^{-7}$	
Alum-phosphate plus polymer	$2.7 * 10^{-4}$	$1.0 * 10^{-7}$	Odegaard (1979)
Lime-phosphate, pH 11	$5.6 * 10^{-5}$	$2.4 * 10^{-7}$	

Since flocculation is a first-order reaction, in order to exhibit a residence time distribution approximating plug flow in a flocculation reactor, Argaman and Kaufman (1970) designed a set of four continuous-stirred tank flocculation rectors (CSTR) in series. Based on the experimental results, they simplified the Equation 2.16 as follows:

[2.17] $$\frac{n_1^o}{n_1^m} = \frac{(1 + K_A G t_i)^m}{1 + K_B G^2 t_i \sum_{i=1}^{m-1} (1 + K_A G t_i)^i}$$

where:

n_1^o – particle concentration when leaving the rapid mixing chamber (mg/L)

n_1^m – particle concentration after the settling chamber (mg/L)

t_i – detention time in each reactor (sec)

m – number of reactors

For one reactor (m=1), Equation 2.17 becomes

$$[2.18] \qquad \frac{n_1^o}{n_1} = \frac{1 + K_A Gt}{1 + K_B G^2 t}$$

3) Differential settling is caused by different settling velocities of particles. Because the settling velocity of particles which have similar densities is proportional to the particle size, the sedimentation of differential particles in heterogeneous suspension provides an additional transport for promoting flocculation. It most likely occurs when at least one of the particles is larger than 10 μm in diameter and the other is significantly different in size (Han and Lawler 1992, Thomas et al. 1999). The collision frequency, β, for this transport mechanism is given by Friedlander (1977)

$$[2.19] \qquad \beta_{DS}(i,j) = \frac{\pi \Delta \rho g \alpha}{72 \mu} (d_i + d_j)^3 (d_i - d_j)$$

where:

$\Delta \rho$ – difference in density between the particle and the fluid (kg/m^3)

g = gravitational constant (9.806 m/s^2)

The three interparticle collision frequency functions are independent and additive (Zhang and Li 2003), that is

$$[2.20] \qquad \beta = \beta_{Br} + \beta_{Sh} + \beta_{DS}$$

2.3.4 Velocity Gradient, G

Velocity gradient, G, is the relative velocity of the two fluid particles at a given distance. The optimum G and Gt (the product of G and detention time) value is of

importance in the coagulation/flocculation process. If G is insufficient, adequate interparticulate collisions will not occur and a proper floc will not be produced. If G is too great, excessive shear forces will prevent the desired floc formation, for high shear rates break up previously formed flocs (Reynolds and Richards 1996).

Spicer and Pratsinis (1996) concluded that increasing fluid shear appeared to narrow the steady state floc size distributions and the large tail of the floc size distribution was pushed to smaller particle sizes by shear-induced fragmentation.

Typical G and detention times for flocculation at 20 $^{\circ}$C are summarized in Table 2.3 (ASCE and AWWA 1998).

Table 2.3. Flocculation design criteria (ASCE and AWWA 1998)

Process	G (sec^{-1})	t (sec)	Gt
Distribution channels mixer to flocculator	100 - 150	Varies	--
High-energy flocculation for direct filtration	20 - 75	900 – 1,500	40,000 – 75,000
Conventional flocculation	10 - 60	1,000 – 1,500	30,000 – 60,000

The power (P) imparted to the liquid by impellers may be determined (Reynolds and Richards 1996). For laminar flow (Reyolds number, Re, <10 to 20), the power imparted by an impeller is as follows:

[2.21] $\qquad P = K_L n^2 D_i^3 \mu$

where:

K_L = impeller constant for laminar flow

n = rotational speed (rpm)

D_i = impeller diameter (m)

For turbulent flow (Re >10,000), the power imparted by an impeller is given by the equation:

$$[2.22] \qquad P = K_T n^3 D_i^5 \rho$$

where:

K_T = impeller constant for turbulent flow

ρ = density of liquid (kg/m^3)

If using paddle-type mechanical flocculators (Bagwell et al. 2001), the power imparted can be expressed as

$$[2.23] \qquad P = F_D v = C_D A \rho \frac{v^3}{2}$$

where:

F_D = drag force of the paddle (N)

C_D = coefficient of drag

A = paddle-blade area at right angle to the direction of movement (m^2)

v = velocity of the paddle blade relative to the water, which is approximately three-

    fourths the peripheral blade velocity (mps)

2.4 Temperature Effects on Water Properties and Coagulation/Flocculation

Low water temperature causes low turbidity removal efficiency and poor effluent quality. Kang et al. (1995) indicated that cold water had a pronounced detrimental effect on flocculation kinetics, slowing the rate of flocculation.

2.4.1 Physical and Physicochemical Effects

Temperature affects physical properties of water. Heinanen (1987) illustrated temperature effect on density, viscosity and dielectric constant of water. Figure 2.5 shows that the dynamic viscosity increases with decreasing temperature. Dielectric constant also increases as temperature decreases (Figure 2.6), the dielectric constant is the ability of a dielectric to store electrical potential energy under the influence of an electric field. Density rises with decreasing temperature to its maximum level at 4°C after which it decreases slightly until the phase change occurs at 0°C where the density sharply decreases (Figure 2.7a and b).

The change in viscosity with varying temperature in the range of 0 to 22 $^\circ$C is far larger than the change in density or dielectric constant in water. As shown in Figure 2.5, when a temperature decreased from 15 to 4°C, the viscosity increased from 1.139 cP to 1.567 cP. Thus the viscosity increase was 38%. However, the density increase was less than 0.1% and the dielectric constant increase was approximately 6% (Figures 2.6 and 2.7). Therefore, the temperature impact is more significant for those process mechanisms which are a function of viscosity.
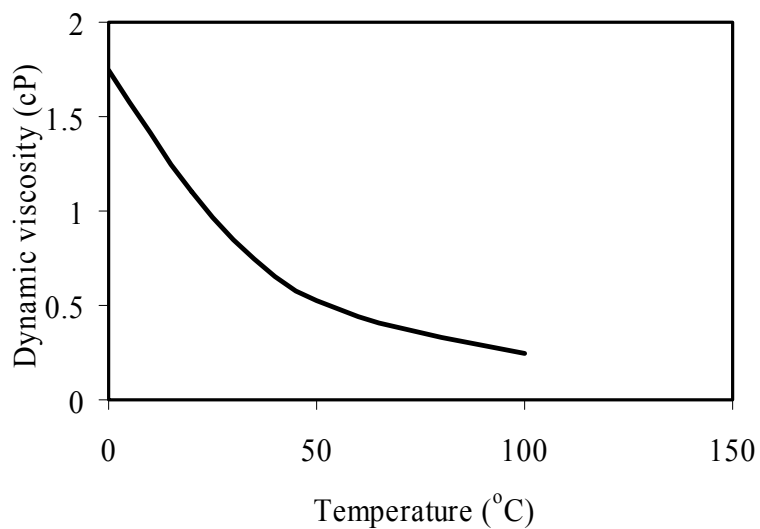
Figure 2.5. Dynamic Viscosity of water as a
function of temperature (Heinanen 1987)
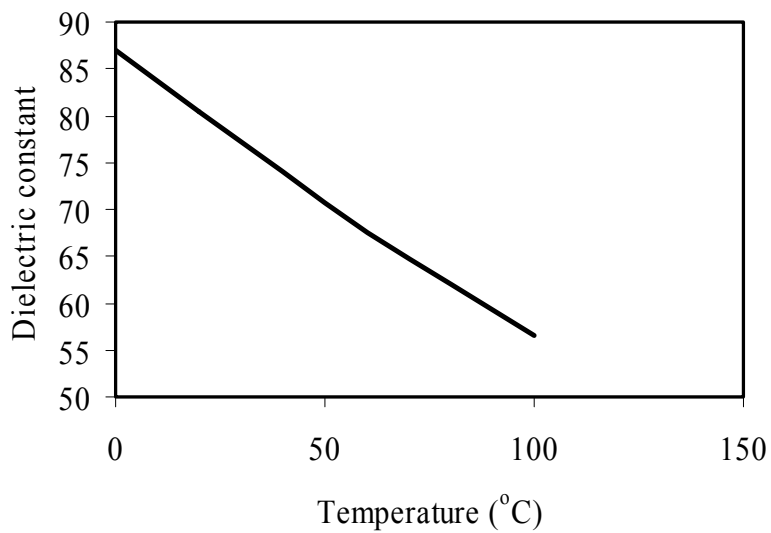
Figure 2.6. Dielectric constant of water as a
function of temperature (Heinanen 1987)
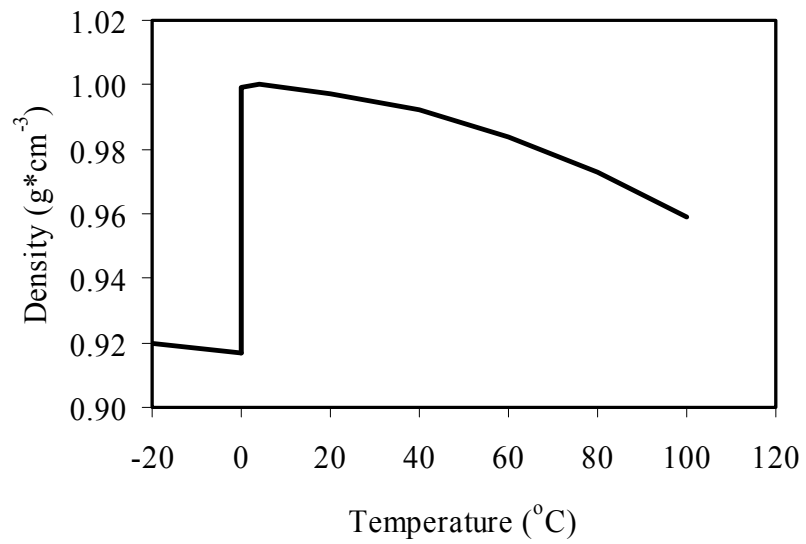
Figure 2.7a. Density of water as a
function of temperature (Heinanen 1987)
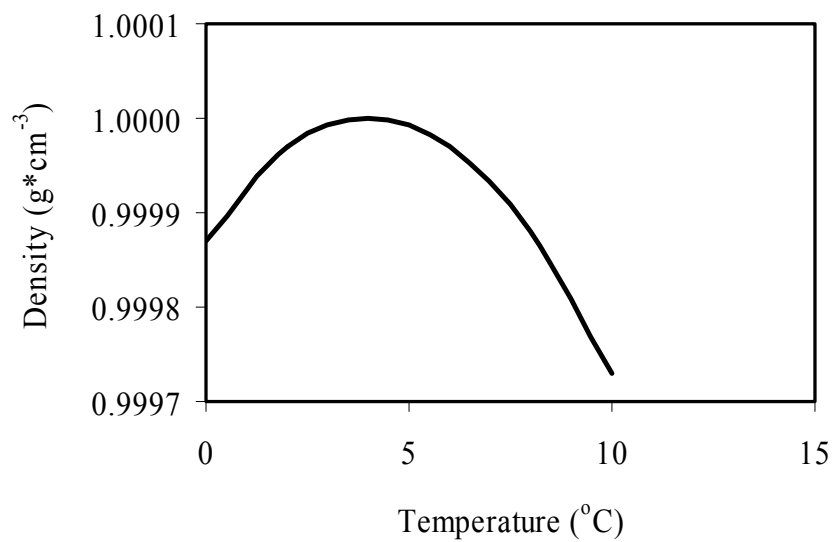
Figure 2.7b. Density of water as a
function of temperature (Heinanen 1987)

The change in viscosity and dielectric constant with temperature is of interest because they lead to the variation of a zeta potential (Z_p), which relates to the stability of colloidal particles in coagulation. Equation 2.1 (in Section 2.3.2) shows the relationship among Z_p, viscosity and dielectric constant.

Mothadi and Rao (1973) found that the zeta potential of kaolinite and bentonite clays coagulated with alum at a given dose and constant pH of 5.0 did not change with temperature variation from 1 to 25°C, while the electrophoretic velocity, which is the migration velocity of a charged particle in an electromagnetic field, decreased with decreasing temperature. The possible reason was that the decreased electrophoretic velocity combined with the increased dielectric constant and the increased viscosity tended to offset one another resulting in very little net impact on the zeta potential at low temperature. Kang et al. (1995) concluded that the zeta potential of kaolin clay was only slightly sensitive to temperature variation from 5 to 23°C.

Temperature affects the flocculation processes. The particle transport processes are described as perikinetic due to Brownian diffusion, orthokinetic due to fluid shear, and differential settling flocculation (in Section 2.3.3). Lawler (1993) and O'Melia (1978) stated that the orthokinetic collision rate greatly exceeded the rate of Brownian diffusion in flocculation, even at a fairly low shear rate. In practical situations, since the size of most particles is larger than 1 μm during the coagulation-flocculation process and when quite a high shear rate is applied, temperature would have little effect on

perikinetic flocculation, which dominates when at least one of the particles is less than 1 μm.

In orthokinetic flocculation, its rate can be affected by the varying temperature because of the effect of the root mean square velocity gradient G. Hanson and Cleasby (1990) found that maintaining a constant value of G (by increasing energy input) to compensate for higher water viscosity at low temperature was a way to increase flocculation rate. In a study on the effect of temperature on flocculation processes, they found that the impeller geometry impacted the particulate removal efficiency at a temperature of 5 $^{\circ}$C, because different impeller geometry produced different percentage of energy which generated turbulence. Matsui et al. (1998) indicated that although lower temperatures slowed the particle destabilization, a decrease in the flocculation rate could be avoided by maintaining a constant G value.

2.4.2 Chemical Effects

Temperature affects the chemical properties of water, such as reaction rates, solubilities, pH, and hydrolysis species of coagulants.

Reaction rates and reaction kinetics decrease with reducing temperature. This relationship is expressed with Arrenius empirical rate law (Snoeyink and Jenkins 1980),

[2.24] $$\ln(k) = \ln(A) - \frac{E_a}{RT}$$

where:

k = reaction rate constant

A= pre-exponential factor (L/mole-sec)

E_a = the activation energy, constant for a given reaction (cal/mole)

R = ideal gas constant (1.99 cal/mole-K)

T = temperature (K)

In general, the solubility of solids and liquids is highly dependant on temperature but only slightly on pressure. In most water-engineering situations, solubility may be considered as a function of temperature alone. The solubilities of most solids decrease as temperature decreases (Bagwell et al. 2001).

Solubility can be best depicted by use of the solubility product constant (K_{sp}). Consider the following equation:

[2.25] $A^+ + B^- = C_{Solid}$

where:

$[A^+]$, $[B^-]$ = the molar concentrations of the ions (mole/L)

[C] = the concentration of a solid substance (mole/L)

Generally stated, the equilibrium constant, K_w, is as follows (Snoeyink and Jenkins 1980):

[2.26] $K_w = \dfrac{[A^+][B^-]}{[C]}$

The concentration of a solid substance can be treated as a constant K_s. Actually, while heterogeneous equilibria occur between crystals of a compound in the solid state and its ions in solution, Equation 2.26 is expressed as follows:

[2.27] $\qquad K_{sp} = K_w K_s = [A^+][B^-]$

where:

K_{sp} = solubility product constant

In an unsaturated solution, the ion product ($[A^+]$ $[B^-]$) is less than K_{sp}. If the ion product is greater than K_{sp}, the solution is supersaturated and will tend to form a precipitate.

Equilibrium constants for chemical reactions vary with temperature. Their relationship can be described by the Van's Hoff equation as follows (Snoeyink and Jenkins 1980):

[2.28] $\qquad \ln \dfrac{K_{w1}}{K_{w2}} = \dfrac{\Delta H^o}{R} \left(\dfrac{1}{T_2} - \dfrac{1}{T_1} \right)$

where:

K_{w1} and K_{w2} = equilibrium constants at T_1 (K) and T_2 (K), respectively

ΔH^o = change in enthalpy (kcal/mole)

In exothermic reactions, an increase in temperature will shift a reaction to a less complete state, ΔH^o is negative and K_w declines as temperature increases, thus solubility declines. This is typically what happens to calcium carbonate in the reaction:

[2.29] $\qquad Ca^{2+} + HCO_3^- = (CaCO_3)_{solid} + H^+$
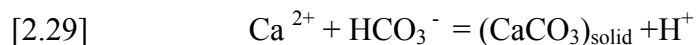
Thus, an increase in temperature will shift the reaction to a less complete state or to the right of Equation 2.29 in this case.

Endothermic reactions occur in most water treatment operations. In endothermic reactions, ΔH^o is positive and K_w will increase as temperature increases, thus solubility increases. The equilibrium equation for aluminum hydroxide can be expressed as follows:

[2.30] $$Al^{3+} + 3OH^- = (Al(OH)_3)_{solid}$$
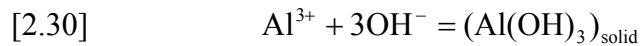
An increase in temperature will shift the reaction to a more complete state or to the left in this case.

Al-Laya and Middlebrooks (1974) compared the impact of water temperatures at 10, 20 and 35°C on algae removal, and found that less coagulant was required at the lower temperatures for the same degree of removal. They concluded that because of the decreased solubility of aluminum hydroxide at lower temperatures, more flocs appeared at the colder temperatures. However, the temperatures used by them were not in the temperature range that this research would conduct.

While water temperature changes, both the equilibrium concentrations of the various metal salt coagulant species and the hydrolysis reaction kinetics might change. Kang et al. (1995) observed the differences in iron (III) solubility and speciation with varying temperature. Thermodynamic data are listed in Table 2.4. Table 2.4 contains both enthalpic data and equilibrium constants at 25 ^{o}C, as well as calculated equilibrium constants at 5 ^{o}C for the mono-meric hydrolysis species of iron (III). They indicated that the impact of temperature on the $Fe(OH)_{3(S)}$ solubility was distinguishable. Temperature

decrease from 25 to 5 $^\circ$C resulted in the theoretical solubility curve of $Fe(OH)_{3(S)}$ shifting about 0.4 pH unit to the alkaline side and lowering about 0.2 log unit of soluble ferric concentrations.

Table 2.4. Iron (III) hydrolysis equilibrium constants and corresponding reaction enthalpy (Kang et al. 1995)

[1]Reaction	H°_f (kcal/mol)	Log K at 25°C	Log K at 5°C
$Fe^{3+} + H_2O = FeOH^{2+} + H^+$	10.4	-2.19	-2.74
$Fe^{3+} + 2H_2O = Fe(OH)_2^+ + 2H^+$	17.1	-5.67	-6.57
$Fe^{3+} + 3H_2O = Fe(OH)_3^0 + 3H^+$	24.8	-12.56	-13.84
$Fe^{3+} + 4H_2O = Fe(OH)_4^- + 4H^+$	31.9	-21.6	-23.28
$Fe(OH)_{3(S)} = Fe^{3+} + 3\ OH^-$	20.7	-38.7	-39.79

[1]Ligand and H_2O molecules are omitted for brevity.

Hem and Roberson (1990) and Dempsey (1987) stated similar results for aluminum. Dempsey (1987) depicted that the theoretical solubility curve of $Al(OH)_{3(S)}$ shifted 0.6-0.8 pH units to the alkaline side and lowering about 0.7 log unit of soluble Al concentration with decreasing temperature from 25 to 1 $^\circ$C.

The control of pH is an essential aspect of coagulation. Heinanen (1987) indicated that an optimum pH existed for floc formation, and this optimum pH increased as water temperature decreased. The optimum pH for coagulation is generally within the range of 5.5 to 7.5 and 5.0 to 8.5 in the water treated with Alum and Ferric, respectively (ASCE and AWWA 1998).

Hanson and Cleasby (1990), Van Benschoten and Edzwald (1990), and Kang et al. (1995) observed the change of optimum coagulation pH at low temperature when adding Al (III) or Fe (III) coagulants. They found that low temperature effects on coagulation/flocculation were offset by increasing the coagulation pH. They demonstrated that the use of constant pOH for correcting system chemistry could lower temperature effects. Using constant pOH means to maintain hydroxyl ion concentration constant as temperature changes. Maintaining constant pOH with varying temperature is achieved simply by increasing the pH of suspension at lower temperature following the changes in pK_w ($-\log [H^+][OH^-]$) with temperature.

Hanson and Cleasby (1990) found that while ferric sulfate acted as a coagulant, there was a pronounced decrease in flocculation kinetics at the cold temperature when the pH was held constant. However, the flocculation kinetics at 20 ^{o}C and 5 ^{o}C were nearly identical when pOH was held constant. This phenomenon can be explained by the fact that at constant pH, the hydroxyl ion concentration decreases when temperature decreases, causing slower particle destabilization rate.

Kang et al. (1995) discovered that the use of constant pOH to adjust water chemistry for temperature change was partially effective for reducing the impact of low temperature on flocculation kinetics, but the improved performance at 5°C at constant pOH did not reach the performance at 23 ^{o}C. Van Benschoten and Edzwald (1990) found that the pH at which Al precipitation occurred was increased from 4.6 at 25 ^{o}C to 5.5 at 4 ^{o}C.

On the other hand, the impact of temperature on pH can also be demonstrated by comparing the variation of pH of a neutral solution with temperature. In general, it is thought that pH of 7 represents neutrality, however this only applies at 25 °C. The variation of equilibrium constant K_w with temperature causes the change in neutral pH results. The neutral pH for water at 0°C is 7.5 (Hooge 2000).

Water temperature may also influence the distribution of the hydrolysis species of Al (III) and Fe (III) both in solution and on particle surfaces due to the change of the rate and extent of reactions involved. In studies of Al hydrolysis reactions, Hem and Roberson (1990) and Apps and Neil (1990) pointed out that the rate of approach to the equilibrium concentration of aluminum hydroxide increased with increasing temperature. Similarly, Flynn (1984) stated that, with increasing temperature and pH, the rate of hydrolysis of Fe (III) salts was accelerated. Temperature effects on the formation of coagulant species in solution could also affect the species adsorbed on particles, and then the surface properties of the particles.

Hanson and Cleasby (1990) investigated the floc internal binding forces (floc strength) at different temperatures by comparing the particle size distributions of various floc samples after floc breakup with an impeller. Both iron and alum flocs formed at 5 °C, even at constant pOH, were much weaker than those at 20 °C. Hutchison and Foley (1974) found that water temperature below 3.3 °C resulted in much slower floc growth than under normal temperature conditions. Morris and Knocke (1984) observed that for the same coagulant dosage, low temperature conditions caused smaller flocs than 20 °C

conditions by using a particle size analyzer to measure floc size distributions. Figure 2.8 shows that increasing alum dosage at low temperature (1 $^\circ$C) actually reduced the size of the coagulated flocs (Morris and Knocke 1984). This result implies that an increase in alum dosage for cold water might not offer any improvement in turbidity removal.
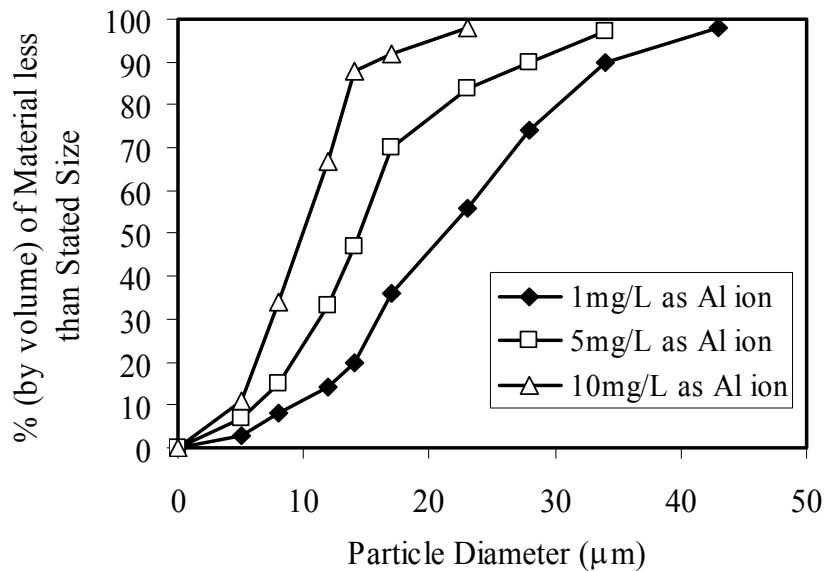
Figure 2.8. Effect of alum coagulant dose on particle size distribution at
1°C (Morris and Knocke 1984)

Morris and Knocke (1984) conducted precipitation rate experiments at low temperature of 1°C and found that significant precipitation occurred for both ferric and aluminum based coagulants within 1 minute. They recognized that precipitation rates were dependant on both reaction rate and crystal growth. They concluded that precipitation rates did not greatly change at 1 $^\circ$C in comparison with 22 $^\circ$C.

It has been reported that polymers could increase water treatment efficiencies under low water temperature conditions. Matsui et al. (1998) indicated that polyaluminium chlorides (PACls) were less sensitive to the change of hydroxyl concentration, and PACls performed better than alum in cold water. Wang et al. (2002) found that even with a lower dosage and shorter coagulation/flocculation time, PACls performed as effectively as aluminum sulfate for the treatment of cold water at 5.5 ^{o}C. Bunker et al. (1995) reported that PACls were effective in treating cold waters with a flocculation time of 2.5 to 5 minutes. This is attributed to the higher-charged polymeric aluminum species, and the lower hydrophilic and more compact flocculated flocs of PACl coagulant. However, there were no reports about how a polymer affected a coagulation/flocculation process when a water temperature approached 0 ^{o}C.

2.5 Summary

The literature review in this chapter outlines coagulation/flocculation processes and mechanisms, as well as a variety of studies on temperature effects on coagulation/flocculation. It also states the effects of diverse water characteristics, coagulants and process parameters combined with temperature change on coagulation/flocculation. Because most of the researches focused on studying the coagulation/flocculation treatment efficiency, a study on coagulation/flocculation processes is necessary. The experiment in the following section mostly concentrates on investigations of coagulation/flocculation processes in the water treated with different types and dosages of coagulants at different water temperatures.

Chapter 3 – Experimental Methods And Procedures

3.1 General

The objectives of the experiments are to obtain data from bench-scale tests in order to evaluate the particulate removal efficiency, and to capture images in order to analyze the floc change during the coagulation/flocculation process. The experiments are conducted under various operating conditions, such as the types and dosages of coagulants as well as temperatures.

3.2 Methodology

3.2.1 Bench-scale Test

Bench-scale tests are designed to show the nature and extent of the chemical treatment on a laboratory scale. A bench-scale test was conducted in square batch reactors ($100*100*180$ mm^3) on a stirring apparatus. The stirring apparatus was equipped with a six-place paddle stirrer with two opposite blades on the shaft, an electric motor with speed controller and a tachometer. Figure 3.1 is a photo of the bench-scale test equipment.

The bench-scale test procedure consisted of an initial period of rapid mixing, followed by a period of slow mixing. After slow mixing, the flocs were allowed to settle for a period, and then samples collected from the top 35 mm of each reactor were analyzed for turbidity, pH and particle count (AWWA 1977).

Figure 3.1. Bench-scale test equipment

3.2.2 Image-processing Test

In the image-processing test, pictures from the bench-scale test process were monitored and analyzed with an advanced image analysis method. As seen in Figure 3.2, the bench-scale test process was photographed by use of a 6-megapixel Fujifilm digital camera equipped with a micro lens. The camera was connected to a computer. The shutter opening was synchronized with a flash unit using camera control software.

The camera control software (Fuji FinePixViewer) was also used to manage image acquisition and storage procedures. All images were stored on the computer hard drive.

Captured digital images were analyzed with particle analysis software (Carnoy 2.0), thus the sizes of particles were determined.

The size of image captured was 4256* 2848 pixels. To calibrate image sizes correctly, a general standard scale in the range of 0 to 200 mm was photographed to determine the number of pixels corresponding to a given standard length for each set of experiments. In all of the experiments, 1 mm was equivalent to 440-445 pixels. The exact value depended on each set of experiments. The position of the flocs photographed was about 5 mm from the inside of the jar wall. The depth of field was 1.0 mm.
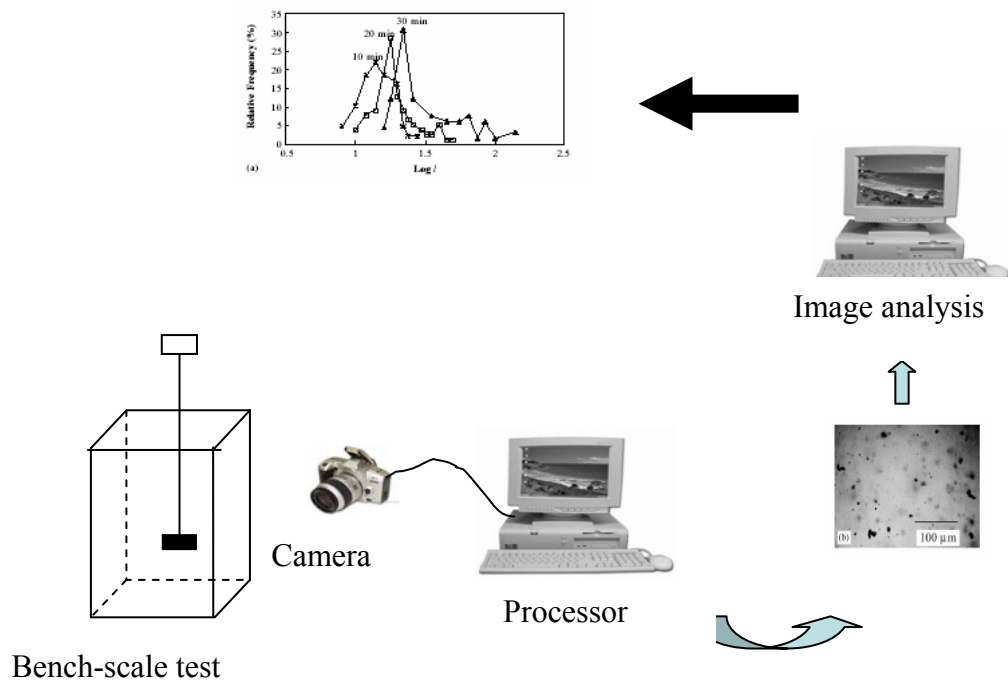
Figure 3.2. Experimental Set-up for Image-processing Test

Multiple digital images were taken throughout the aggregation process so floc size distributions at different flocculation time could be recorded and analyzed. Moreover, the evolution of flocs could be investigated from floc sizes and shapes at different flocculation time.

3.3 Experimental Apparatus and Description

The following experimental apparatuses were used in this research work.

Table 3.1. List of experimental apparatus

Item	Type
Six-place paddle stirrer	Model No.300, Phipps & Bird Inc., Virginia, USA
Square batch reactor	100*100*180 mm, Made by the Engineering Shop of the University of Saskatchewan
Environmental Control Chamber	Chamber located in the Environmental Engineering laboratory
Freezer	Danby Model: DCF 1519WE, Guelph, Canada
Container for tests at a water temperature of $0^{o}C$	Designed and built by Yan Jin
Digital Camera	6-megapixel, Fuji FinePix S2 Pro., Japan
Micro lens	Nikon, USA
Computer	IBM, Window$^{©}$ XP Professional
Camera control software	Fuji FinePixViewer Ver.3.1.02E

The experiments at a water temperature of 22 ^{o}C were conducted in Room 1C36 of the environmental engineering laboratory at the University of Saskatchewan. All other experiments were conducted in a controlled low temperature environmental control

chamber (ECC) of the environmental engineering laboratory. In order to protect the computer from low temperature and moisture, it was set outside of the ECC (Figure 3.3). Figure 3.4 shows the experimental apparatus in the ECC.

Figure 3.3. Outside of ECC

The raw water sample, which was taken from the South Saskatchewan River, was stored in a 400 L tank placed in the ECC. Each time when the experiment started, the water sample was fully mixed in order to keep the consistency of the concentrations of colloidal particles and suspended solids.

Figure 3.4. Experimental apparatus in ECC

The 400 L tank was blocked up above the floor as it was found that the floor temperature within the ECC was 10 °C when air temperature was 2-3 °C (Hooge 2000).

Average water quality of the South Saskatchewan River is shown in Table 3.2 (City of Saskatoon Environmental Operations Annual Report 2001). The turbidity, particle count and pH, which are closely related to the research, were measured in each test (details in Chapter 4).

Table 3.2. Average water quality of the South Saskatchewan River
(City of Saskatoon Environmental Operations Annual Report 2001)

Characteristic	River water
Conductivity at 25°C	472 umhos/cm
pH	8.5
Turbidity	2.7 NTU
Calcium	46 mg Ca/L
Magnesium	18 mg Mg/L
M-Alkalinity	157 mg CaCO$_3$/L
P-Alkalinity	4 mg CaCO$_3$/L
Soluble Organic Carbon	3.1 mg C/L
Total Dissolved Solids	278 mg/L
Total Suspended Solids	9 mg/L
Fecal Coliform	181 CFU/100mL
Fecal Streptococcus	539 CFU/100mL
Total Coliform	377 CFU/100mL
Cryptosporidium	<1 ct/10L
Giardia	<1-24 ct/10L

Coagulants were dry aluminum sulfate and ferric sulfate. Anionic copolymer of acrylamide, which is provided by ClearTech Ltd., was chosen as a coagulant aid. It is widely used in Saskatchewan waterworks. Both coagulants and the coagulant aid were mixed with distilled water to form a standard solution. Table 3.3 shows the characteristics of the anionic copolymer of acrylamide ($CH_2=CHCONH_2$).

Table 3.3. Characteristics of anionic copolymer of acrylamide
(Provided by ClearTech Ltd., 2003)

Characteristics	Value
Water Solubility	5 g/L
Bulk Density	0.8 g/mL
Viscosity	1500 cP at 5 g/L 600 cP at 2.5 g/L 250 cP at 1.0 g/L

The water temperature could be easily adjusted to 22 °C when the water sample was placed in the environmental engineering laboratory for 1-2 days. The water temperature could be adjusted from 4 °C to 1 °C in the ECC. However, the water temperature could not be adjusted to 0 °C because the temperature of the ECC could not be adjusted to 0 °C. When the ECC temperature was close to 0 °C, the surface of the fan in the ECC was covered with ice. The fan did not work normally, and the temperature of the ECC would rise.

Through trials, an apparatus was designed and built to conduct the experiment at a water temperature of 0 °C (Figure 3.5).

The method to adjust a water temperature to 0 °C was as follows:

- The water sample of 1 °C was taken from the 400 L tank in the ECC and stored in a freezer (- 10 °C) for 15 minutes.

- Ice, which had been formed in the freezer, was used to fill in the space between the apparatus and the square batch reactor, as shown in Figure 3.5.
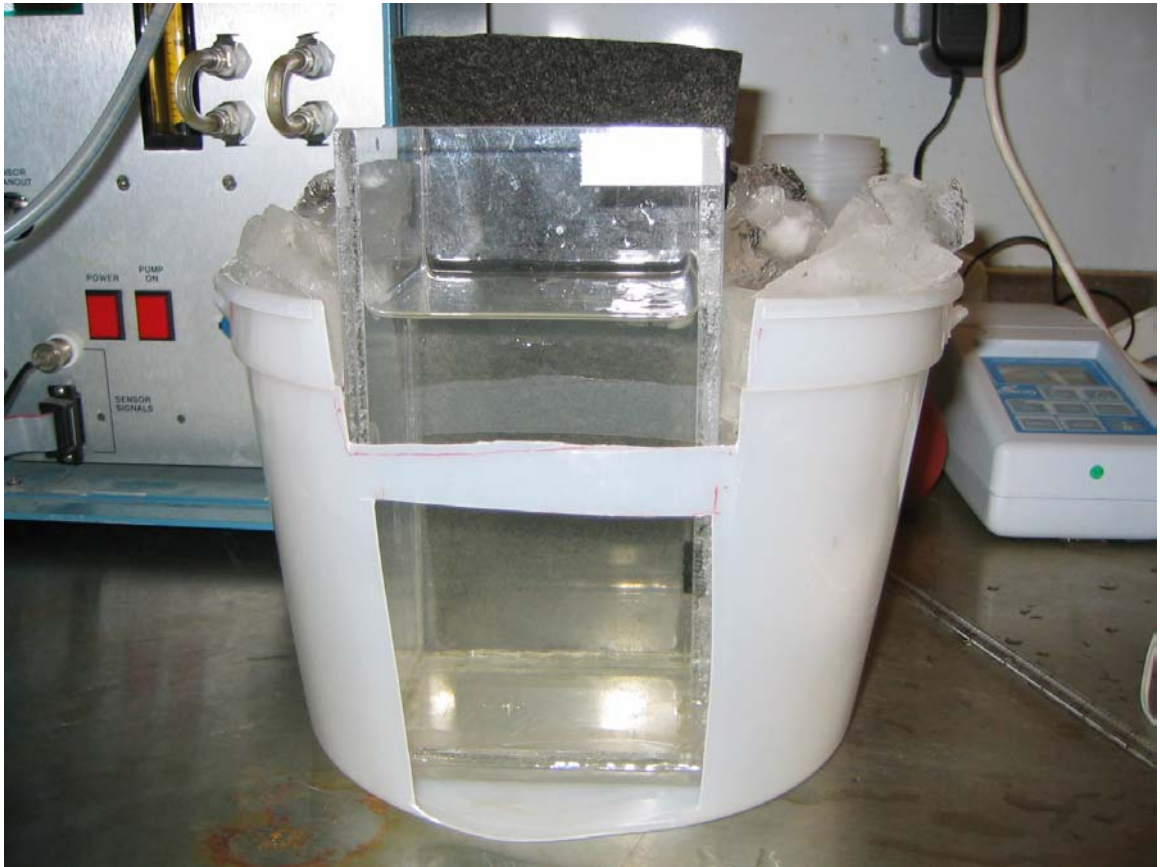
Figure 3.5. Apparatus for experiment at a water temperature of 0 °C

- The water sample was put into the square batch reactor, and mixed by the paddle stirrer for about 5 minutes at 35 rpm. The water temperature declined to 0 °C and then kept at 0 °C until the end of the flocculation process.

The experimental apparatus for experiments at a water temperature of 0 °C in the ECC

is shown in Figure 3.6.

Figure 3.6. Experimental apparatus for the experiment

at a water temperature of 0 °C in ECC

Before the camera was utilized to photograph aggregation processes, a variety of tests

were conducted with the camera control software to determine the best settings for

capturing images with good resolution, such as adjusting the position of the flash and

the camera as well as choosing the photographic parameters, like focus and shoot speed.

Clear images could be captured in the slow mixing period (35 rpm), but couldn't be obtained in the fast mixing (110 rpm) due to the fast movement of particles. Thus, the image processing was limited to the slowing mixing processes.

3.4 Analytical Instrumentation and Description

Table 3.4 summarizes the analytical instrumentation.

Table 3.4. List of analytical instrumentation

Item	Type
Particle Counter	Met One WGS-267/LB-1020 Grab Sampler, USA
Turbidimeter	HACH 2100P, Loveland, USA
Temperature	Digital Temperature Indicator, VWR Canlab
pH meter	HACH EC10
Image Enhancement Software	Adobe Photoshop Elements
Particle Analysis Software	Carnoy 2.0, Flanders-Belgium, USA

Turbidity is a unit of measurement quantifying the degree to which light traveling through a water column is scattered by suspended particulate material and soluble colored compounds in the water. It provides an estimate of the muddiness or cloudiness of the water due to clay, silt, finely divided organic and inorganic matter, soluble colored organic compounds, plankton, and microscopic organisms (Greenberg et al. 1992). Turbidity was measured in this research using the nephelometric standard method. This method is based on a comparison of the intensity of light scattered by the sample under defined conditions with the intensity of light scattered by a standard

reference suspension under the same conditions (Greenberg et al. 1992). It is an important indicator used to evaluate effectiveness of a treatment process in water treatment.

Although a turbidimeter is extensively used as an indicator to determine particulate removal effectiveness, it cannot be used to measure the reduction of particle counts and particulate size distribution. A particle counter can overcome the disadvantages of the turbidimeter. It is becoming a popular tool in the research of water treatment. The WGS-267 Particle counter shown in Figure 3.7 was utilized in the experiment and was operated by using a computer and the Universal Utility Software (UUS). The count data were uploaded into the computer. It was used to observe the variation of particle count by comparing the water quality between raw water samples and finished water samples. The size ranges (μm) of measurement are 2-5, 5-10, 10-15, 15-20, 20-40, and >40.

A high-resolution digital camera equipped with a micro lens could record the coagulation process without disturbing the floc characteristics. Based on Carnoy 2.0 particle analysis software, the sizes of particles/flocs were determined.

Figure 3.7. WGS-267 Particle counter

Before using Carnoy 2.0 particle analysis software to analyze a particle image, it was necessary to process image threshold, which converts color images to black-and-white images, by use of Adobe Photoshop software. This step could effectively filter out random noise.

In this research work, the turbidimeter and the particle counter were utilized as the basis of evaluating the treatment efficiency of coagulation/flocculation processes under various operating conditions. The advanced high pixel photography technique was used to analyze the particle change during coagulation/flocculation processes.

3.5 Experimental Parameters

The experiments were conducted using tightly controlled experimental conditions. Experimental parameters of bench-scale tests were determined based on Laboratory Manual of Simplified Procedures for Water Examination (AWWA 1977) and Handbook of Public Water Systems (Bagwell et al. 2001). The experimental parameters used in this work are summarized in Table 3.5.

Because a paddle-type mechanical flocculator was used in the research, the velocity gradients in flocculation were calculated on the basis of Equations 2.12 and 2.23. The calculation is shown in Table 3.6.

Table 3.6 shows that all G values at different temperatures were within the recommended range of 10 to 60 sec^{-1} (Table 2.3). There was a small difference among G values at low temperatures of 0 ^{o}C, 1 ^{o}C and 4 ^{o}C. The G value at 22 ^{o}C was somewhat higher. The research was intended to be consistent with other published research regarding temperature effects on flocculation kinetics where the bench-scale test was conducted using a fixed rotational speed (Kang et al. 1995). Thus, in this research, the bench-scale tests were conducted by use of a fixed rotational speed not a fixed G value.

Table 3.5. Summary of experimental parameters

Parameter	Description
Water sample	The South Saskatchewan River water
Coagulant/ Coagulant aid	$Al_2 (SO_4)_3.16H_2O$ (Dosing solution 10 g/L), $Fe_2 (SO_4)_3.9H_2O$ (Dosing solution 10 g/L), anionic copolymer of acrylamide (Dosing solution 0.2 g/L)
Temperature	Temperature 22 ± 0.5 ^oC, 4 ± 0.5 ^oC, [1]1 ± 0.5 ^oC, $0+0.5$ ^oC
Bench-scale test procedure	Fast mixing for 1.5 min (110 rpm), slow mixing for 20 min (35 rpm), and then settling 1 hr
Photography	1 sheet per 20 sec., 60 sheets per test
Analysis item	Temperature, turbidity, pH, particle count
Image analysis	Floc projected area

[1]1 ^oC of water temperature was conducted in the experiments of image-processing test, not in bench-scale test.

Table 3.6. Velocity gradients at different temperatures

T (^oC)	Density (kg/m^3)	Viscosity (N-s/m^2)	Reynolds	P (N-m/s)	G sec^{-1}
0	999.87	0.001792	1820	0.001209	26
1	999.93	0.001732	1884	0.001209	26
4	1000.00	0.001568	2081	0.001209	28
22	997.80	0.000961	3387	0.001207	35

$n = 0.58$ rps, $W_i = 0.025$ m, $D_i = 0.075$ m
$C_D = 1.2$, $v = \pi D_i n*0.75$ m/s

3.6 Experimental Procedure

3.6.1 Bench-scale Test

The typical bench-scale test procedure in this research work consisted of the following steps:

1) Using a submersible pump, fully mix the raw water stored in a 400 L tank. The water is collected from the intake of the Saskatoon Water Treat Plant. Then take the water sample out and analyze pH, turbidity and particle counts of the water sample. The volume of the water sample was based on test requirements.

2) Set the environmental control chamber (ECC) or the environmental engineering laboratory to desired temperature and allow all batch water to stabilize at desired temperature.

3) Place the six-place paddle stirrer on the illuminated test stand.

4) Use a 1000 mL graduated cylinder to place 1000 mL of raw water in each square batch reactor.

5) Place reactors 1 to 6 numbering from the left, on the test stand directly under the paddles.

6) With a pipette, add dose of coagulant solution to each reactor as rapidly as possible.

7) Turn on the stirrer motor and adjust the stirring speed to 110 rpm.

8) Continue fast mixing for 1.5 minutes at 110 rpm, and then adjust the stirred speed to 35 rpm (slow stirring) for 20 minutes.

9) Stop the stirrer motor and allow the sample to settle for one hour.

10) Use a pipette to draw 50 mL samples of treated water from the top 35 mm of each reactor.

11) Measure turbidity and pH of the treated sample.

12) Perform particle count tests by putting the intake of the particle counter into each reactor at top 35 mm of water.

13) Repeat tests at different dosages, coagulants, or temperatures.

3.6.2 Image-processing Test

In the image-processing test, a bench-scale test process was photographed by using a high-resolution camera connected to a computer. The experimental procedure of the bench-scale test was mentioned in Section 3.6.1. The procedure of the image-processing tests is as follows:

1) Fix the camera and flash in front of a square batch reactor placed on the test stand directly under the paddles.

2) Adjust and set optimum photographic conditions.

3) Connect the camera to the computer and then use the camera control software to set the parameters of shutter opening on the computer.

4) Photograph a scale which was placed in the reactor to determine the number of pixels corresponding to a given standard length.

5) Photograph entire slow mixing period of 20 minutes at the stir speed of 35 rpm.

6) Process image threshold by use of Adobe Photoshop software.

7) Using Carnoy 2.0 particle analysis software, calibrate image sizes by determining the number of pixels corresponding to a given standard length.

8) Using Carnoy 2.0 particle analysis software, analyze the captured digital images and then obtain the sizes of particles or flocs.

9) Evaluate the aggregation process by analyzing and comparing the characteristics of the particles or flocs.

10) Repeat tests at different coagulants, dosages, or temperatures.

3.6.3 Image Threshold Analysis

Processing image threshold is to convert a color image to a black-and-white image with the use of Adobe Photoshop software, on the basis of different light intensities of the matters. By setting a threshold level, focused flocs are converted to white, and unfocused flocs and background are converted to black. In the analysis of image threshold, an image was divided into two sections, and the analysis was conducted using 70% of each section. This was done for two reasons: (1) a large image file of 35 MB caused the computer to freeze frequently during the subsequent use of Carnoy 2.0 particle analysis software, however, when analyzing 70% of each section, the particle analysis could be conducted normally; (2) the analysis results could be compared between the two sections. The precision of average projected area of flocs should be kept at ± 5%, otherwise, the threshold analysis had to be redone until the required precision was met. The procedure of the image threshold analysis in this research consisted of the following steps:

1) Choose an image photographed at 3 minutes of slow mixing, and adjust the threshold level to ensure that more than 95% of focused particles or flocs are in

white areas and more than 95% of unfocused particles or flocs are in black areas.

2) Choose an image photographed at 20 minutes of slow mixing, and repeat step 1, obtaining another threshold level.

3) Set a threshold level based on two levels obtained from step 1 and 2 to ensure that more than 90% of focused particles or flocs are in white areas and more than 90% of unfocused particles or flocs are in black areas.

4) Compare the threshold image and real image, and manually adjust non-conforming flocs. For example, adjust focused flocs whose edges are filtered out, and unfocused flocs which are not filtered out due to some bright spots.

5) Convert the image to black-and-white color using the threshold determined from steps 3 and 4.

Chapter 4 – Test Results And Discussion

4.1 Overview

Three series of bench-scale tests were conducted at water temperatures of 22 ^{o}C, 4 ^{o}C and 0 ^{o}C, and seven groups of image-processing tests were conducted at water temperatures of 22 ^{o}C, 4 ^{o}C, 1 ^{o}C and 0 ^{o}C. Other operating parameters that varied from test to test included the dosages and types of coagulants (aluminum sulfate, ferric sulfate, and anionic copolymer of acrylamide). A summary of the test conditions for each test run is shown in Table 4.1a and b. The dosages of the coagulants in Table 4.1b were determined based on both residual turbidities and particle count residuals of the treated water in the aforementioned three bench-scale tests.

The raw water was collected from the intake of Saskatoon Water Treatment Plant (SWTP) on October 21st and 23rd, 2003. The water was stored in a 400 L tank in the environmental control chamber (ECC) at a temperature of 4 °C or less. It was well mixed by use of a submersible pump before every test. The turbidity of the water ranged from 9.5 to 10.7 NTU and the pH was from 8.35 to 8.5. Because the sampling locations of the raw water were different between the SWTP and this research, the turbidity was different between them. Figure 4.1 shows the average distribution of the particle size of the duplicate raw water samples. The size distribution of particles in the raw water indicated that around 73% of the total particle counts was in the 2-10 μm size range.

Table 4.1a. Test run summary (Bench-scale tests)

Test run No.	Temp. (^{o}C)	Initial Turb. (NTU)	Initial Particle count (#/100mL)	[1]Coagulant	[2]Dosage range (mg/L)
1	22, 4 and 0	10.7	1,400,000	AS	0.5-100
2	22, 4 and 0	9.5	1,229,000	FS	0.5-100
3	22, 4 and 0	10.7	1,400,000	JC polymer	0.02-1.6

[1]AS – aluminum sulfate; FS –ferric sulfate; JC polymer – water-soluble charged anionic copolymer of acrylamide as a coagulant aid, together with a fixed AS dosage of 50mg/L

[2]For specific dosage values, refer to Section 4.1

Table 4.1b. Test run summary (Image-processing tests)

Test run No.	Temp. (^{o}C)	Coagulant	Dosage (mg/L)
4	22, 4, 1 and 0	AS	50
5	22, 4, 1 and 0	AS	20
6	22, 4, 1 and 0	AS	5
7	22, 4, 1 and 0	FS	50
8	22, 4, 1 and 0	FS	20
9	22, 4, 1 and 0	FS	5
10	22, 4, 1 and 0	JC Polymer	*0.2/1.4

* Polymer dosages: 0.2 mg/L at 22 ^{o}C & 4 ^{o}C, and 1.4 mg/L at 1 ^{o}C & 0 ^{o}C

Initial turbidity: 10.5 NTU. Initial particle count: 1,115,000 (#/100 mL)
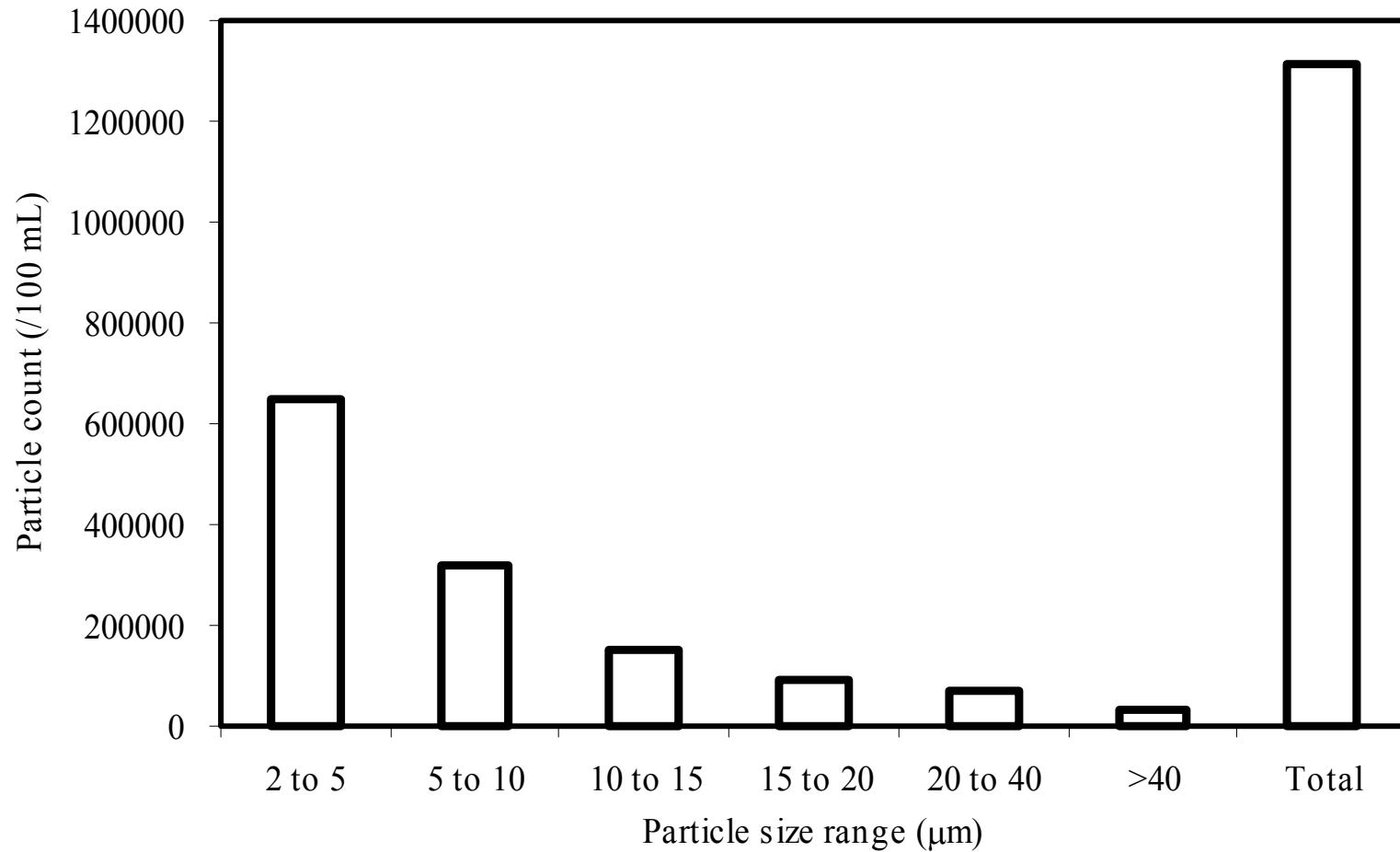
Figure 4.1. Particle size distribution of the South Saskatchewan River Water
(Collected from the intake of the Saskatoon Water Treatment Plant)
(Average duplicate samples on Oct. 23 and Nov. 03, 2003)

In each of the image-processing tests, sixty images of the flocculation process were captured and stored in the computer. Floc projected area was measured by use of Carnoy 2.0 particle analysis software. Then, the average projected areas of the flocs were calculated, and the projected-area distributions of the flocs were obtained by using histogram analysis software.

A systematic method based on the bench-scale test, floc size analysis, flocculation kinetics and image observation was formed to evaluate the aggregation processes. The treatment efficiencies at different temperatures were obtained based on the bench-scale test. Floc size analysis described floc growth with increasing time and floc size change with different temperature or coagulant dosage. Floc size analysis included the average projected area and the distribution of the projected area. An analysis of flocculation kinetics described the performance of floc aggregation and breakup. Image observation demonstrated the process of floc formation. The results and discussion are presented in the remaining sections of this chapter.

4.2 Bench-scale Tests

Bench-scale tests were conducted by adding different types and dosages of coagulants into the water. Duplicate tests were conducted, and all of the results were averaged based on the duplicate tests.

The first bench-scale test was conducted in the water treated with different dosages of aluminum sulfate (0.5, 5, 10, 20, 40, 50, 60, 65, 80, and 90 mg/L). The residual

turbidity and the particle count residuals at 22 °C, 4 °C, and 0 °C are shown in Figures 4.2 and 4.3, respectively.

Figure 4.2 illustrates that residual turbidities tended to decrease with increasing AS dosages, but the turbidities began to level off after the point of 20 mg/L of AS dosage. A dosage greater than 50 mg/L resulted in marginal gains in treatment efficiency. The turbidities tested at 22 °C were close to those tested at 4 °C under the same AS dosage conditions. Both of them were lower than those tested at 0 °C.

Figure 4.3 shows that particle count residuals declined with increasing AS dosages, but the particle count residuals began to level off after the point of 40 mg/L of AS dosage at 22 ^{o}C and after 20 mg/L at 4 ^{o}C and 0 ^{o}C. A dosage greater than 50 mg/L resulted in marginal gains in treatment efficiency. The results between Figures 4.2 and 4.3 are consistent.

The second bench-scale test was conducted in the water treated with ferric sulfate (0.5, 5, 10, 20, 30, 40, 50, 60, 70, 80, 90, and 100 mg/L). Figure 4.4 presents the relationship between residual turbidity and FS dosage at different water temperatures. The relationship between the particle count residual and FS dosages at different water temperatures is shown in Figure 4.5. Figure 4.4 indicates that residual turbidity decreased with increasing FS dosages. The residual turbidity started to level off after the point of 20 mg/L of FS dosage.
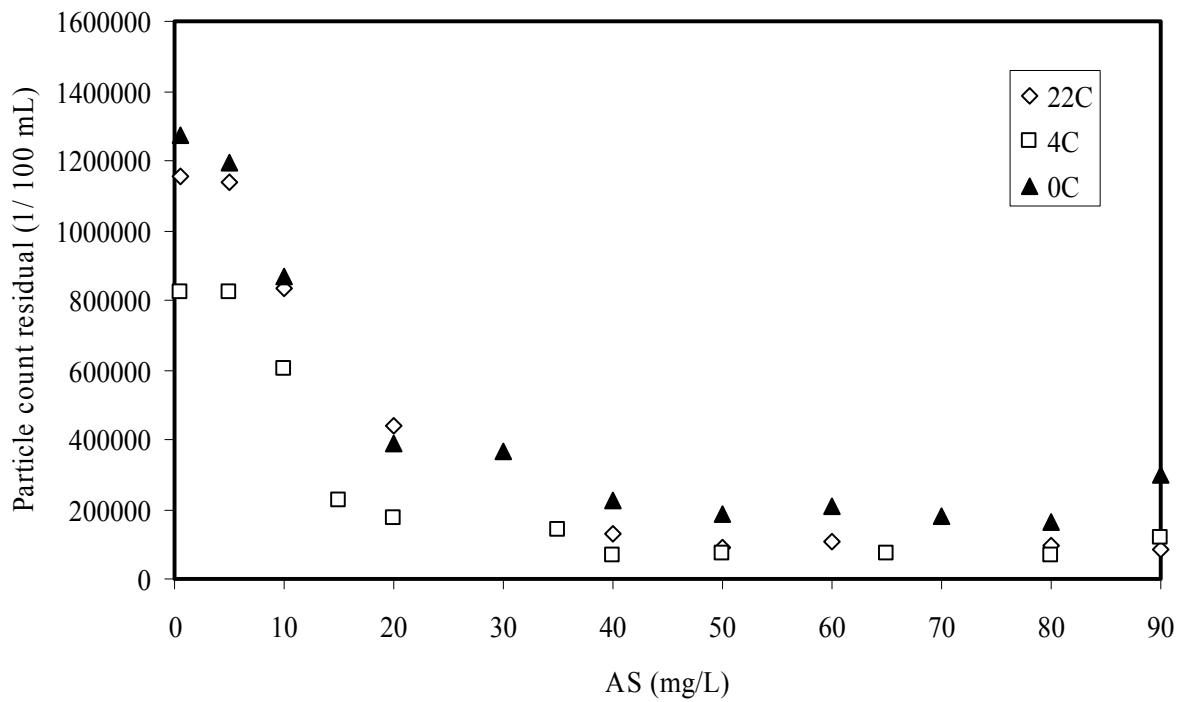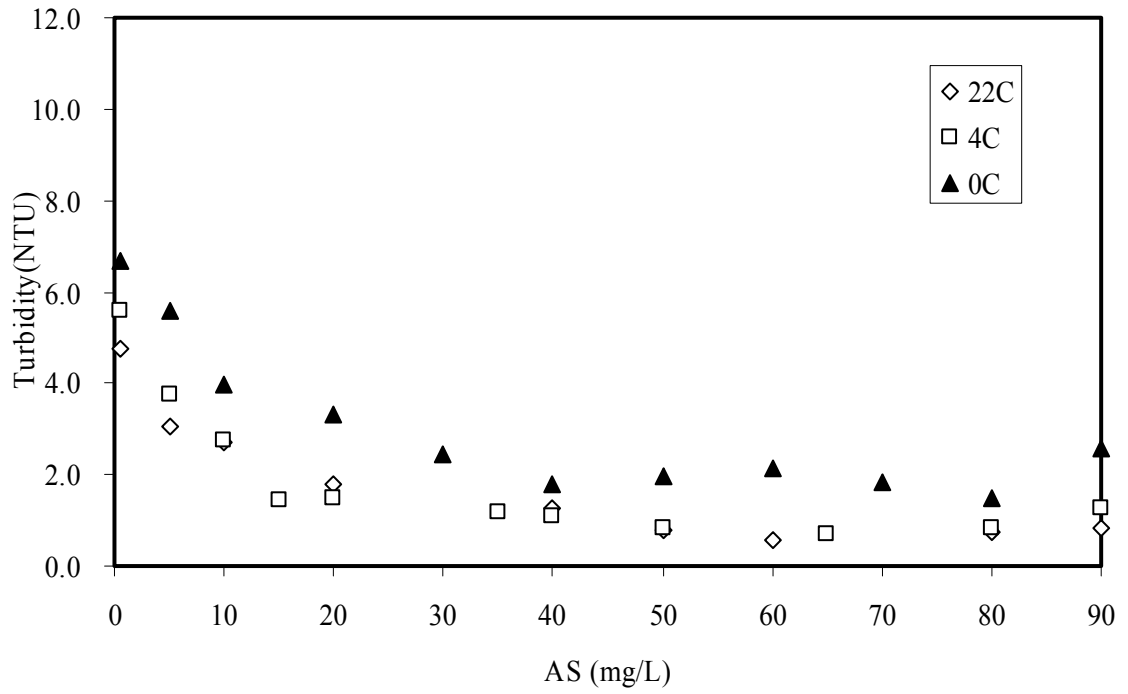
Figure 4.3. Particle count residual vs AS dosage
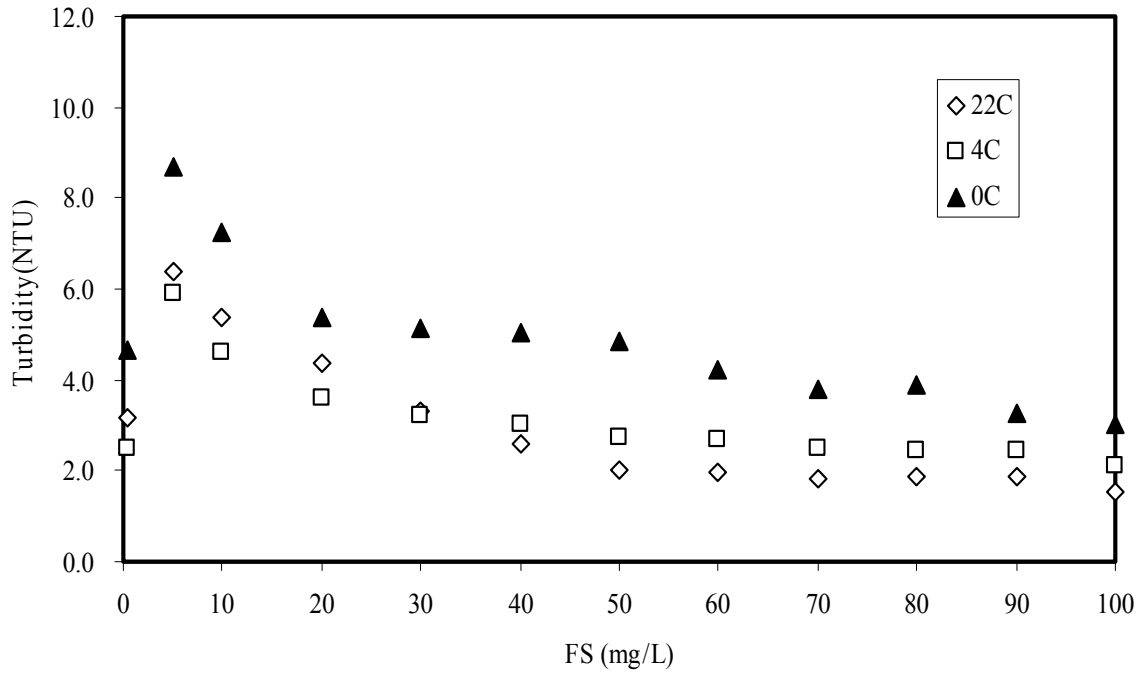
Figure 4.4. Residual Turbidity vs FS dosage
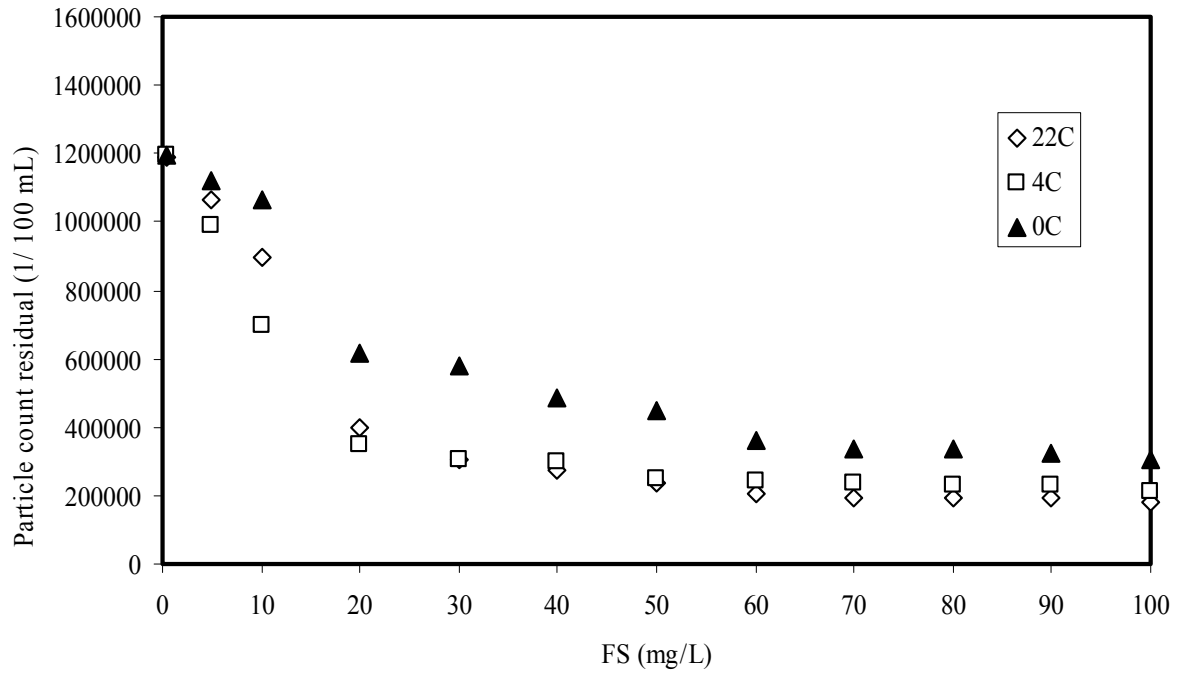
Figure 4.5. Particle count residual vs FS dosage

When the dosage was more than 40 mg/L, the residual turbidities tested at 0 °C were higher than those tested at 22 °C and 4 °C, with the turbidities at 22 °C being the lowest. A FS dosage greater than 50 mg/L resulted in marginal gains in treatment efficiency.

Figure 4.5 shows that particle count residuals declined with increasing FS dosages. The particle count residuals began to level off after the point of 20 mg/L of FS dosage. The turbidities tested at 22 °C were close to those tested at 4 °C under the same FS dosage conditions. Both of them were lower than those tested at 0 °C. The results between Figures 4.4 and 4.5 are consistent.

The third bench-scale test was conducted in the water treated with JC polymer. JC polymer was anionic copolymer of acrylamide (0.02-1.6 mg/L) as a coagulant aid together with AS coagulant (a fixed dosage of 50 mg/L). Table 4.2 lists the test results with different polymer dosages at 22 °C, 4 °C, 1 °C and 0 °C.

Table 4.2 indicates that floc count decreased more than 80% after 3 minutes of slow mixing at water temperatures of 22 °C, 4 °C and 1 °C. However, a higher dosage of polymer was required to cause such a decrease in the floc count as water temperature decreased. The dosages were 0.04, 0.15 and 0.6 mg/L at 22 °C, 4 °C, and 1 °C, respectively. When the water temperature was close to 0 °C, there was no such decrease in the floc count, even though the polymer dosage of 1.6 mg/L was added. Thus, the

polymer did not significantly change the coagulation/flocculation process when the

water temperature was close to 0 °C.

Table 4.2. Bench-scale tests at different temperatures

Temp. (^{o}C)	JC polymer (mg/l)	Turb. (NTU)	Particle count (#/100 mL)	Change of floc count
22	0.02	0.9	116500	No evidence
	0.04	1.0	125500	
	0.06	0.8	109500	
	0.10	0.9	122000	
	0.14	0.8	89500	*Swift decrease of floc count
	0.18	0.9	96000	
	0.20	0.7	88000	
	0.40	0.7	86500	
	0.60	0.9	116000	
	1.00	0.9	110000	
4	0.02	0.7	98500	
	0.06	1.0	108000	No evidence
	0.10	0.8	94500	
	0.15	0.7	74000	
	0.20	0.7	72500	*Swift decrease of floc count
	0.40	1.0	119500	
	1.00	0.7	78500	
1	0.10	2.0	286500	
	0.20	2.1	274000	No evidence
	0.40	1.6	200500	
	0.60	0.9	98000	
	0.80	1.1	156000	*Swift decrease of floc count
	1.00	0.9	106000	
	1.40	0.9	111500	
	1.60	1.0	122500	
0	0.60	2.4	310500	
	0.70	1.7	206000	
	0.80	2.1	252500	No evidence
	1.00	1.9	218000	
	1.40	1.6	178000	
	1.60	1.7	180000	

*Swift decrease of floc count: more than 80% of decrease in floc count after 3 minutes of slow mixing.

Figures 4.6a and 4.6b, plotted from Table 4.2, show that residual turbidities and particle count residuals varied with JC polymer dosages. At 22 °C and 4 °C, the dosage change of the polymer didn't cause significant turbidity and particle count variation. The turbidities and particle count residuals declined with the increased polymer dosages at 1 °C and 0 °C.

Table 4.3 outlines that residual turbidities and particle count residuals varied with JC polymer dosages under different settling time at 22 °C. It demonstrates that 20 minutes of settling time was insufficient when no polymer was added because there were high residual turbidity of 2.1 NTU and particle count of 275,000 #/100 mL, but enough when the polymer was added (1.0 NTU of turbidity and 124,000 #/100 mL of particle count or less). Therefore, the settling time could be greatly decreased when the polymer was added. The particle count residuals after 60 minutes were somewhat lower than those after 20 minutes with JC polymer.

Table 4.3. Turbidity after different settling time at 22 $^{\circ}$C

JC Polymer	60 min settling		20 min settling	
(mg/l)	Turbidity (NTU)	Particle count (#/100 mL)	Turbidity (NTU)	Particle count (#/100 mL)
0.00	0.8	120000	2.1	275000
0.18	0.9	96000	1.0	121500
0.20	0.7	88000	0.7	98000
0.40	0.7	86500	0.7	103000
0.60	0.9	116000	1.0	124000
1.00	0.9	110000	0.9	118000
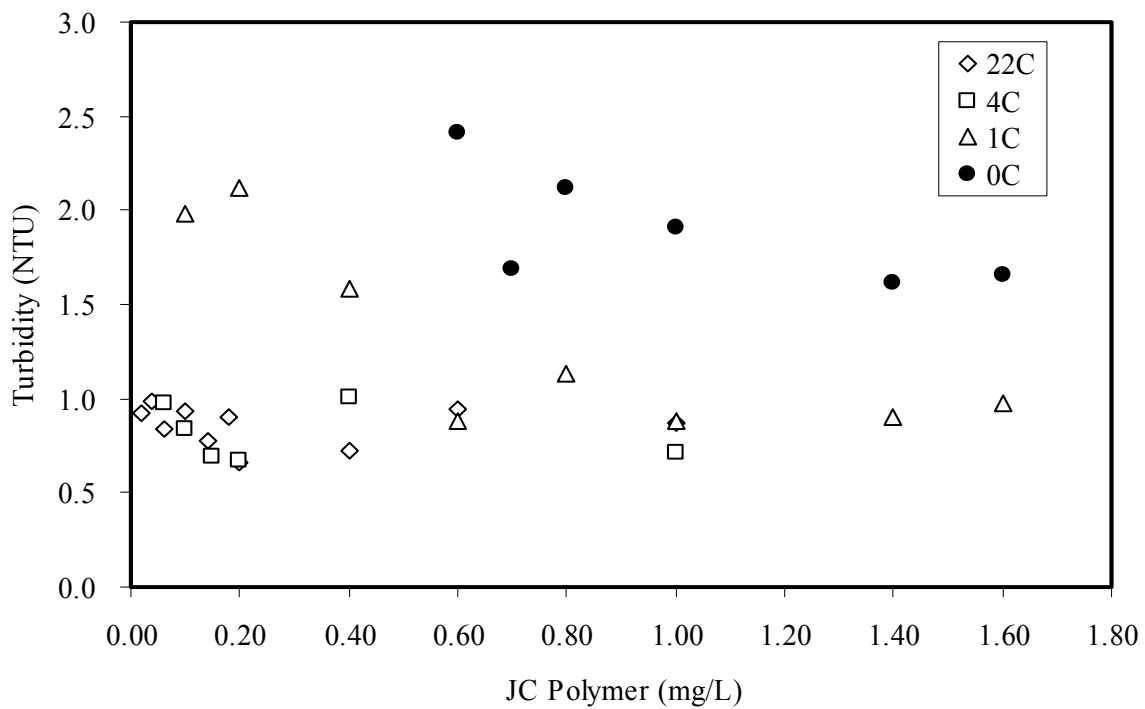
Figure 4.6a. Residual turbidity vs. polymer dosage
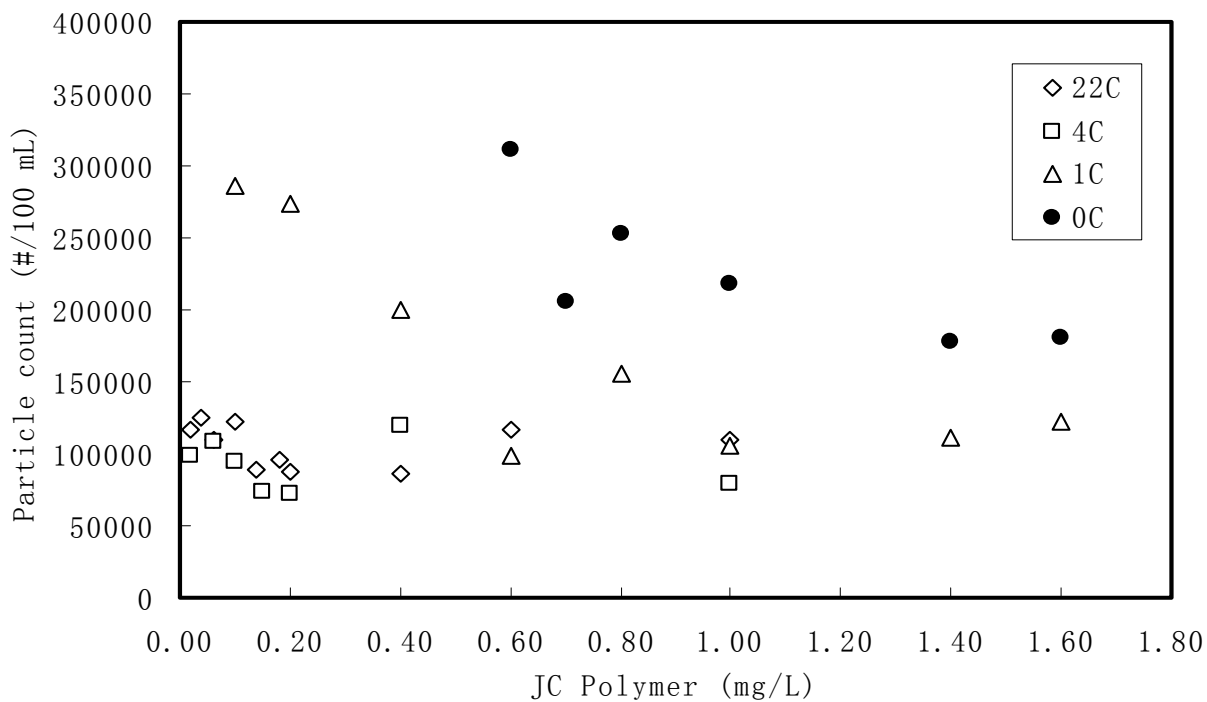
Figure 4.6b. Particle count vs. polymer dosage

4.3 Floc Size Analysis

Seven groups of image-processing tests were conducted in water treated with different types and dosages of coagulants. The following floc size analysis was based on the image photographed after 3, 5, 10, 15 and 20 minutes of slow mixing. The image analysis was conducted based on four equal time periods of 5 minutes each (5, 10, 15 and 20 minutes) because floc size changes were evident at each 5 minutes interval during image observation. The image analysis after 3 minutes was necessary, as floc count decreased more than 80 % after only 3 minutes when JC polymer was added at 22 $^{\circ}$C, 4 $^{\circ}$C and 1 $^{\circ}$C.

4.3.1   AS Tests

4.3.1.1 Analysis of Floc Average Projected Area

The floc average projected area is given as

[4.1] $$S_{average} = \frac{\Sigma_{i=1}^{n} S_i}{n}$$

where:

$S_{average}$ = floc average projected area (μm^2)

n   = floc count

S_i = projected area of floc i (μm^2)

Figure 4.7 exhibits the evolution of the average projected area of the flocs in the water treated with AS dosages of 50, 20 and 5 mg/L, respectively. In the water treated with AS dosages of 50 and 20 mg/L, the average projected area tended to decline with decreasing water temperature, but the average projected areas at 1 $^{\circ}$C were close to

those at 4 °C. For instance, at the end of the slow mixing, the average projected areas in the water treated with AS at 50 mg/L at 0 °C, 1 °C, 4 °C, and 22 °C were $47*10^3$, $82*10^3$, $89*10^3$ and $143*10^3$ μm^2, respectively.

The average projected areas in the water treated with an AS dosage of 50 mg/L were over 1.3 and 5.5 times larger than those with AS at 20 and 5 mg/L, respectively, after 5 minutes of slow mixing. Thus, the average projected area decreased as the AS dosage reduced.

The average projected area increased with time when the water was treated with AS at 50 and 20 mg/L. However, the floc growth at 0 °C was slower than that at 1 °C, 4 °C, and 22 °C with the growth at 22 °C being fastest.

An AS dosage of 5 mg/L or less produced poor coagulation/flocculation results regardless of the temperature tested. The average projected area was similar at different temperatures, and the variation of the average projected area was small with increasing time. The average projected areas of the flocs at 0 °C, 1 °C, 4 °C, and 22 °C after 20 minutes of flocculation time were $4*10^3$, $4*10^3$, $5*10^3$ and $3*10^3$ μm^2, respectively, while the average projected area of the particles in the raw water was $2*10^3$ μm^2.
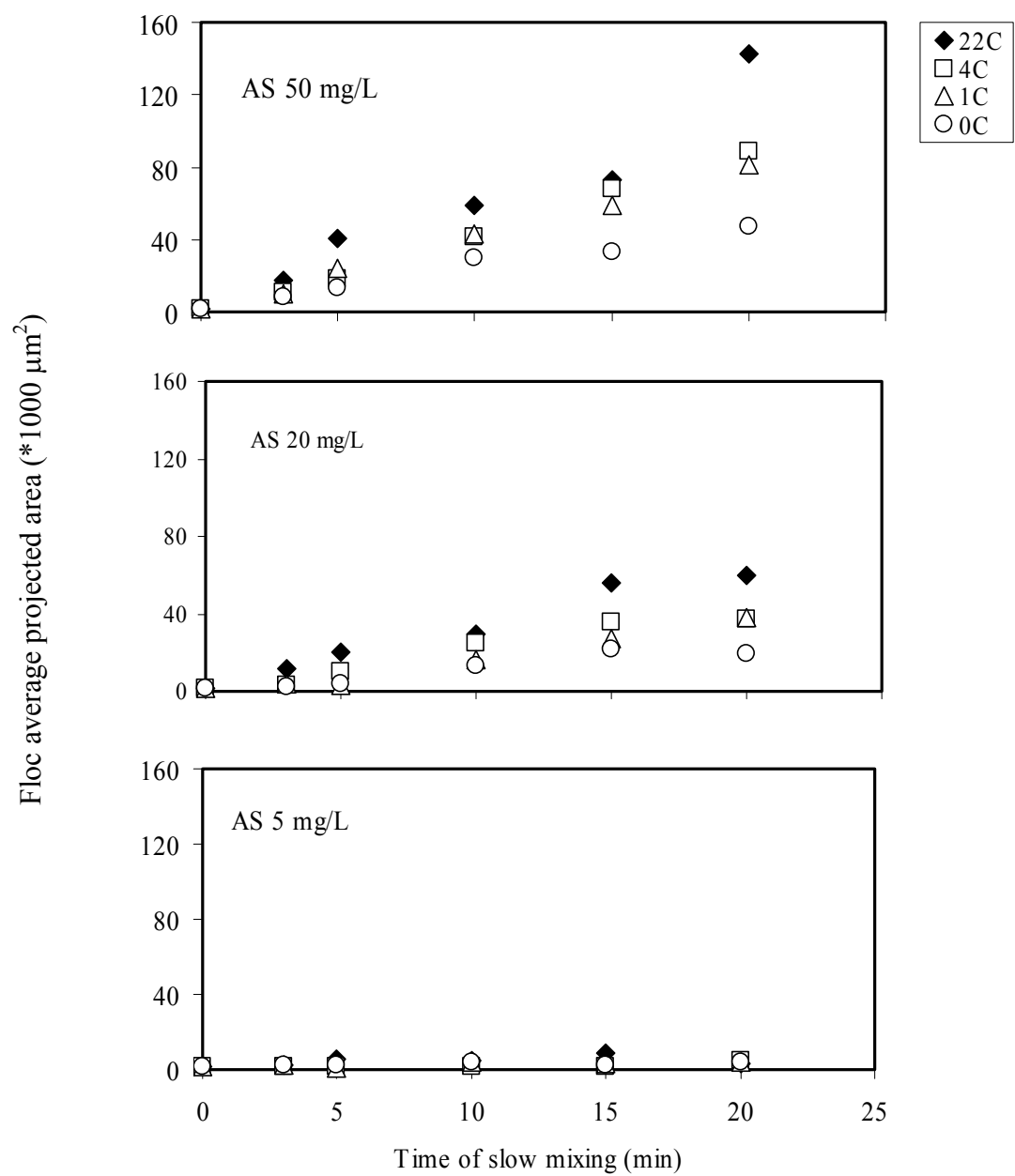
Figure 4.7. Floc average projected-area versus time with AS

77

4.3.1.2 Analysis of Floc Projected-area Distribution

The projected-area distributions of the flocs in the water treated with AS dosages of 50, 20 and 5 mg/L are plotted in Figures 4.8, 4.9 and 4.10, respectively. The projected area cited in the figures was the midpoint of the range. A peak location in the distribution was the position where there was the largest percentage of floc count.

1) Floc size change (comparison under the same time condition)

Firstly, in the water treated with AS at 50 and 20 mg/L, increasing temperature shifted the distribution of projected area into the larger sizes. Under the same time conditions (after 10 minutes), the projected areas at the peak locations at 0 °C were smaller than those at 22 °C, 4 °C and 1 °C with the values at 22 °C being the largest. The projected areas at the peak locations at 4 °C were similar to those at 1 °C. As seen in Figure 4.8, at the end of slow mixing, the projected area at the peak location at 0 °C was $45*10^3$ μm^2 while the values at 1 °C, 4 °C and 22 °C were $65*10^3$, $85*10^3$, and $145*10^3$ μm^2, respectively.
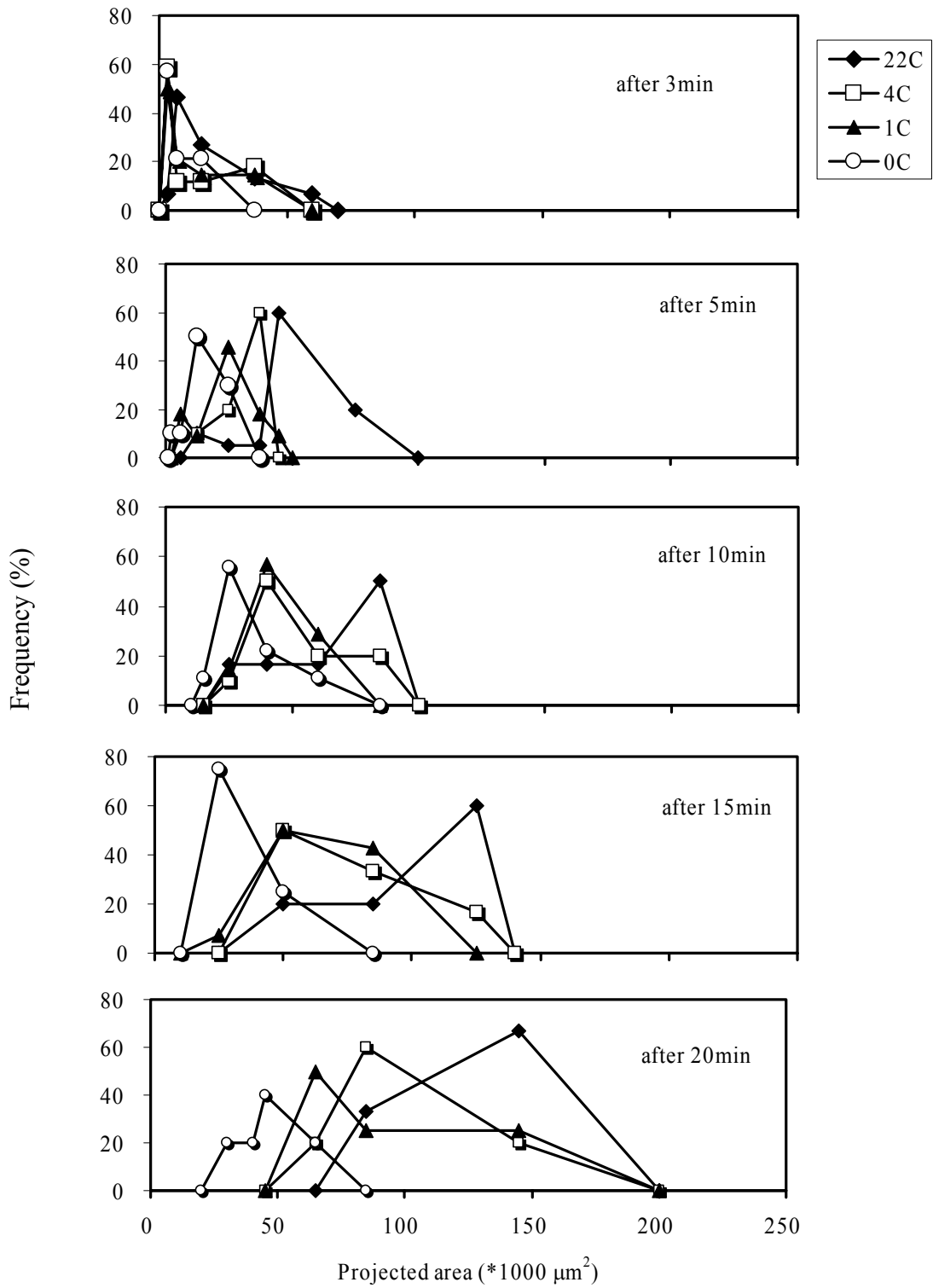
Figure 4.8. Floc projected-area distribution with AS at 50 mg/L
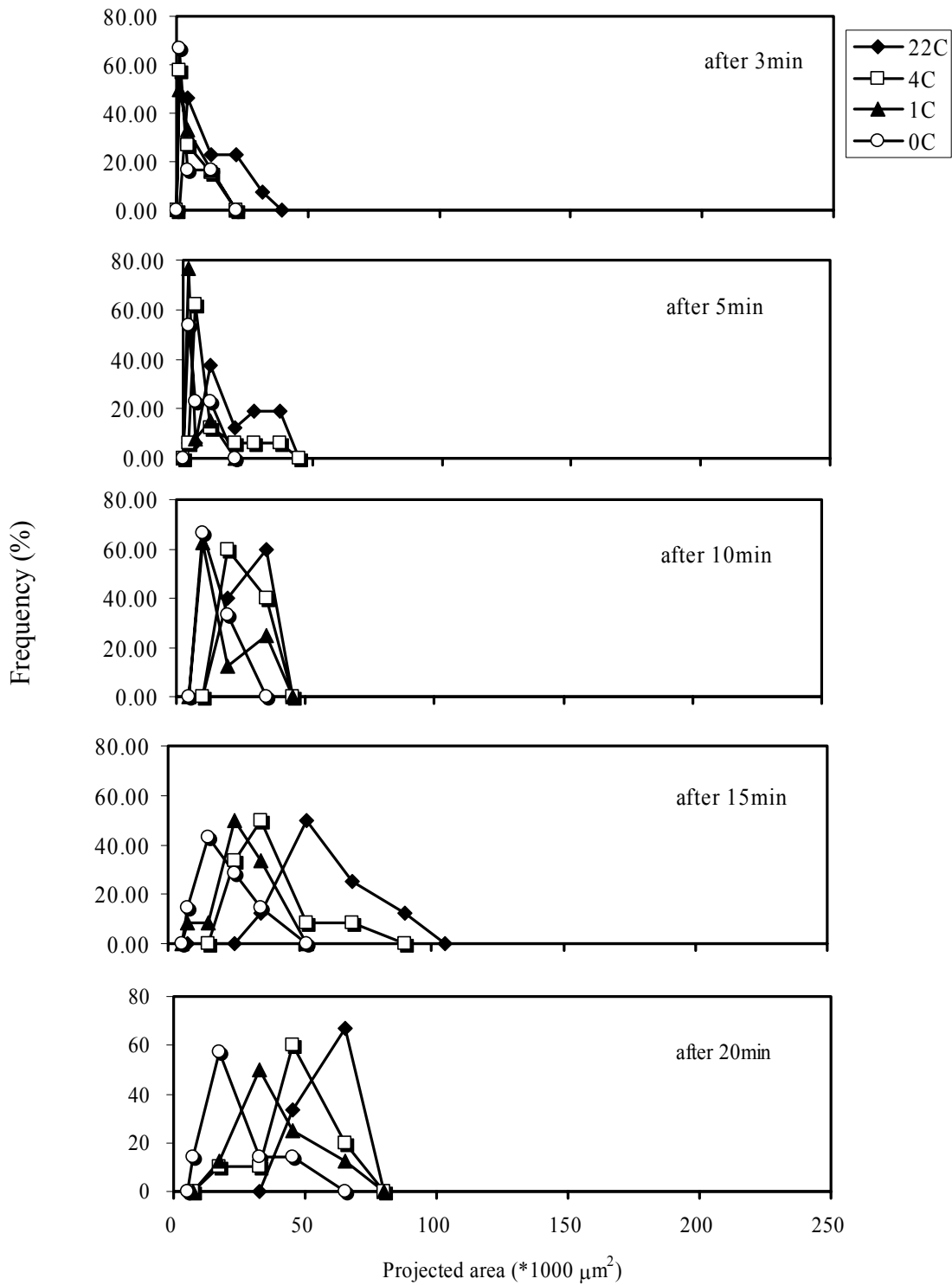
Figure 4.9. Floc projected-area distribution with AS at 20 mg/L
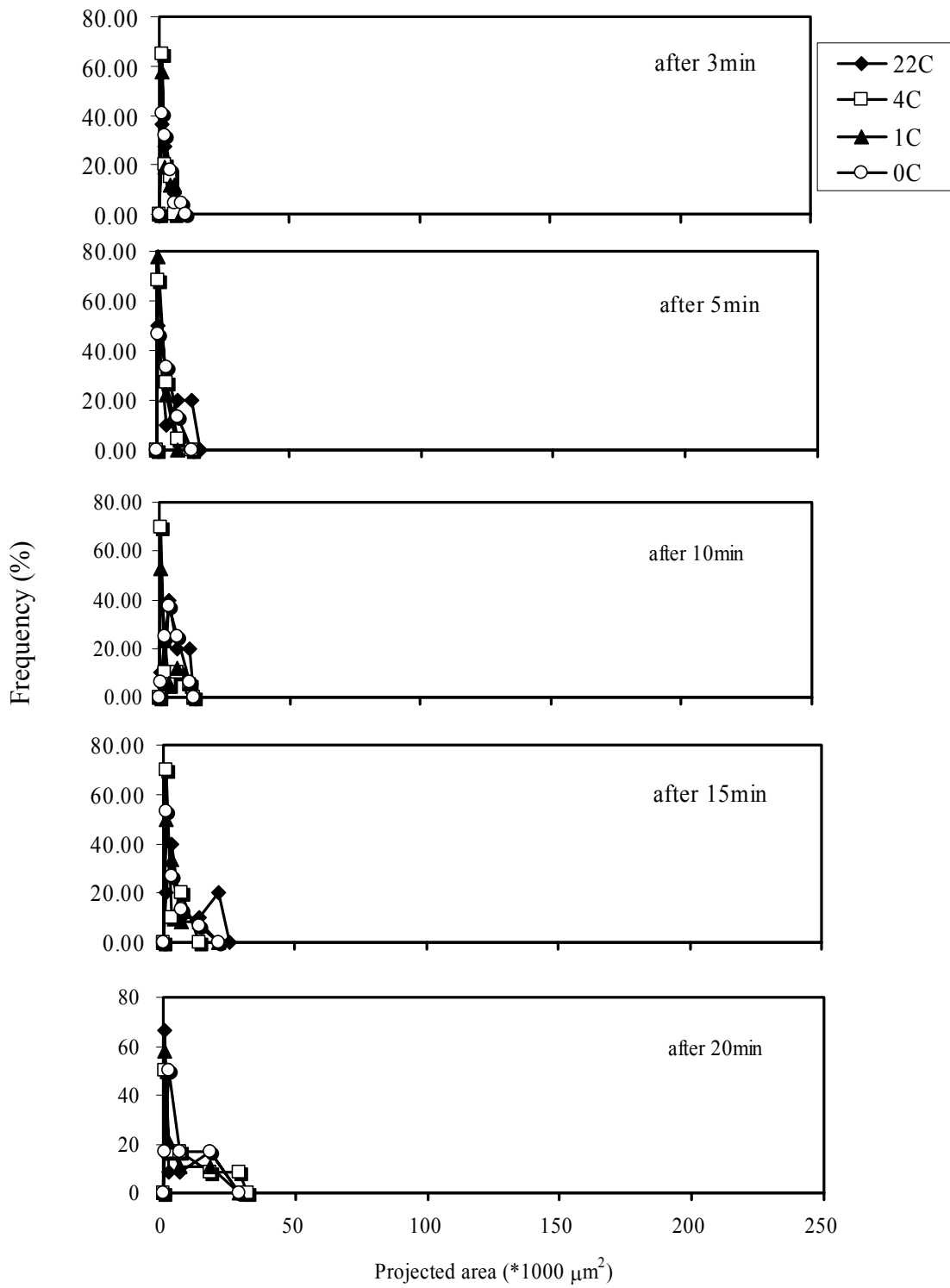
Figure 4.10. Floc projected-area distribution with AS at 5 mg/L

Secondly, decreasing dosage reduced the overall projected areas of the flocs, shifting the entire projected-area distribution into the smaller sizes. The projected areas at the peak locations in the water treated with AS at 50 mg/L were over 1.4 times larger than those with AS at 20 mg/L after 5 minutes of slow mixing. Spicer and Pratsinis (1996) obtained similar result when their polystyrene suspension was treated with various alum concentrations. However, the result conflicted with the research by Morris and Knocke (1984) who stated that increasing alum dosage at low temperature actually reduced the size of the coagulated flocs. The result obtained with the use of a particle size analyzer by Morris and Knocke may not represent the real situation.

Thirdly, an AS dosage of 5 mg/L resulted in small change of floc size. All of the projected areas at the peak locations at 22 °C, 4 °C, 1 °C and 0 °C were less than $4*10^3$ μm^2 in the entire aggregation processes. The projected areas at the peak locations didn't shift to larger size classes with increasing temperature (in comparison with $2*10^3$ μm^2 of average projected area of the particles in the raw water).

2) Floc growth

The average movement rate of the peak location, which expresses the rate of floc growth, is defined as follows:

[4.2] $$R = \frac{A_2 - A_1}{t_2 - t_1}$$

where:

R $\quad$ = rate of floc growth (μm^2/min)

A_1 $\quad$ = projected area at the peak location at t_1 time (μm^2)

A_2 = projected area at the peak location at t_2 time (μm^2)

t_1, t_2 = time of slow mixing (min)

Clearly, low temperature caused slow floc growth. In the water treated with AS at 50 and 20 mg/L, there was a very fast movement of the projected-area distribution towards larger size classes at 22 °C, while this movement was slow at 0 °C. The movement at 4 °C was similar to the movement at 1 °C. For example, in the water treated with AS at 50 mg/L, the rates of floc growth, R, in the period of 3 to 20 min of slow mixing were $10*10^3$, $7*10^3$, $5*10^3$ and $3*10^3$ μm^2/min at 22 °C, 4 °C, 1 °C and 0 °C, respectively.

The floc growth rates in the water treated with AS at 50 mg/L were larger than the rates with AS at 20 mg/L. For instance, the floc growth rates in the water treated with AS at 50 and 20 mg/L at the water temperature of 22 ^{o}C were $10*10^3$ and $4*10^3$ μm^2/min, respectively.

In the water treated with AS at 5 mg/L, the variation of the projected-area distributions with time was slight. The impact of water temperature on floc growth was small. An AS dosage of 5 mg/L resulted in poor floc growth.

4.3.2 FS Tests

4.3.2.1 Analysis of Floc Average Projected Area

Figure 4.11 shows the evolution of the average projected areas of the flocs in the water treated with FS dosages of 50, 20 and 5 mg/L, respectively. Firstly, in the water treated

with FS at 50 and 20 mg/L, the average projected area decreased as water temperature reduced. For example, after 20 minutes of slow mixing, the average projected areas in the water treated with FS at 50 mg/L at 0 °C, 1 °C, 4 °C, and 22 °C were $32*10^3$, $79*10^3$, $101*10^3$ and $142*10^3$ μm^2, respectively.

Secondly, the average projected area declined with decreasing FS dosage. The average projected areas in the water treated with a FS dosage of 50 mg/L were over 1.4 and 4.8 times larger than those with 20 and 5 mg/L, respectively after 5 minutes of slow mixing.

Finally, when the FS dosage was 5 mg/L, all of the average projected areas were small, no matter what water temperature was. The results were similar to those with AS at 5 mg/L. The average projected areas at 0 °C, 1 °C, 4 °C, and 22 °C after 20 minutes of slow mixing were $5*10^3$, $6*10^3$, $6*10^3$ and $14*10^3$ μm^2, respectively. The biggest value of $14*10^3$ μm^2 at 22 °C was much smaller than $79*10^3$ and $142*10^3$ μm^2 with 20 and 50 mg/L, respectively.
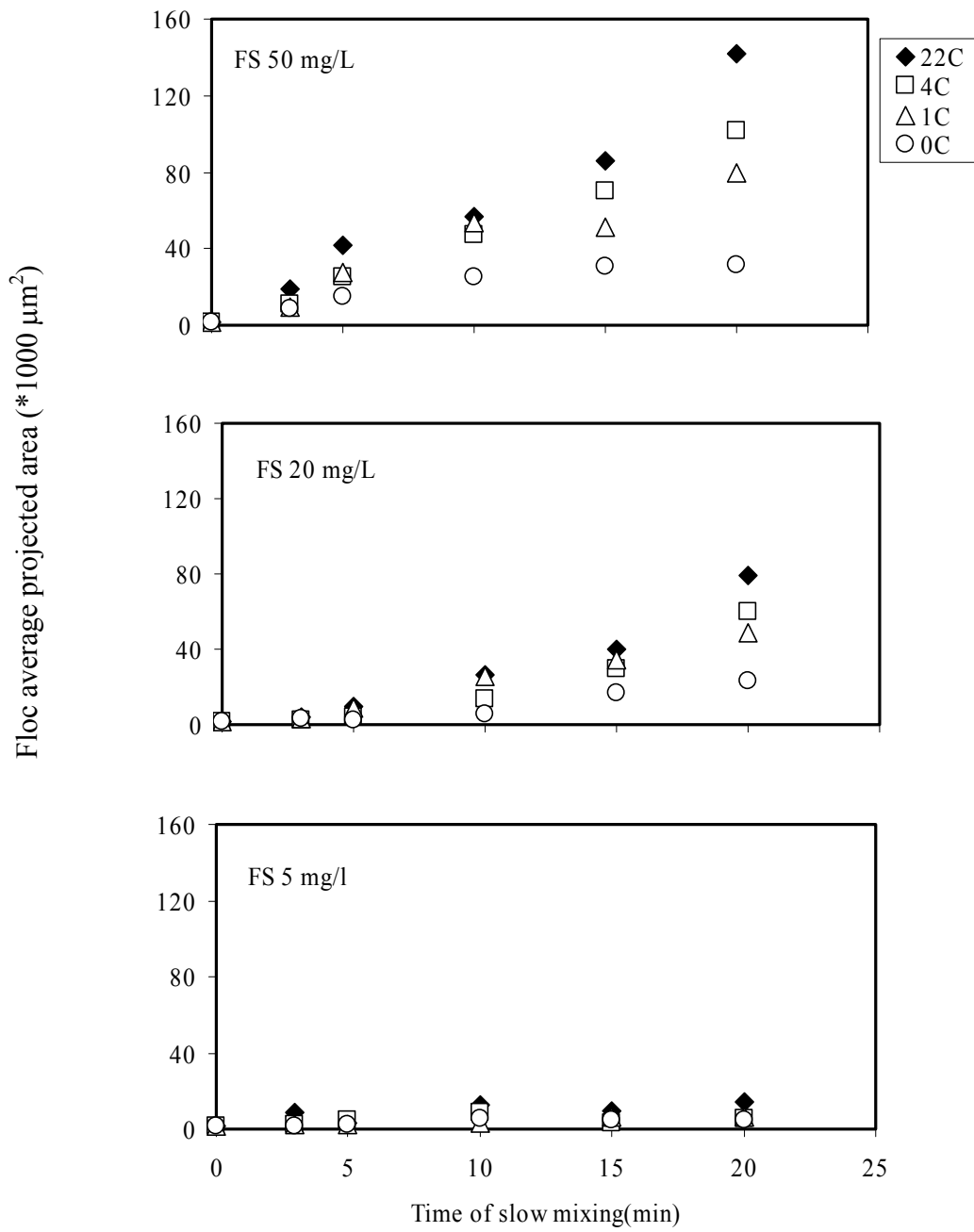
Figure 4.11. Floc average projected-area versus time with FS

4.3.2.2 Analysis of Floc Projected-area distribution

Figures 4.12, 4.13 and 4.14 demonstrate that the projected-area distributions of the flocs at different temperatures in the water treated with FS dosages of 50, 20 and 5 mg/L, respectively.

1) Floc size change (comparison under the same time condition)

As seen in Figures 4.12 and 4.13, the projected area distribution moved to the smaller sizes with decreasing water temperature. In the water treated with the FS dosage of 50 mg/L, the projected area at the peak location at 0 °C after 20 minutes was $35*10^3$ μm^2, while the values at 1 °C, 4 °C and 22 °C were $60*10^3$, $90*10^3$, and $150*10^3$ μm^2, respectively.

Decreasing dosage reduced the large tail of the projected-area distribution and decreased the overall projected area, shifting the entire projected-area distribution into the smaller sizes. The projected areas at the peak locations in the water treated with FS at 50 mg/L were over 1.0 times larger than those with FS at 20 mg/L after 5 minutes of slow mixing.

Figure 4.14 indicates that in the water treated with the FS dosage of 5 mg/L, with increasing temperature, the projected areas at the peak locations didn't shift to larger size classes. All of the projected areas at the peak locations at 22 °C, 4 °C, 1 °C and 0 °C were less than $6*10^3$ μm^2 , while the average projected area of the particles in the raw water was $2*10^3$ μm^2. Thus, the change of floc size was small.
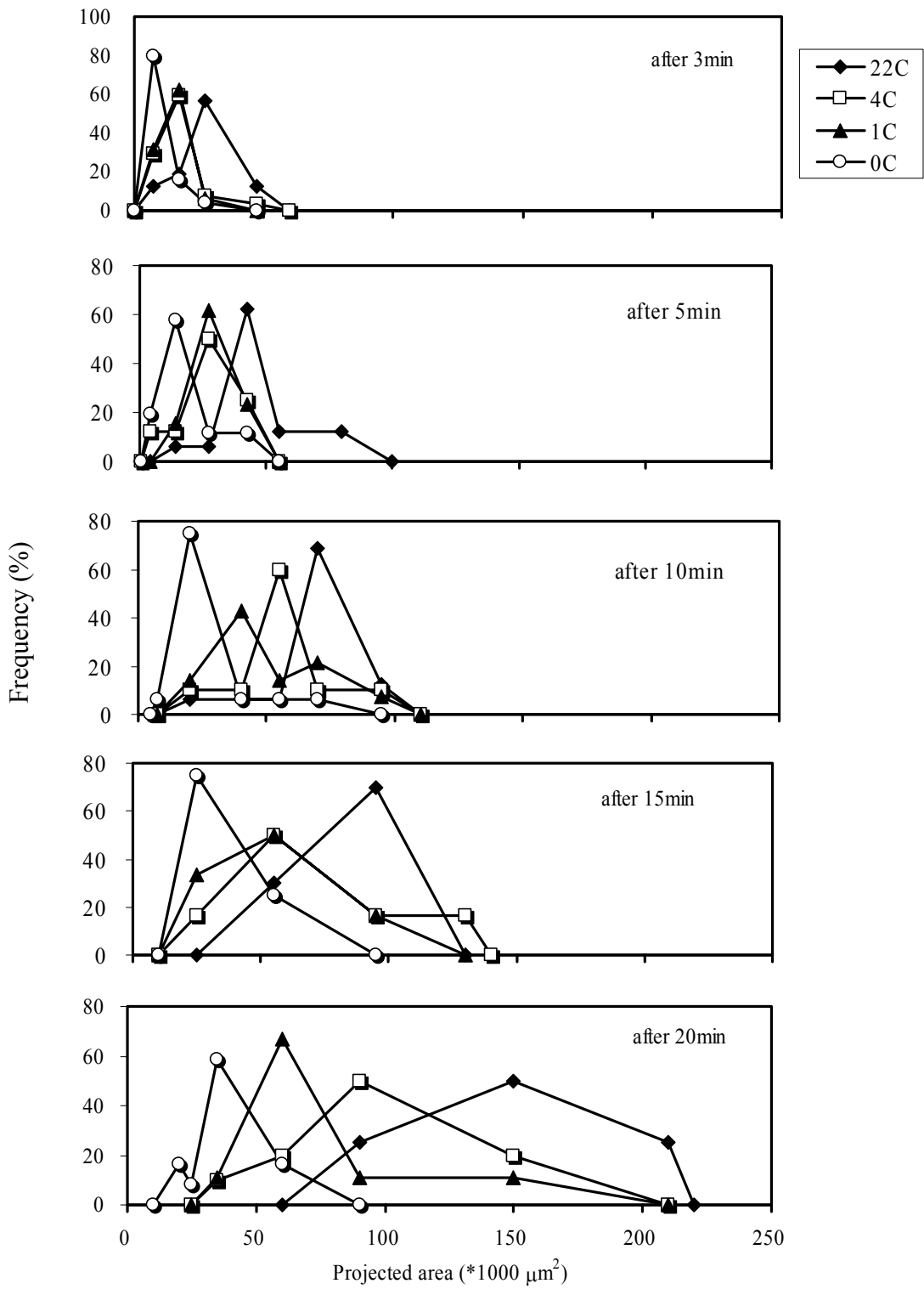
Figure 4.12. Floc projected area distribution with FS at 50 mg/L
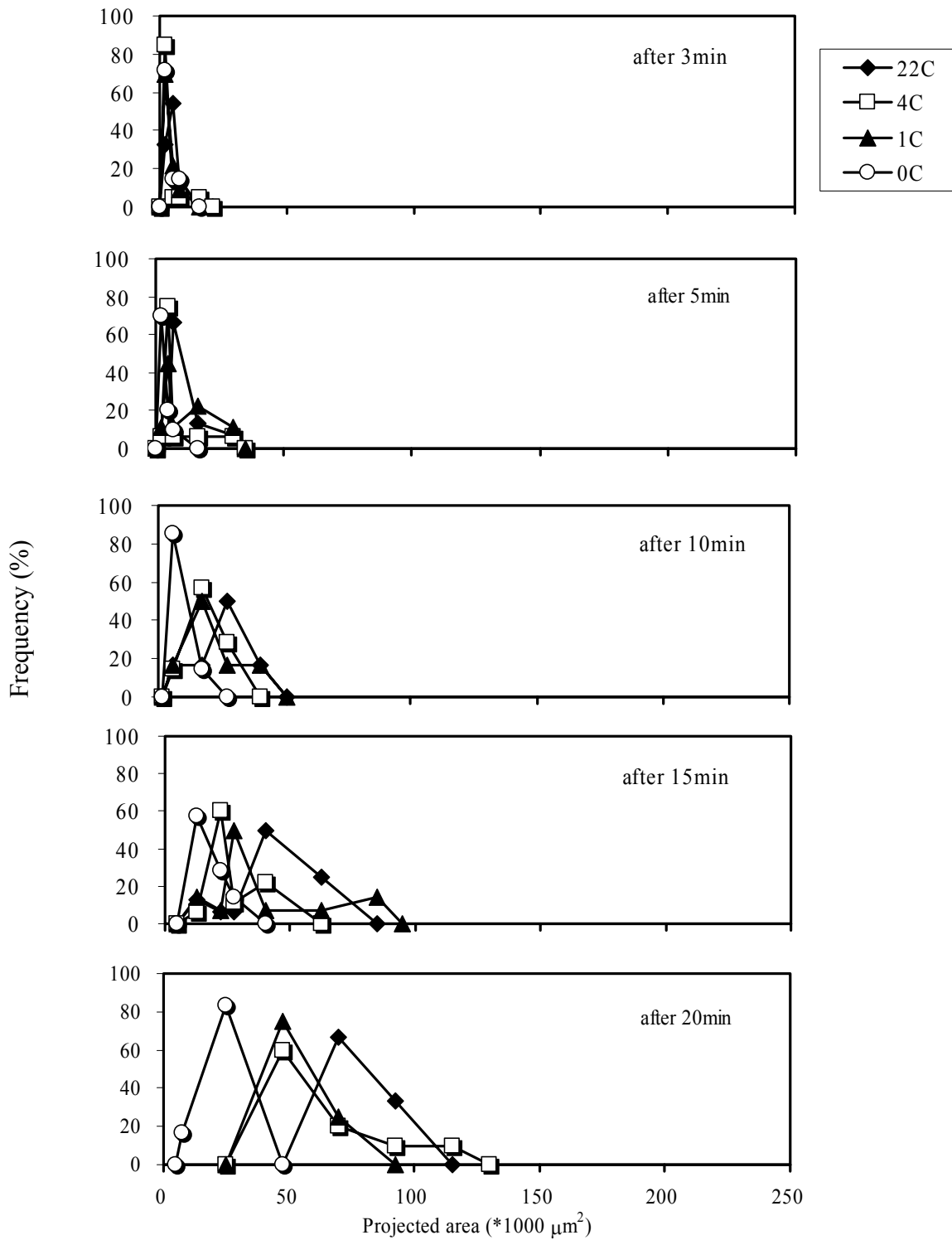
Figure 4.13. Floc projected area distribution with FS at 20 mg/L
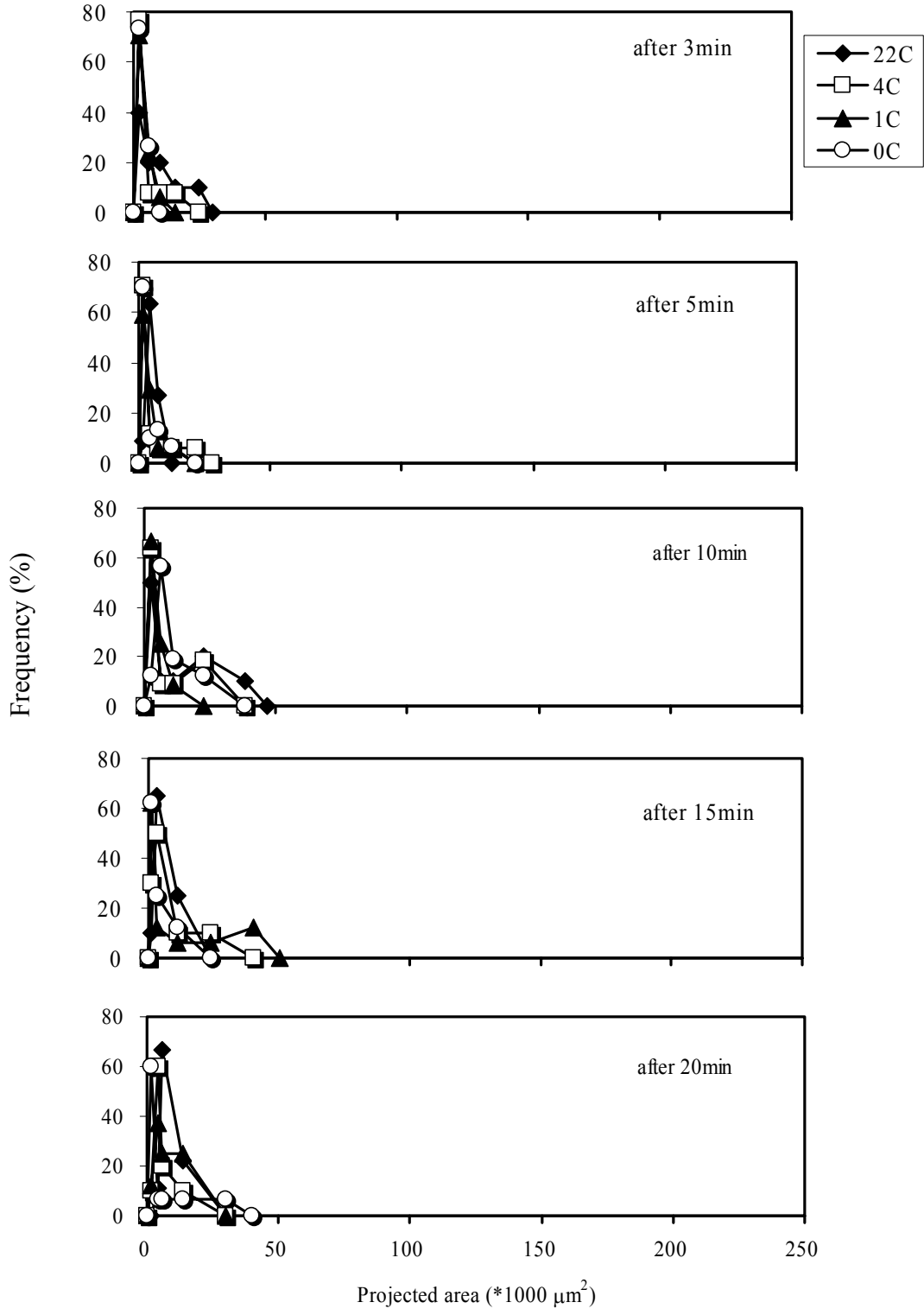
Figure 4.14. Floc projected area distribution with FS at 5 mg/L

2) Floc growth

In the water treated with FS at 50 and 20 mg/L, floc growth became slow with decreasing water temperature, particularly at 0 °C. The movement of the projected-area distribution towards larger size classes at 22 °C was very fast, but this movement at 0 °C was extremely slow. For instance, the floc growth rates in the water treated with FS at 50 mg/L were $7*10^3$, $5*10^3$, $3*10^3$ and $2*10^3$ μm^2/min at 22 °C, 4 °C, 1 °C and 0 °C, respectively. Kang et al. (1995) also indicated that low water temperature slowed the rate of flocculation in a kaolin clay suspension treated with ferric nitrate.

Clearly, the projected-area distribution in the water treated with FS at 50 mg/L moved forward with time faster than in the water treated with FS at 20 mg/L. For instance, the average rates of the peak movements in the water treated with FS at 50 and 20 mg/L at the water temperature of 22 °C were $7*10^3$ and $3*10^3$ μm^2/min, respectively. Thus, decreasing dosage caused slow floc growth.

In the water treated with FS at 5 mg/L, the projected-area distribution varied slightly with time, and water temperature effect on floc growth was small.

4.3.3 JC Polymer Tests

When adding JC polymer into the water, the coagulation/flocculation process was different from the process with AS and FS. The coagulation/flocculation process with JC polymer was faster. The flocs formed were extremely large after only about 3 min of slow mixing except when the water temperature was 0 $^\circ$C. There were only 1 to 4 particles in each picture photographed. Therefore, it was difficult to conduct the analysis for floc size distribution. Hence, only the analysis for the average projected areas of the flocs in the water treated with JC polymer was carried out.

The average projected areas of the flocs with flocculation time in the water treated with JC polymer are shown in Figure 4.15. In comparison with Figure 4.7, results indicate that JC polymer decreased the effect of low water temperature and greatly shortened flocculation time, when the water temperature was not less than 1 $^\circ$C. However, JC polymer didn't significantly improve the aggregation process when the temperature approached 0 $^\circ$C. At the water temperatures of 22 $^\circ$C, 4 $^\circ$C and 1 $^\circ$C, large flocs (larger than 0.5 mm^2 in projected area) were formed. The flocs quickly grew within 3 minutes of slow mixing. After 3 minutes, the average projected areas of the flocs began to level off and flocculation was completed. At the water temperature of 0 $^\circ$C, the polymer didn't cause the formation of large floc. The average projected areas tended to level off after at least 15 minutes and the flocculation time was not shortened.
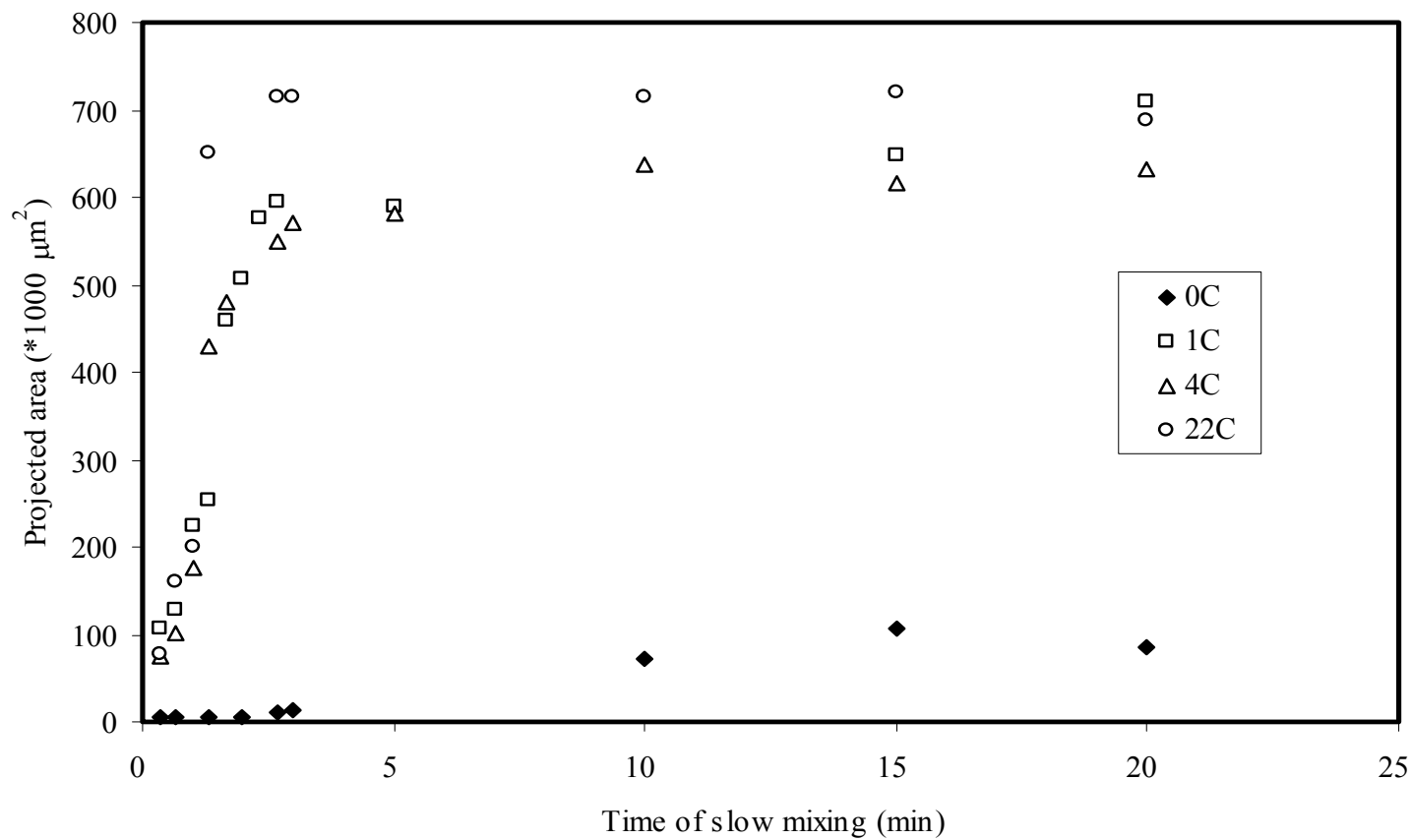
Figure 4.15. Average projected area vs. time in the water treated with JC Polymer
(Dosage 0.2mg/L at 22 & 4 ^{o}C, 1.4 mg/L at 1 & 0 ^{o}C)

Floc size defined in the research:
    Large floc – floc projected area ≥ 0.5 mm^2
    Medium floc – floc projected area between 0.1 to 0.5 mm^2
    Small floc – floc projected area ≤ 0.1 mm^2

Wang et al. (2002) demonstrated that, compared with the AS, PACls could give the same effective performance even with shorter coagulation/flocculation time during the treatment of cold water at 5.5 °C. The flocculation time of 5 minutes was sufficient for PACls to treat cold water of 5.5 °C.

4.4 Comparison between Aluminum Sulfate and Polymer

Figure 4.16, plotted from Figures 4.7 and 4.15, presents the effect of AS and JC polymer on the aggregation processes. Table 4.4 shows the effect of AS and JC polymer on residual turbidities. The results indicate that (1) floc sizes in the water treated with JC polymer were much larger than in the water treated with AS at water temperatures of 22 °C, 4 °C and 1 °C. The floc size with the JC polymer was over 30 times of that without the polymer at 3 minutes of slow mixing. Moreover, the residual turbidities in the water treated with JC polymer were smaller than those with AS at 22 °C and 4 °C; (2) at a water temperature of 0°C, the floc sizes in the water treated with the JC polymer were slightly larger than those without the polymer. In addition, the residual turbidity of 1.6 NTU in the water treated with JC polymer was lower than the turbidity of 2.0 NTU with AS. Therefore, the JC polymer slightly improved the floc growth and increased treatment efficiency at water temperature of 0 °C.
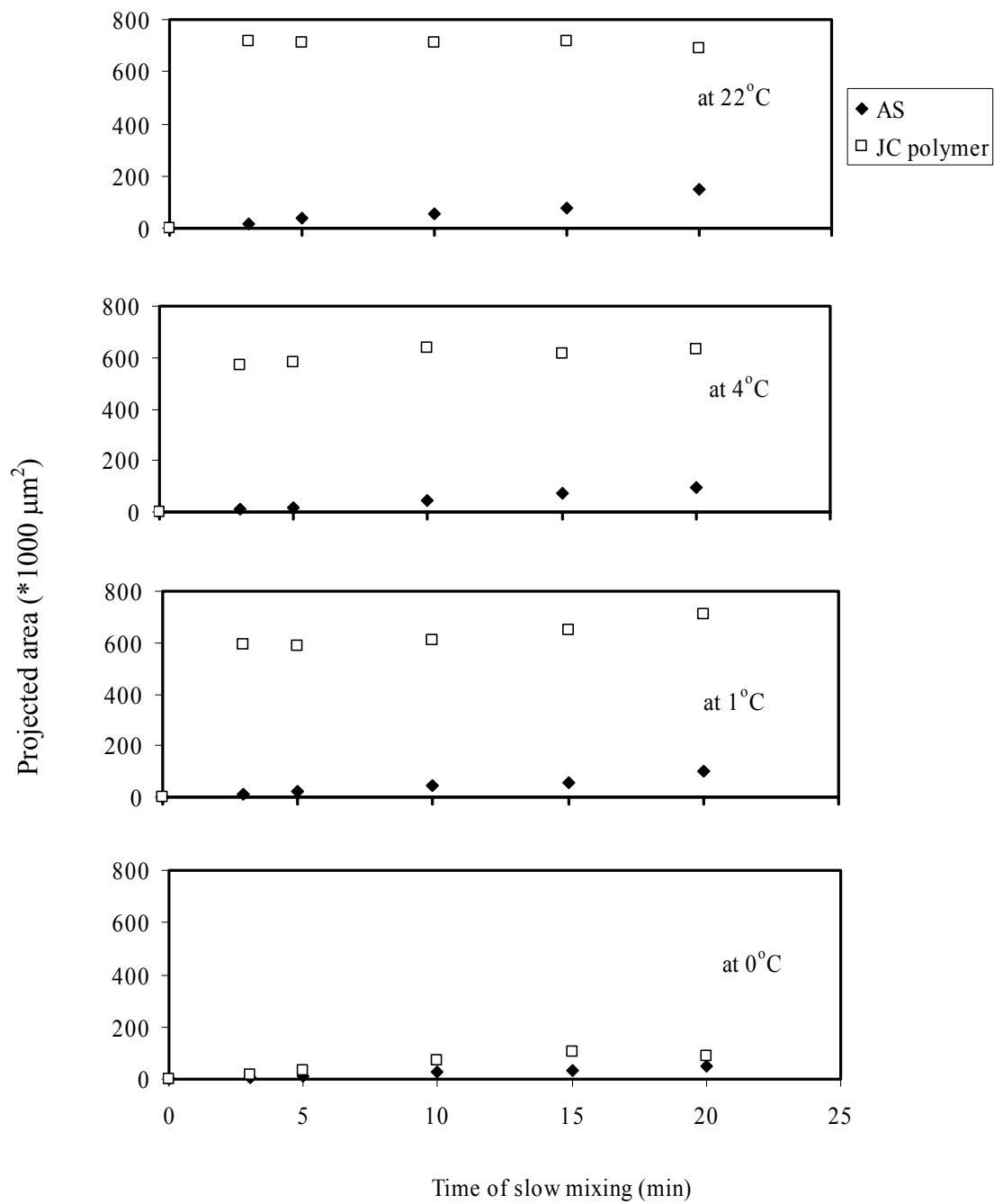
Figure 4.16. Average projected area vs. time in
water treated with AS and JC polymer
(AS: 50 mg/L; JC polymer: 0.2mg/L at 22 & 4 ^{o}C,
and 1.4 mg/L at 1 & 0 ^{o}C)

Table 4.4. Residual turbidity with AS and JC polymer

	Residual turbidity (NTU)		
	at 22 ^{o}C	at 4 ^{o}C	at 0 ^{o}C
AS	0.8	0.8	2.0
JC polymer	0.7	0.7	1.6

4.5 Comparison between Aluminum Sulfate and Ferric Sulfate

The effects of different coagulants on aggregation are compared in Figure 4.17. Clearly, both the average floc size and floc growth in the water treated with AS were similar to those with FS under the same temperature conditions.

On the other hand, comparing Figure 4.2 and Figure 4.4, the residual turbidities of particles in the water treated with AS were lower than those with FS under the same conditions. For instance, the residual turbidities of particles in the water treated with 50 mg/L of AS and FS at 22 ^{o}C were 0.8 NTU and 2.0 NTU, respectively. In addition to coagulation/flocculation, sedimentation processes determine the residual turbidities in water treatment. Different floc shape and density resulted in different floc sedimentation efficiency. The different sedimentation performance may cause different turbidities between AS and FS.
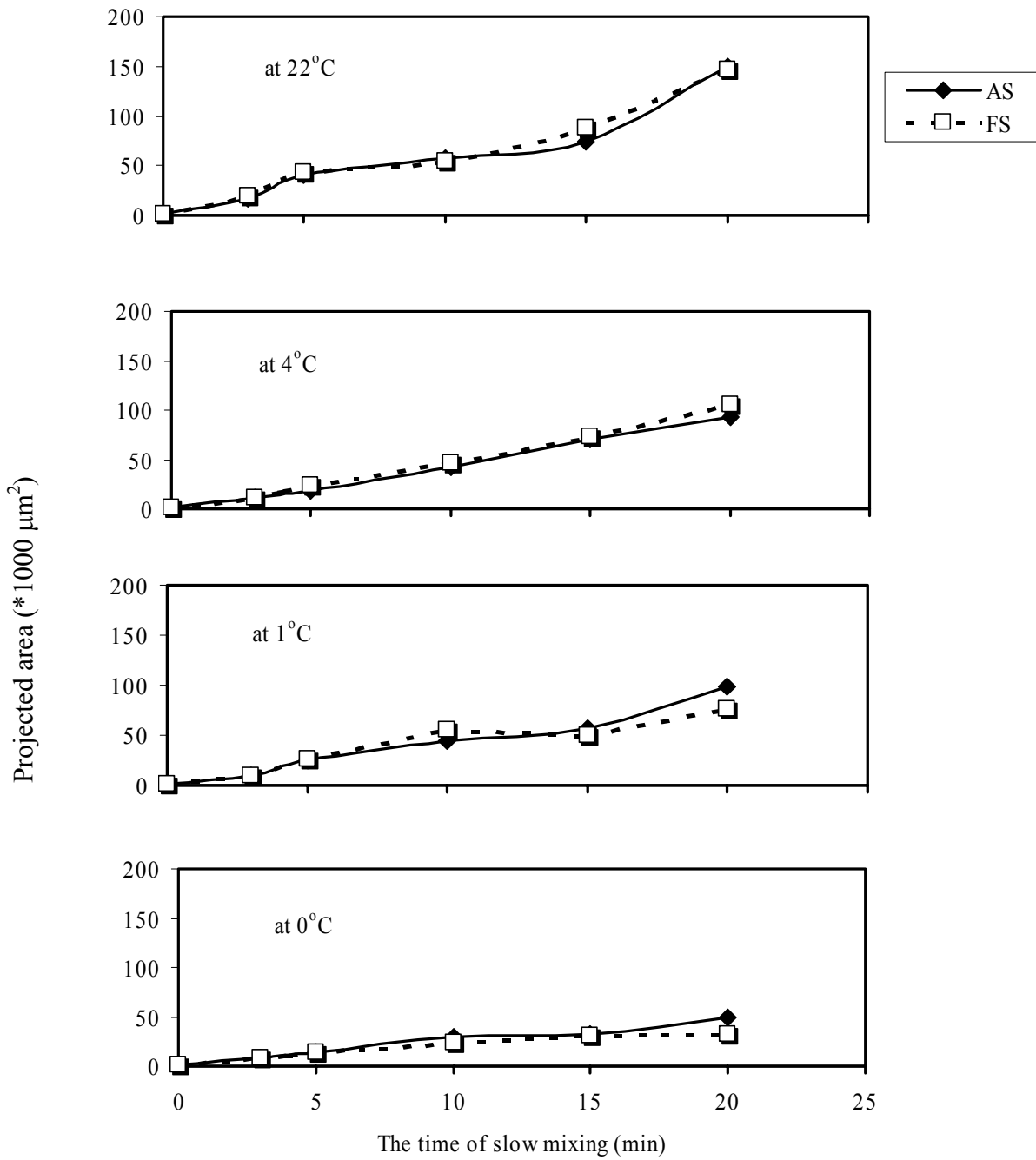
Figure 4.17. Average projected area vs. time in water treated
with AS at 50 mg/L and FS at 50 mg/L

4.6 Flocculation Kinetics

Equation 2.18 given by Argaman and Kaufman (1970) was used in this research. It is represented by

[4.3] $$\frac{n_o}{n_t} = \frac{\frac{1}{t} + K_A G}{\frac{1}{t} + K_B G^2} = 1 + \frac{K_A G - K_B G^2}{\frac{1}{t} + K_B G^2}$$

where:

n_o = particle count per 4256 * 2848 pixels of the raw water (ct/4256 * 2848 pixels)

n_t = particle count per 4256 * 2848 pixels at t time (ct/4256 * 2848 pixels)

t = flocculation time in a reactor (sec)

Rearranging of Equation 4.2 gives

[4.4] $$\frac{1}{n_t} = \frac{1}{n_o} + \frac{K_A G - K_B G^2}{n_o} \bullet \frac{1}{(\frac{1}{t} + K_B G^2)}$$

This equation is a linear equation of the type (y=b +Sx). Thus a plot will give a straight line on arithmetic paper. At first, K_B was chosen from reported data (Table 2.2). A straight line based on $1/(1/t+K_B G^2)$ and $1/n_t$ was drawn in a plot, and the value of R^2 was obtained. Over 30 values of K_B were chosen to obtain 30 R^2 values, and then the largest R^2 value was chosen. After that, K_A was calculated based on the following:

[4.5] $$K_A = \frac{S n_0 + K_B G^2}{G}$$

where:

S = slope of the line in figure

Figures 4.18 and 4.19 show flocculation kinetics for the water treated with AS and FS at 50 mg/L under different temperature conditions, respectively. Kinetic parameters are summarized in Table 4.5.

Table 4.5. Flocculation Kinetic Parameters

Coagulant	Temperature (^{o}C)	Aggregation Constant K_A	Breakup Constant K_B (sec)	Multiple Correlation Coefficient R^2
AS 50 mg/L	22	$4.4 * 10^{-4}$	$3.0 * 10^{-7}$	0.98
	4	$2.1 * 10^{-4}$	$8.8 * 10^{-7}$	0.99
	0	$2.0 * 10^{-4}$	$9.8 * 10^{-7}$	0.94
FS 50 mg/L	22	$4.5 * 10^{-4}$	$4.2 * 10^{-7}$	0.99
	4	$2.1 * 10^{-4}$	$9.9 * 10^{-7}$	0.99
	0	$2.0 * 10^{-4}$	$10.0 * 10^{-7}$	0.95

The results in this research agreed with the model (Equation 2.18) because all R-squared (R^2) for regressions were high (more than 0.94). As well, both K_A and K_B at 22 ^{o}C were close to the reported data, respectively (refer to Table 2.2).
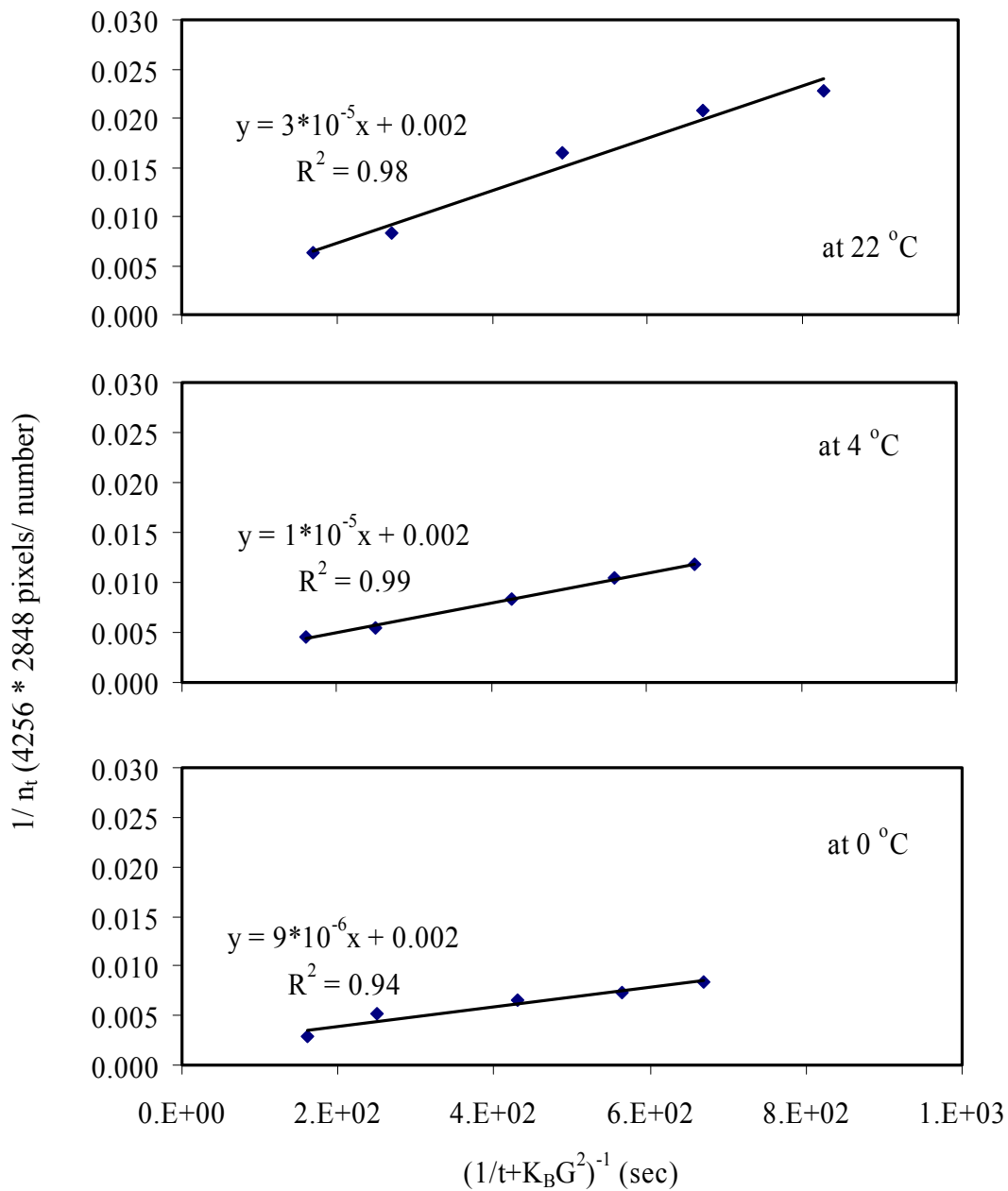
Figure 4.18. Flocculation in water treated with AS at 50 mg/L
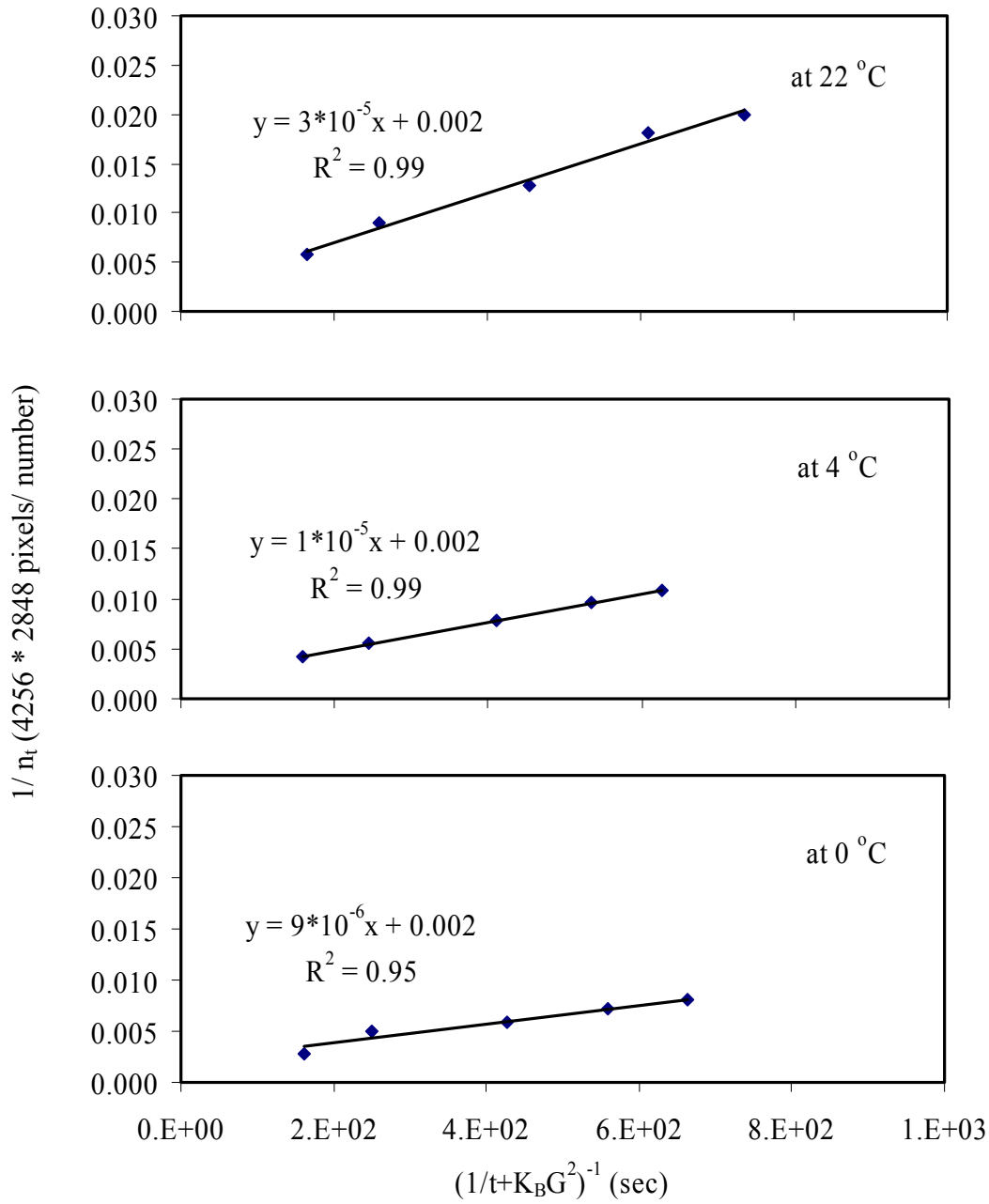
Figure 4.19. Flocculation in water treated with FS at 50 mg/L

After reviewing 30 sets of data of K_B, K_A and R^2, the results are summarized in Table 4.6. Table 4.6 indicates that the values of K_B or K_A in each range had similar flocculation performance.

Table 4.6. Relationship among K_B, K_A and R^2

Temp. ($^{\circ}$C)	Coagulant 50 mg/L	*K_B range (sec) K_B*E-07	*K_A range K_A*E-04	R^2
22	AS	2.3-5.5	4.4-4.5	0.98
	FS	3.2-6.0	4.4-4.5	0.99
4	AS	5.0-10.0	2.0-2.1	0.99
	FS	6.0-15.0	2.0-2.3	0.99
0	AS	8.8-15	2.0-2.2	0.94
	FS	9.5-11	2.0-2.1	0.95

*The ranges of K_B and K_A were determined based on the largest R^2 values with 2 significant digits.

In the water treated with AS and FS at 50 mg/L, as water temperature decreased, aggregation constant (K_A) declined and breakup constant (K_B) increased. K_B is dependent on the floc internal binding forces (floc strength). K_A at 22 $^{\circ}$C was larger than that at 4 $^{\circ}$C and 0 $^{\circ}$C, while K_A at 4 $^{\circ}$C was close to that at 0 $^{\circ}$C. K_B at 22 $^{\circ}$C was smaller than that at 4 $^{\circ}$C and 0 $^{\circ}$C. Hence, floc aggregation declined and floc strength became weaker with decreasing temperature. Hanson and Cleasby (1990) demonstrated that both iron and alum flocs formed at 5 $^{\circ}$C were much weaker than those at 20 $^{\circ}$C.

Comparing K_A and K_B in the water treated with AS and FS under the same water temperature conditions, the values of K_A and K_B with AS were close to those with FS. The results indicate that floc aggregation performance in the water treated with AS was similar to that with FS. The flocs strength with FS was also close to that with AS.

4.7 Image Observation

The method of image observation is to observe floc information and then discover some phenomena of the aggregation processes. Since aggregation mechanisms are complicated and observational error cannot be avoided, the following description may not accurately represent the processes. This section focuses on the image observation of the water treated with AS and JC polymer, except for FS, as FS performance was similar to that with AS in aggregation processes.

The comparison of floc sizes at 22 °C, 4 °C and 0 °C in the water treated with AS at 50 mg/L is as follows: After 1 minute of slowing mixing (Figure 4.20), the floc sizes at 22 °C were larger than those at 4 °C and 0 °C. This indicates that the formation of precipitates and the destabilization of particles by sweep-floc coagulation (enmeshment by a precipitate) at 22 °C were faster than at 4 °C and 0 °C.

After 10 minutes (Figure 4.21), the floc sizes at 22 °C were evidently larger than those at 4 °C, and the floc sizes at 4 °C were larger than those at 0 °C. Low temperatures decreased the aggregation performances of particles and flocs.

At the end of the flocculation process (Figure 4.22), the floc sizes at 22 °C and 4 °C were obviously larger than those at 0 °C, while the sizes at 22 °C were the largest. This indicates that low temperature affected aggregation processes, and the water temperature of 0 °C caused small floc size.
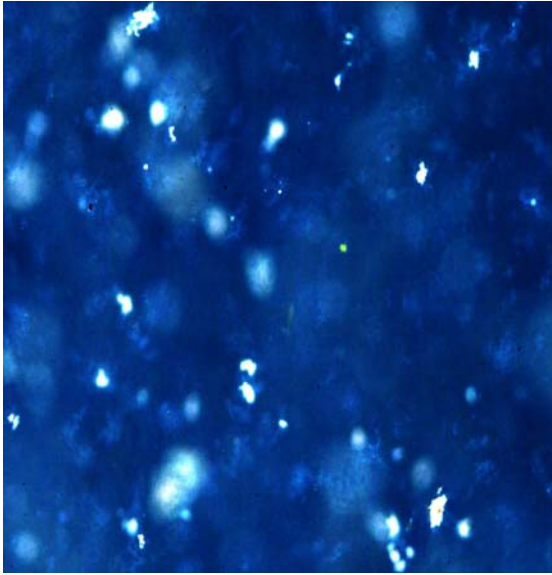
(a) 22 $^{\circ}$C
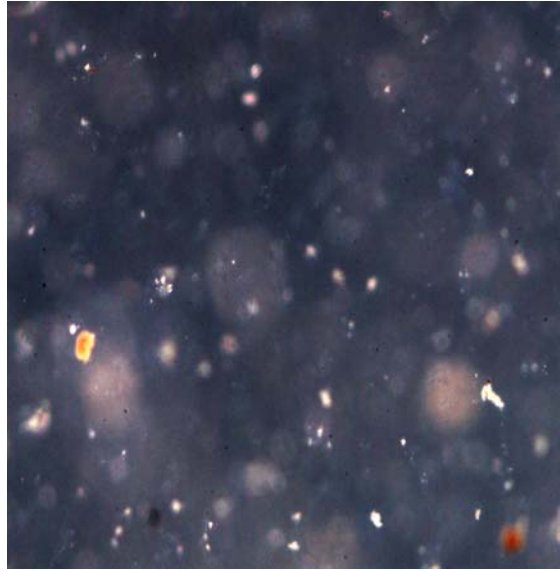
(b) 4 $^{\circ}$C
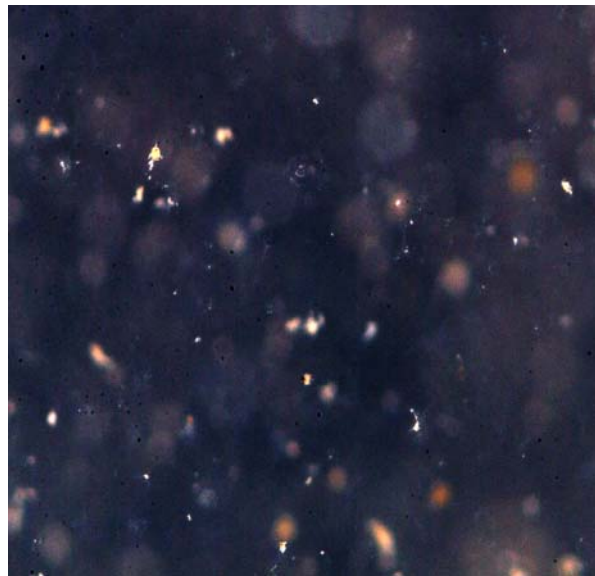
(c) 0 $^{\circ}$C

Figure 4.20. Images in water treated with AS at 50 mg/L after 1 min
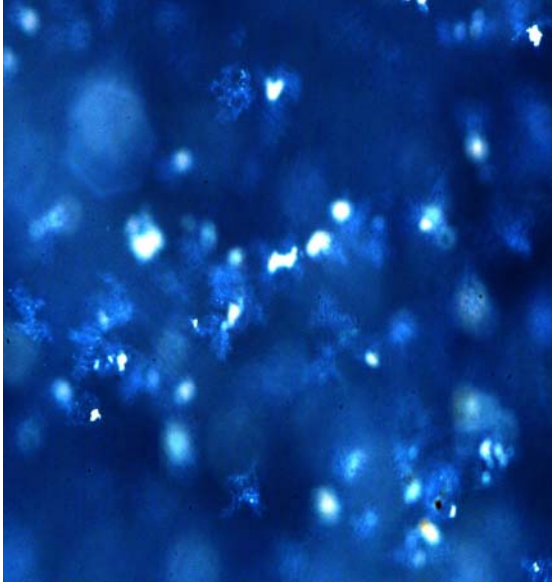
(a) 22 $^{\circ}$C
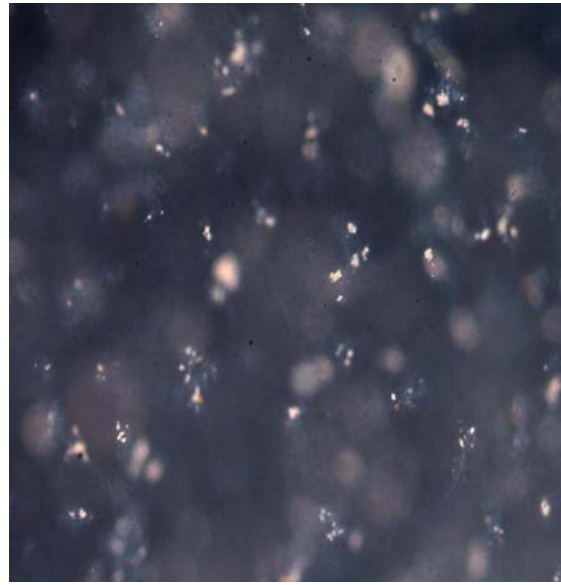
(b) 4 $^{\circ}$C
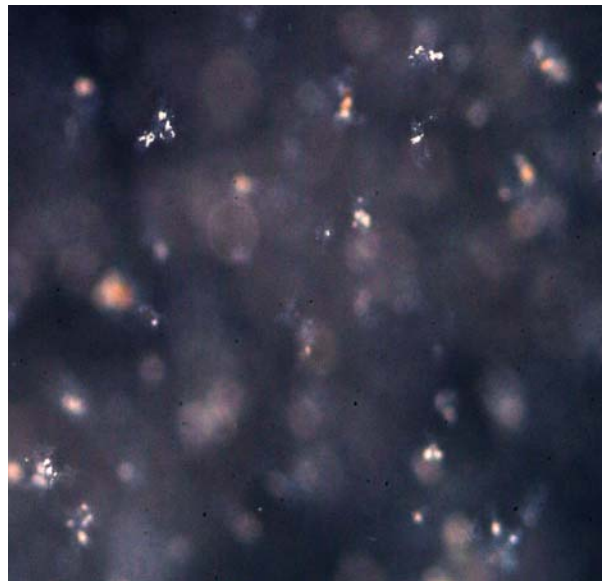
(c) 0 $^{\circ}$C

Figure 4.21. Images in water treated with AS at 50 mg/L after 10 min
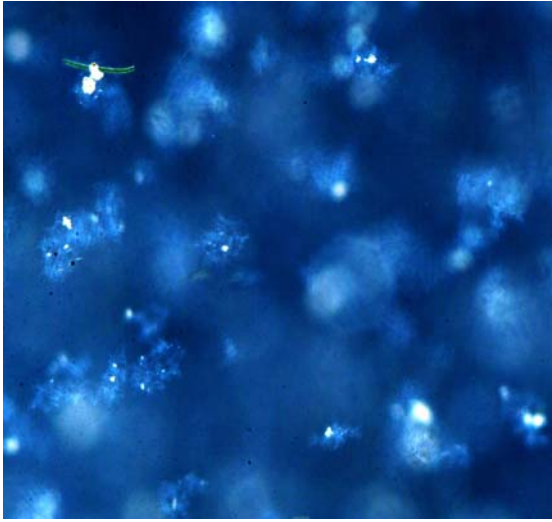
(a) 22 $^{\circ}$C
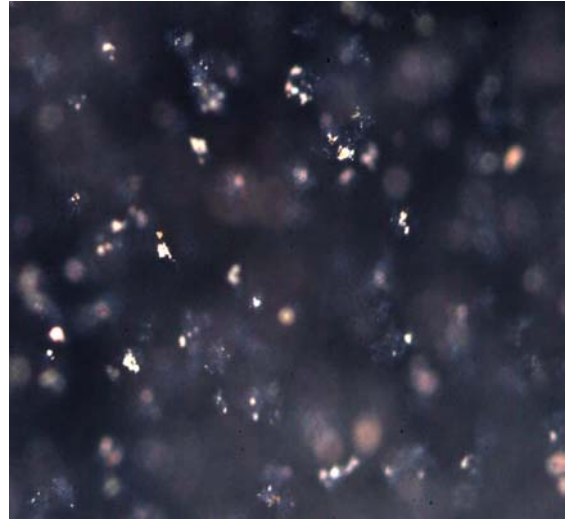
(b) 4 $^{\circ}$C

(c) 0 $^{\circ}$C

Figure 4.22. Images in water treated with AS at 50 mg/L after 20 min

The description of the aggregation process in the water treated with JC Polymer is as follows:

As shown in Figure 4.23a, the formed flocs were big at the beginning of slow mixing (at the end of fast mixing). This indicates that at the water temperature of 22 °C, almost all particles were destabilized and formed into flocs during 1.5 minutes of fast mixing period. After 1 minute, the formed flocs were much larger (Figure 4.23b). After 3 minutes, large porous flocs were formed, and the flocculation process was completed (Figure 4.23c). This indicates that flocculation time was extremely short. Similar processes were observed at water temperatures of 4 °C and 1 °C.

The process at the water temperature of 0 °C was very different from the above-mentioned process. Large floc did not form. It could be seen that when slow mixing started, a lot of short chains had been made from the polymer, and a number of particles had been attached to the short chains. Attachment occurred to form a bridge (Figure 4.24a). With increasing time, more and more particles were destabilized, the flocs became bigger and bigger. However, the shape of the flocs was filamentous, as shown in Figures 4.24b and 4.24c. Throughout the flocculation process, the flocs were filamentous and there was no large porous floc formed.

(a) at the beginning of slow mixing
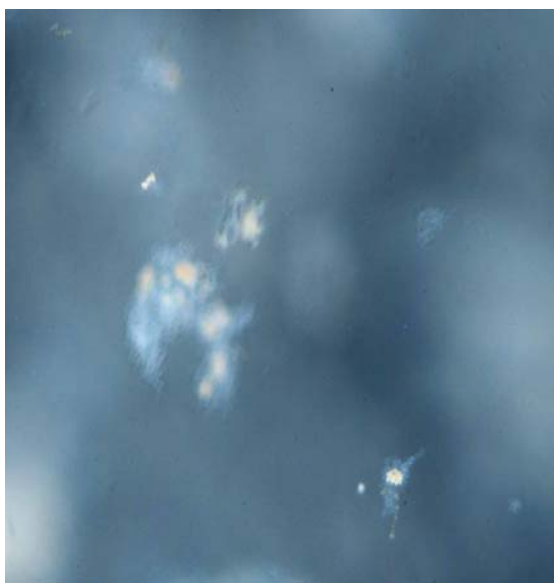
(b) after 1 min of slow mixing

(c) after 3 min of slow mixing

Figure 4.23. Images at 22 °C in water treated with JC polymer
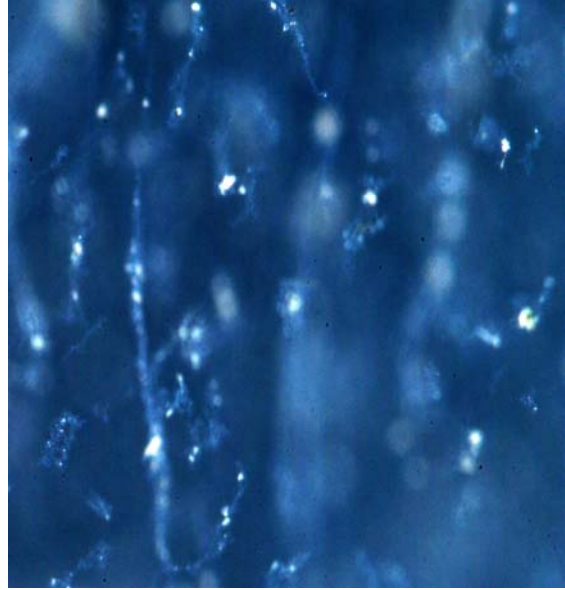
(a) at the beginning of slow mixing   (b) after 10min of slow mixing
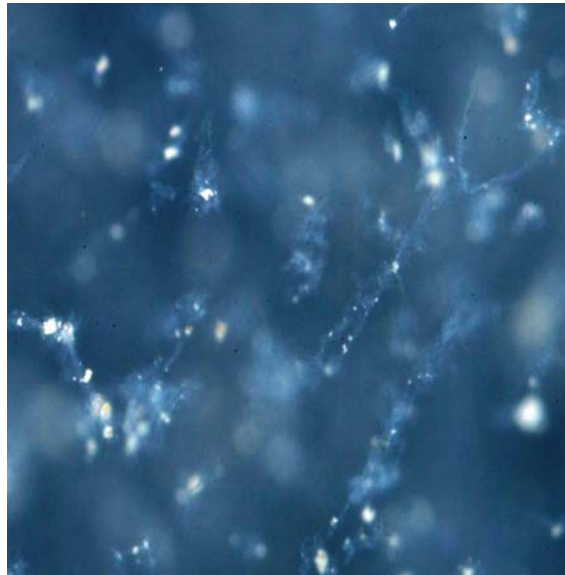
(c) at the end of slow mixing

Figure 4.24. Images at 0 °C in water treated with JC polymer

Chapter 5 – Summary, Conclusions and Recommendations

5.1 Summary

Although various studies have examined temperature effects on coagulation/flocculation efficiencies, little work has been performed to directly observe coagulation/flocculation processes due to the limitation of measurement technologies. In recent years, a microscopic image technique has been used to study the coagulation/flocculation process, but it requires sample handling that disturbs the floc characteristics during measurement. This method results in large deviation from practical processes. An advanced high resolution photographic technique has been used in the present work. This technique overcomes the disadvantages of microscopic image techniques, for the images are obtained directly while the flocculation process is still taking place.

Based on this technique, a systematic method of evaluating aggregation processes was formed in this project. The systematic method included: the bench-scale test, floc size analysis, flocculation kinetic analysis and image observation. Several conclusions were reached regarding aggregation processes under different conditions based upon the application of the method.

5.2 Conclusions

A 6-megapixel digital camera equipped with a micro lens was found to be useful for obtaining time-varying in situ images of aggregation. In combination with FUJI FinePixViewer camera control software, Adobe Photoshop software for floc threshold

setting and Carnoy 2.0 particle analysis software, this procedure provided a convenient means of obtaining data to calculate size distribution. Once the size distribution was calculated, the floc growth and floc size change in the aggregation process were analyzed.

The experimental results in this research agreed with the model for flocculation kinetics given by Argaman and Kaufman (1970). In the water treated with AS and FS at 50 mg/L, the aggregation constant (K_A) declined and breakup constant (K_B) increased, as water temperature decreased. Floc aggregation performance declined with decreasing water temperature.

Under the same water temperature conditions, the values of K_A and K_B for AS were close to those for FS, respectively. Floc aggregation performance in the water treated with AS were similar to that with FS.

Low water temperature has a detrimental impact on coagulation/flocculation processes. A water temperature of 0 °C resulted in a slow floc growth and small floc size. Although the floc growth rates at 4 °C and 1 °C were less than those at 22 °C, they were higher than at 0 °C. In the water treated with AS at 50 mg/L, the floc growth rates were $10*10^3$, $7*10^3$, $5*10^3$ and $3*10^3$ μm^2/min at 22 °C, 4 °C, 1 °C and 0 °C, respectively.

The coagulant dosage is an important factor in aggregation processes. A dosage greater than 50 mg/L of aluminum sulfate or ferric sulfate resulted in marginal gains in treatment efficiency. Decreasing dosages caused lower floc growth rates and smaller floc sizes.

When the dosage was 5 mg/L or less, there was a poor floc formation and very small floc size. The floc growth rates in the water treated with AS at 50 and 20 mg/L at a water temperature of 22 $^{\circ}$C were $10*10^3$ and $4*10^3$ μm^2/min, respectively. After 5 minutes of slow mixing, the average projected areas of the flocs in the water treated with an AS dosage of 50 mg/L were over 1.3 and 5.5 times larger than those with AS at 20 and 5 mg/L, respectively. The floc growth process in flocculation with AS was similar to the process with FS.

The coagulant aid, anionic copolymer of acrylamide, can significantly reduce the impact of low temperature due to the function of interparticle bridging, when the temperature is not less than 1 °C, but it only improves the aggregation slightly when the temperature approaches 0 °C, for the interparticle bridging is not significantly efficient. At water temperatures of 22 °C, 4 °C and 1 °C, floc size with the polymer was over 30 times of that without the polymer at 3 minutes of slow mixing. Flocculation completed in 3 minutes of slow mixing, while 20 minutes was required without polymer. Twenty minutes of sedimentation with polymer yielded similar results when compared to one hour of sedimentation without polymer. The polymer greatly shortened the required time of flocculation and settlement. When the temperature was close to 0 °C, the polymer did not cause the formation of large floc (larger than 0.5 mm^2 in projected area), nor did it shorten the time of flocculation and sedimentation.

5.3 Recommendations

This research focuses on finding an effective measurement technique for capturing the images throughout the aggregation process and forming a systematic method of evaluating aggregation processes. Recommendations for future studies are presented in the following paragraphs.

Since the test focused on the impact of water temperature and coagulant on aggregation processes, other parameter changes were not considered. Therefore, more tests could be performed based on different Gt values, settling time and pH. The test with different alkalinities could be performed if insufficient alkalinity quantity is present in water.

Although the advanced high resolution photographic technique can be used to analyze floc size change and floc growth rate, it cannot be used to measure floc density and porosity. Since different floc density and porosity resulted in different floc sedimentation efficiency, they should be measured to find the reason why the treatment efficiency with AS was higher than that with FS.

The position of the flocs photographed was about 5 mm from the inside of the jar in this research. In order to reduce the wall effects, a longer focal length should be considered. The photographic technique in this research can measure floc size greater than 8 μm. Using more advanced equipment could allow for the measurement of smaller flocs. An image analysis software with the function of measuring floc major axis and short axis

should also be considered in the future, as different floc shape causes different flocculation and sedimentation performance.

The research found that anionic copolymer of acrylamide at 1.6 mg/L or less together with AS at 50 mg/L could not improve aggregation significantly when temperature approached 0 °C. Different dosages of AS and anionic copolymer of acrylamide could be tested to determine if they have similar performances.

References:

Adhin, A. and Rebhun, M., 1974. High-rate contact flocculation-filtration with cationic polyelectrolytes. JAWWA, 66(2): 109-117.

Agraman, Y. and Kaufman, W.J., 1970. Turbulence and flocculation. J. Sanit. Eng. Div. ASCE, 96: 223.

Al-Laya, M.A. and Middlebrooks, E.J., 1974. Algae removal by chemical coagulation. Water and Sewage Works, 121(9): 76-80.

American Society of Civil Engineers (ASCE) and American Water Works Association (AWWA), 1998. Water treatment plant design. McGraw-Hill, New York.

American Water Works Association (AWWA), 1984. Introduction to water treatment. Denver, Colorado.

American Water Works Association (AWWA), 1977. Simplified procedures for water examination laboratory manual. Denver, Colorado.

Apps, J.A. and Neil, J.M., 1990. Solubilities of aluminum hydroxides and oxydydroxides in alkaline solutions: correlation with thermodynamic properties of $Al(OH)_4^-$. Chemical Modeling of Aqueous Systems II, Proc., 196th Meeting of American Chemical Society: ACS Symp. Series 416, ACS, Washington, D.C.: 414-428.

Argaman, Y.A. and Kaufman W.J., 1970. Turbulence and flocculation. J. Sanit. Eng. Div. ASCE, 96: 223.

Argaman, Y.A., 1971. Pilot-plant studies of flocculation. JAWWA, 63 (12): 775-777.

Bagwell, T., Henry, H.B. and Kenneth, M.B., 2001. Handbook of public water systems. 2nd Edition, HDR Engineering Inc., New York.

Binnie, C., Kimber, M. and Smethurst. G., 2002. Basic water treatment. Thomas Telford Ltd., London.

Borstnik, A., Stark, H. and Zumer, S., 2000. Temperature-induced flocculation of colloidal particles immersed into the isotropic phase of a nematic liquid crystal. Physical Review E. Statistical Physics, Plasmas, Fluids, and Related Inter-disciplinary Topics, 61 (3): 2831.

Bratby, J., Miller, M.W. and Marais, G.V.R., 1977. Design of Flocculation systems from batch test data. Water S. Afr., 3(4): 173-182.

Bunker, D.Q., Edzwald, J.K., Dahlquist, J. and Gillberg, L., 1995. Pretreatment considerations for dissolved air flotation: water type, coagulants and flocculation. Wat. and Sci. Tech., 31(3): 63-71.

Camp, T.R. and Stein, P.C., 1943. Velocity gradients and internal work in fluid motion. J. Boston Soc. Civ. Eng. 30: 219-237.

Campbell, S., Lykins, J.R., Goodrich, J.A., Post, D. and Lay, T., 1995. Package plants for small systems: A field study. JAWWA, 87(11): 39-47.

City of Saskatoon Environmental Operations Annual Report, 2001. Utility Services Department, Saskatoon.

Dempsey, B.A., 1987. Chemistry of coagulants. Influence of coagulation on the selection, operation, and performance of water treatment facilities and processes, Seminar of the American Water Works Association (AWWA), Denver. Colorado: 19-30.

Driscoll, C.T. and Letterman, R.D., 1988. Chemistry and fate of Al(III) in treated drinking water. J. Envir. Engrg. Div., ASCE. 114(2): 21-37.

Edzwald, J.K., 1987. Coagulation-sedimentation-filtration processes for removing organic substances from drinking water. Control of organic substances in water and wastewater, Noyes Data Corporation, Noyes Data Corporation, Park Ridge, New Jersey: 26-64.

Flynn, C.M., 1984. Hydrolysis of inorganic iron (III) salts. Chemical Rev., 84(1): 31-41.

Friedlander, S.K., 1977. Smoke, Dust and Haze, Wiley-interscience, New York.

Francois, R.J. and Bekaert, N.V., 1986. Influence of mixing parameters and water quality on the flocculation of kaolinite with aluminum sulfate. Chemistry for protection of the Environment, Proc., 5th Int. Conf., Elsevier, New York: 273-296.

Greenberg, A.E., Clesceri, L.S., and Eaton, A.D., 1992. Standard methods for the examination of water and wastewater. APHA and AWWA, 18th Edition, Washington, DC.

Han, M. and Lawler, D.F., 1992. The (relative) insignificance of G in flocculation. JAWWA, 82(11): 56-73.

Hanson, A.T., and Cleasby, J.L., 1990. The effects of temperature on turbulent flocculation: fluid dynamics and chemistry. JAWWA 82(11): 56-73.

Health Canada, 1996. Guidelines for Canadian drinking water quality, Sixth Edition.

Heinanen, J., 1987. Effect of temperature on water treatment. Jour. Aqua Fennica, (17)2: 201-220.

Hem, J.D. and Roberson, C.E., 1990. Aluminum hydrolysis reaction and products in mildly acidic aqueous system. Chemical modeling of aqueous systems II, proc., 196th Meeting of American Chemical Society: ACS Symp. Series 416, Washington, D. C.: 429-446.

Hooge, P.A., 2000. Evaluating adsorption clarification at cold water temperature for drinking water treatment. M.Sc. thesis, University of Saskatchewan, Saskatoon.

Hutchison, W. and Foley, P.D., 1974. Operational and experimental results of direct filtration. JAWWA, 66(2): 79-85.

Kang, L.S. and Cleasby, J.L., 1995. Temperature effects on flocculation kinetics using Fe(III) coagulant. Journal of Environmental Engineering, 121(12).

Lawler, D.F., 1993. Physical aspects of flocculation: from microscale to macroscale. Separation of Particles from Water, J. Gregory, ed., Pergamon Press Ltd., Oxford, England: 165-180.

Li, D.M. and Jin, T.G., 2003. Application of cationic high-molecular flocculent in treatment of low temperature and low turbidity water. China Water and Wastewater, 19 (3): 40

Machesky, M.L., 1990. Influence of temperature on ion adsorption by hydrous metal oxides. Chemical modeling of aqueous systems II, proc., 196th Meeting of American Chemical Society: ACS Symp. Series 416, ACS, Washington, D. C.: 282-292.

Matsui, Y., Yuasa, A., Furuya, Y. and Kamei, T., 1998. Dynamic analysis of coagulation with alum and PACl. JAWWA, 90(10): 96-106.

Montgomery, J.M., 1985. Water treatment principles and design. John Wiley & Sons, Inc.

Morris, J.K. and Knocke, W.R., 1984. Temperature effects on the use of metal-ion coagulants for water treatment. JAWWA, 76(3): 74-79.

Mothadi, M.F. and Rao, O.N., 1973. Effect of temperature on flocculation of aqueous dispersions, Water Res., 7: 747-767.

Mpofu, P., Addai-Mensah, J., and Ralston, J., 2004. Temperature influence of nonionic polyethylene oxide and anionic polyacrylamide on flocculation and dewatering behavior of kaolinite dispersions. Journal of Colloid and Interface Science, 271 (1): 145-156.

Odegaard, H., 1979. Orthokinetic flocculation of phosphate precipitates in a multi-component reactor with non-ideal flow. Prog. Water Tech., 11(1): 61-88.

O'Melia, C.R., 1978. Coagulation in wastewater treatment plant design, Ann Arbor Science, Ann Arbor, MI.

O'Melia, C.R., 1978. Coagulation in wastewater treatment. The scientific basis of flocculation, (NATO advanced Study Inst. Series, Series E, Appl. Sci. No. 27), K. J. Ives, ed., Sijthoff and Noordhoff, Alpenaan den Rijn, the Netherlands: 219-268.

O'Melia, C.R., Gray, K.A. and Yao, C.H., 1989. Polymeric inorganic coagulants, American Water Works Association Research Foundation, Denver, Colorado.

Spicer, P.T. and Pratsinis, S.E. 1996. Shear-induced flocculation: the evolution of floc structure and the shape of the size distribution at steady state. Water Res., 30(5): 1049-1056.

Reynolds, T.D. and Richards, P.A., 1996. Unit operations and processes in environmental engineering. 2nd Edition, PWS Publishing Company.

Sanks, R.L., 1979. Water treatment plant design. Ann Arbor Science Publishers Inc.

SaskH$_2$O, 2003. Water information quick facts, the Government of Saskatchewan.

Schultz, C.R., Singer, P.C., Gandley, R. and Nix, J.E., 1984. Evaluating buoyant coarse media flocculation. JAWWA, 76(8):51-63.

Shea, T.G., Gates, W.E. and Argaman, Y.A., 1971. Experimental evaluation of operating variables in contact flocculation. JAWWA, 63(1): 41-48.

Smoluchowski, M., 1917. Versuch einer Mathematischen Theorie der Koagulationskinetik Kolloider Losungen. Z. Phys. Chem. 92: 129-168.

Snoeyink, V.L. and Jenkins, D., 1980. Water chemistry, John Wiley and Sons, Inc., New York.

Speight, J.G. and Lee, S., 2000. Environmental technology handbook, Taylor & Francis.

Streeter V.L. and Wylie, E.B., 1979. Fluid mechanics, McGraw-Hill Book Company.

Swift, D.L. and Friedlander, S.K., 1964. The coagulation of hydrosols by Brownian motion and laminar shear flow. J. Coll. Sci. 19: 621.

Thomas, D.N., Judd, S.J. and Fawcett, N., 1999. Flocculation modeling: a review. Water Res., 33(7):1579-1592.

Van Benschoten, J.E. and Edzwald, J.K., 1990. Chemical aspects of coagulation using aluminum salts hydrolytic reactions of alum and polyaluminum chloride. Water Res., 24(12): 1519-1526.

Vesilind, P.A., Peirce, J.J. and Weiner, R.F., 1988. Environmental engineering. Butterworth Publishers.

Vik, E.A. and Eikebrokk, B., 1989. Coagulation process for removal of humic substances from drinking water. Aquatic humic Substances: influence on fate and treatment of pollutants, proc., 193rd Meeting of the American Chemical Society: Adv. in Chemistry Series 219, ACS, Washington, D. C.: 385-408.

Wang, X.C., Jin, P.K. and Gregory, J., 2002. Structure of Al-humic flocs and their removal at slightly acidic and neutral pH. Water Supply, 2(2): 99-106.

Wang, Y.L., Guo, J.L. and Tang, H.X., 2002. Pilot testing of dissolved air flotation (DAF) in a highly effective coagulation-flocculation integrated (FRD) system. Journal of Environmental Science and Health - Part A Toxic/Hazardous Substances and Environmental Engineering, 37(1): 95-111.

Water Services Association of Australia (WSSA), 1992. Assessment of coagulants for water treatment. Report No: 41.

Xie, Y.F., 2000. Xie's Bar Theory for water coagulation. The 2000 water works operators' association of Pennsylvania annual meeting.

Zhang, J.J. and Li, X.Y., 2003. Modeling particle-size distribution dynamics in a flocculation system. American Institute of Chemical Engineers Journal, 49(7): 1870.

Appendix A – Bench-scale Tests

Table A.1. Results of bench-scale test (with aluminum sulfate)

22 °C						
	Turbidity(NTU)			Particle count (1/100 mL)		
AS(mg/l)	test1	test2	ave.	test1	test2	ave.
0.5	4.9	4.7	4.8	1077000	1237000	1157000
5	3.0	3.1	3.1	1036000	1240000	1138000
10	2.6	2.8	2.7	807000	857000	832000
20	1.8	1.7	1.8	412000	464000	438000
40	1.2	1.4	1.3	140000	122000	131000
50	0.7	0.9	0.8	94000	86000	90000
60	0.6	0.5	0.6	104000	112000	108000
80	0.7	0.7	0.7	95000	91000	93000
90	0.8	1.0	0.9	87000	81000	84000
4 °C						
	Turbidity(NTU)			Particle count (1/100 mL)		
AS(mg/l)	test1	test2	ave.	test1	test2	ave.
0.5	5.7	5.5	5.6	759000	891000	825000
5	3.7	3.7	3.7	849000	795000	822000
10	2.8	2.7	2.8	585000	621000	603000
15	1.5	1.4	1.5	232000	214000	223000
20	1.4	1.6	1.5	163000	187000	175000
35	1.1	1.2	1.2	145000	137000	141000
40	1.0	1.2	1.1	66000	68000	67000
50	0.9	0.7	0.8	77000	71000	74000
65	0.7	0.6	0.7	79000	71000	75000
80	0.7	0.8	0.8	66000	68000	67000
90	1.2	1.3	1.3	124000	111000	117000
0 °C						
	Turbidity(NTU)			Particle count (1/100 mL)		
AS(mg/l)	test1	test2	ave.	test1	test2	ave.
0.5	6.6	6.8	6.7	1317000	1233000	1275000
5	5.5	5.7	5.6	1145000	1241000	1193000
10	3.9	4.0	4.0	884000	850000	867000
20	3.2	3.4	3.3	402000	372000	387000
30	2.3	2.5	2.4	384000	348000	366000
40	1.9	1.7	1.8	209000	241000	225000
50	2.0	2.0	2.0	180000	188000	184000
60	2.2	2.0	2.1	219000	203000	211000
70	1.7	1.8	1.8	174000	192000	183000
80	1.4	1.6	1.5	174000	152000	163000
90	2.4	2.6	2.5	276000	324000	300000
Initial turbidity: 10.7 NTU, initial particle count: 1,400,000						

Table A.2. Results of bench-scale test (with ferric sulfate)

22 °C						
	Turbidity(NTU)			Particle count (1/100 mL)		
FS(mg/l)	test1	test2	ave.	test1	test2	ave.
0.5	3.1	3.2	3.2	1137000	1241000	1189000
5	6.5	6.3	6.4	1025000	1111000	1068000
10	5.3	5.5	5.4	968000	824000	896000
20	4.4	4.4	4.4	389000	405000	397000
30	3.2	3.4	3.3	289000	325000	307000
40	2.5	2.7	2.6	289000	261000	275000
50	1.9	2.0	2.0	228000	242000	235000
60	2.0	2.0	2.0	211000	203000	207000
70	1.7	1.9	1.8	205000	185000	195000
80	2.0	1.8	1.9	187000	203000	195000
90	1.8	1.9	1.9	196000	188000	192000
100	1.6	1.4	1.5	167000	197000	182000
4 °C						
	Turbidity(NTU)			Particle count (1/100 mL)		
FS(mg/l)	test1	test2	ave.	test1	test2	ave.
0.5	2.4	2.6	2.5	1281000	1113000	1197000
5	6.0	5.8	5.9	1040000	942000	991000
10	4.5	4.6	4.6	664000	734000	699000
20	3.6	3.5	3.6	354000	340000	347000
30	3.1	3.3	3.2	322000	286000	304000
40	3.0	3.0	3.0	292000	310000	301000
50	2.6	2.7	2.7	244000	258000	251000
60	2.8	2.6	2.7	258000	228000	243000
70	2.4	2.5	2.5	249000	225000	237000
80	2.3	2.5	2.4	249000	213000	231000
90	2.5	2.4	2.5	224000	236000	230000
100	2.0	2.1	2.1	220000	204000	212000
0 °C						
	Turbidity(NTU)			Particle count (1/100 mL)		
FS(mg/l)	test1	test2	ave.	test1	test2	ave.
0.5	4.5	4.6	4.6	1242000	1148000	1195000
5	8.6	8.7	8.7	1077000	1167000	1122000
10	7.4	7.2	7.3	1146000	978000	1062000
20	5.3	5.5	5.4	579000	651000	615000
30	5.0	5.1	5.1	593000	559000	576000
40	5.2	5.0	5.1	507000	469000	488000
50	4.8	4.9	4.9	441000	459000	450000
60	4.3	4.1	4.2	341000	383000	362000
70	3.7	3.9	3.8	342000	324000	333000
80	4.0	3.8	3.9	321000	353000	337000
90	3.2	3.3	3.3	330000	318000	324000
100	3.1	2.9	3.0	297000	315000	306000
Initial turbidity: 9.5 NTU, initial particle count: 1,229,000 (1/100 mL)						

Table A.3. Results of bench-scale test (with anionic copolymer of acrylamide)

Temp. °C	JC polymer (mg/l)	Turbidity (NTU)			Particle count (1/100 mL)		
		test1	test2	ave	test1	test2	ave
22	0.02	0.8	1.0	0.9	111000	122000	116500
	0.04	0.8	1.1	1.0	123000	128000	125500
	0.06	0.7	0.8	0.8	102000	117000	109500
	0.10	0.8	0.9	0.9	121000	123000	122000
	0.14	0.8	0.8	0.8	92000	87000	89500
	0.18	0.8	0.9	0.9	101000	91000	96000
	0.20	0.6	0.8	0.7	84000	92000	88000
	0.40	0.7	0.7	0.7	82000	91000	86500
	0.60	0.8	1.0	0.9	109000	123000	116000
	1.00	0.8	0.9	0.9	103000	117000	110000
4	0.02	0.6	0.7	0.7	104000	93000	98500
	0.06	1.1	0.9	1.0	101000	115000	108000
	0.10	0.9	0.7	0.8	94000	95000	94500
	0.15	0.6	0.8	0.7	71000	77000	74000
	0.20	0.7	0.7	0.7	74000	71000	72500
	0.40	1.0	0.9	1.0	123000	116000	119500
	1.00	0.7	0.6	0.7	76000	81000	78500
1	0.10	2.0	2.0	2.0	292000	281000	286500
	0.20	2.0	2.2	2.1	281000	267000	274000
	0.40	1.6	1.5	1.6	197000	204000	200500
	0.60	1.0	0.8	0.9	108000	88000	98000
	0.80	1.2	1.0	1.1	164000	148000	156000
	1.00	0.9	0.8	0.9	98000	114000	106000
	1.40	0.8	1.0	0.9	106000	117000	111500
	1.60	1.1	0.9	1.0	118000	127000	122500
0	0.60	2.5	2.3	2.4	307000	314000	310500
	0.70	1.6	1.8	1.7	217000	195000	206000
	0.80	2.0	2.2	2.1	243000	262000	252500
	1.00	1.8	2.0	1.9	211000	225000	218000
	1.40	1.7	1.5	1.6	172000	184000	178000
	1.60	1.6	1.8	1.7	182000	178000	180000
Initial turbidity: 9.5 NTU, initial particle count: 1,229,000 (1/100 mL)							

Table A.4. Particle size distribution of the South Saskatchewan River water

	Particle size range (μm)						
	2 to 5	5 to 10	10 to 15	15 to 20	20 to 40	>40	Total
Oct. 23, 03	614000	291000	141000	88000	66000	29000	1229000
Nov.03, 03	680000	347000	166000	99000	71000	37000	1400000
ave.	647000	319000	153500	93500	68500	33000	1314500

Table A.5. Turbidity after different settling time

Temp.	JC polymer	Turbidity (NTU)					
		60min*			20min*		
^oC	(mg/l)	test1	test2	ave.	test1	test2	ave.
	0.00	0.7	0.9	0.8	2.0	2.2	2.1
	0.18	0.8	0.9	0.9	0.9	1.0	1.0
	0.20	0.6	0.8	0.7	0.6	0.7	0.7
22	0.40	0.7	0.7	0.7	0.6	0.8	0.7
	0.60	0.8	1.0	0.9	0.9	1.1	1.0
	1.00	0.8	0.9	0.9	0.8	1.0	0.9

* time of settling

Table A.6. Particle count after different settling time

Temp.	JC polymer	Particle count (#/100 mL)					
		60min*			20min*		
^oC	(mg/l)	test1	test2	ave.	test1	test2	ave.
	0.00	113000	127000	120000	287000	263000	275000
	0.18	101000	91000	96000	112000	131000	121500
	0.20	84000	92000	88000	94000	102000	98000
22	0.40	82000	91000	86500	107000	99000	103000
	0.60	109000	123000	116000	112000	136000	124000
	1.00	103000	117000	110000	114000	122000	118000

* time of settling

Appendix B – Floc Size Analysis

Table B.1. Projected area of flocs with AS at 50 mg/L

| | Raw water | Projected area of flocs (1000*μm2) | | | | | | | | | | | | | | | | | | | | |
| | | 22 °C | | | | | 4 °C | | | | | 1 °C | | | | | 0 °C | | | | |
	0 min	3 min	5 min	10 min	15 min	20 min	3 min	5 min	10 min	15 min	20 min	3 min	5 min	10 min	15 min	20 min	3 min	5 min	10 min	15 min	20 min
Test 1	0.2	20.6	28.7	71.1	137.2	169.9	4.2	16.2	22.5	59.0	199.1	0.8	27.1	65.8	30.5	97.5	20.0	1.8	21.4	31.0	72.5
	0.3	16.6	11.4	47.8	38.6	86.3	5.2	9.1	71.0	30.8	72.7	22.1	37.3	60.4	58.9	72.6	3.4	12.6	25.7	40.8	38.1
	0.9	39.8	39.8	74.3	64.3	191.6	2.2	4.2	38.9	88.5	64.4	26.7	27.4	44.2	24.5	83.5	5.0	30.7	12.1	41.7	25.2
	1.4	0.9	40.3	24.2	43.5		21.6	36.8	51.1	108.2	72.7	5.8	24.0	28.6	93.9	77.4	2.3	15.1	33.9	35.1	59.0
	1.2	24.6	62.1	54.4	89.8		5.5	3.5	28.2	30.6	52.9	15.6	40.7	35.1	98.7		12.2	13.1	17.7	34.1	52.4
	0.5	24.4	26.5	74.0			4.0	35.0		105.7		4.6	38.7	11.5	11.7		5.6	5.9	48.3	30.1	
	0.2	1.2	29.1				3.4	20.5				4.0	34.9	64.3	75.8		1.9	8.1	62.1	27.2	
	1.8	40.8	32.8				37.4	6.0				8.8	5.0				6.4	29.9	13.2	15.1	
	1.5	69.1	95.5				4.3	17.2				0.9	22.6				4.2	11.8	29.8		
	6.8	4.3	44.1				7.7	29.7				28.3	2.2				18.1	8.1			
	0.3	7.7					2.1					2.4	13.4				2.7				
	0.4	1.7					19.2					7.0					15.1				
	0.2	2.7					30.6					10.4					3.7				
	2.0	3.2					0.6					2.2					9.5				
	1.3	4.4					1.7														
	0.2						33.0														
	7.2						8.8														
Ave 1	1.5	17.5	41.0	57.6	74.7	149.3	11.3	17.8	42.3	70.5	92.4	10.0	24.8	44.3	56.3	82.7	7.9	13.7	29.4	31.9	49.4

(Continue on next page)

Table B.1. – continue

	Raw water	22 °C					4 °C					1 °C					0 °C				
	0 min	3 min	5 min	10 min	15 min	20 min	3 min	5 min	10 min	15 min	20 min	3 min	5 min	10 min	15 min	20 min	3 min	5 min	10 min	15 min	20 min
Test 2	1.8	6.5	18.4	95.7	94.3	125.6	1.6	5.6	32.2	46.6	54.9	25.5	41.9	51.2	18.7	72.8	5.7	22.6	14.7	13.5	27.5
	1.4	24.2	58.6	45.5	32.6	88.9	37.0	26.5	55.9	57.4	62.8	6.6	18.2	31.2	84.2	84.6	8.1	1.2	31.2	32.8	32.3
	2.0	1.9	14.9	61.5	68.2	146.3	15.6	37.2	73.5	85.8	88.3	5.6	35.3	58.3	92.3	73.6	7.8	25.3	47.2	37.2	68.1
	4.4	22.8	34.1	65.4	49.1	187.4	5.8	4.5	22.7	43.3	137.2	18.9	5.0	64.8	71.8	91.5	16.5	7.4	17.9	29.6	43.6
	3.0	7.2	45.3	35.8	136	81.4	7.5	23.3	37.5	94.8	80.1	8.9	29.6	30.1	38.5		0.6	6.3	51.1	42.7	53.8
	1.0	8.0	25.0	71.2	47.5	185.7	2.5	30.7	20.1			3.9	8.8	29.4			18.1	18.6	18.7	48.7	
	0.4	6.8	40.1	87.5	71.8		6.1	11.5				3.5	31.6	25.8			7.5	14.3	27.3	35.4	
	0.5	7.5	88.3	21.1			3.1	18.5				1.9	24.2				5.9	9.4			
	0.8	14.4	44.7				14.5	9.6				20.0	5.6				4.7	13.8			
	2.0	17.2	27.3				28.6	38.1				2.4	37.1				2.7	18.1			
	0.1	0.6					2.3	2.6				12.9	16.7				3.4	5.2			
	0.8	64.3					5.1					27.3					5.8	12.5			
	2.3	48.9					0.3					0.9					24.2				
		3.2					33.1										12.3				
		5.8					3.8										2.1				
		41.6																			
		0.8																			
Ave. 2	1.6	16.6	39.7	60.5	71.3	135.9	11.1	18.9	40.3	65.6	84.7	10.6	23.1	41.5	61.1	80.6	8.4	12.9	29.7	34.3	45.1
Ave.	1.6	17.0	40.4	59.1	73.0	142.6	11.2	18.4	41.3	68.0	88.5	10.3	24.0	42.9	58.7	81.7	8.1	13.3	29.5	33.1	47.3

Table B.2. Projected area of flocs with AS at 20 mg/L

| | Projected area of flocs (1000*μm^2) | | | | | | | | | | | | | | | | | | | |
| | 22 °C | | | | | 4 °C | | | | | 1 °C | | | | | 0 °C | | | | |
	3 min	5 min	10 min	15 min	20 min	3 min	5 min	10 min	15 min	20 min	3 min	5 min	10 min	15 min	20 min	3 min	5 min	10 min	15 min	20 min
Test 1	4.6	3.0	17.4	12.7	40.9	0.6	0.4	15.1	38.1	38.7	0.6	0.5	6.8	19.2	68.1	2.2	7.0	21.9	16.9	25.4
	4.7	41.5	16.6	104.2	80.0	1.0	0.7	18.8	22.4	16.6	3.7	9.4	6.5	14.0	29.7	9.0	1.8	10.2	12.6	19.2
	8.0	10.6	40.3	67.1	60.5	1.6	4.2	22.6	20.4	38.8	5.5	0.2	11.9	8.4	11.5	1.5	12.9	15.0	54.7	11.5
	2.7	31.5	32.7	34.1		5.3	23.2	27.7	25.2	34.4	4.9	0.5	9.9	49.3	43.5	0.5	2.8	10.3	29.9	46.9
	5.3	30.5	36.6			6.6	1.4	43.1	34.5	37.2	0.4	2.7	12.8	49.4		2.0	4.4	9.6	21.7	9.0
	19.6	12.2				10.3	26.1		72.1	54.2	4.2	0.5	22.0	25.3		0.7	0.6	8.4	11.1	10.6
	21.5	14.2				3.1	4.3				0.3	6.6	25.1			0.7	0.4		8.7	13.9
	8.0	20.6				2.7	35.6				8.9	8.6	31.2			1.4	5.8			
	3.6					12.3	0.2				1.8	2.4				0.5	5.5			
	13.1					0.6	29.0				0.9	1.1				8.1	7.4			
	16.2					0.2	4.5				10.1	1.3				5.2	2.4			
	37.1					3.0	25.2				15.1	3.4				7.4	1.3			
	5.4					0.3	0.7				0.7	0.3				0.9	2.4			
						8.1	3.9				5.7					0.2				
						2.1	0.9				2.2					0.9				
						3.9	0.6				0.8					1.7				
						0.4					0.4					0.7				
						0.2					0.2					0.2				
						1.0														
						0.6														
						16.0														
						0.5														
						0.6														
						0.5														
						0.3														
						1.0														
Ave. 1	11.5	20.5	28.7	54.5	60.4	3.2	10.1	25.5	35.5	36.6	3.7	2.9	15.8	27.6	38.2	2.4	4.2	12.6	22.2	19.5

(Continue on next page)

Table B.2. – continue

| | Projected area of flocs (1000*μm^2) | | | | | | | | | | | | | | | | | | | |
| | 22 °C | | | | | 4 °C | | | | | 1 °C | | | | | 0 °C | | | | |
	3 min	5 min	10 min	15 min	20 min	3 min	5 min	10 min	15 min	20 min	3 min	5 min	10 min	15 min	20 min	3 min	5 min	10 min	15 min	20 min
Test 2	15.1	23.5	33.7	23.3	72.2	10.3	3.1	18.1	27.5	17.3	0.4	0.3	8.1	47.6	46.3	0.3	10.3	16.2	50.3	7.3
	3.5	2.9	15.2	73.9	47.3	0.4	0.3	27.3	69.1	45.8	2.3	0.8	23.7	41.5	37.4	0.8	5.8	13.7	27.5	23.4
	5.9	32.3	24.8	49.5	71.5	0.3	10.6	19.6	33.7	21.9	2.2	4.5	9.6	27.6	58.8	0.6	1.8	8.7	14.1	37.8
	23.1	12.2	43.3	40.8	45.2	0.6	4.7	21.3	24.6	48.3	1.6	1.2	31.2	21.8	27.4	8.1	0.8	7.2	6.6	17.3
	2.9	28.2	45.4	97.7	51.9	2.3	24.1	14.5	24.4	56.6	0.8	1.6	16.5	24.1	18.2	0.9	0.5	14.7	15.7	24.6
	13.3	13.6	18.1		63.4	0.8	3.5	23.9	37.2		15.7	7.6	7.7	17.0		3.4	5.3	13.3	22.4	6.9
	3.9	10.5				8.8	22.3	44.6			0.1	5.4		6.8		6.2	4.4	18.6	12.3	18.3
	34.9	8.7				3.7	1.6				0.7	3.1				2.1	0.7			
	17.6	44.2				0.3	40.2				3.6	0.9				0.2	7.9			
	5.6					2.9	1.6				2.8	3.4				4.5	7.1			
	11.9					4.4	3.6				0.3	0.4				0.3	0.6			
	5.7					1.2	0.9				0.5					0.7				
	14.2					0.2					9.1					7.4				
	5.3					2.2					14.1					1.1				
	2.3					8.2					2.3					1.7				
						0.3														
						3.5														
						13.6														
						1.5														
						0.5														
Ave. 2	11.0	19.6	30.1	57.0	58.6	3.3	9.7	24.2	36.1	38.0	3.8	2.7	16.1	26.6	37.6	2.6	4.1	13.2	21.3	19.4
Ave.	11.3	20.1	29.4	55.8	59.5	3.2	9.9	24.8	35.8	37.3	3.7	2.8	15.9	27.1	37.9	2.5	4.2	12.9	21.8	19.5

Table B.3. Projected area of flocs with AS at 5 mg/L

| | Projected area of flocs (1000*μm^2) | | | | | | | | | | | | | | | | | | | |
| | 22 °C | | | | | 4 °C | | | | | 1 °C | | | | | 0 °C | | | | |
	3 min	5 min	10 min	15 min	20 min	3 min	5 min	10 min	15 min	20 min	3 min	5 min	10 min	15 min	20 min	3 min	5 min	10 min	15 min	20 min
Test1	1.5	3.3	0.1	3.4	0.3	4.4	0.3	0.3	0.1	11.6	0.1	3.0	0.1	0.6	23.0	2.6	3.7	0.6	0.3	8.6
	8.2	0.3	8.0	12.4	0.2	0.2	1.3	0.1	0.9	0.2	4.5	0.2	4.1	0.2	1.4	4.5	1.1	0.7	4.5	1.5
	0.1	0.7	11.7	24.2	0.1	0.1	0.5	0.5	1.1	6.4	0.2	5.3	5.3	3.4	1.9	0.2	9.4	0.4	0.6	2.3
	3.6	16.2	3.9	3.3	3.7	0.4	0.2	0.1	0.5	0.3	1.5	0.7	2.6	0.3	0.2	6.1	0.4	6.3	0.6	8.4
	8.0	8.6	0.5	0.8	12.9	0.3	1.1	0.2	1.5	1.6	0.1	0.6	6.4	2.0	0.1	2.7	6.2	0.7	11.5	2.0
	2.2	13.4			0.3	1.6	2.9	6.1	0.2	1.3	1.0	0.7	0.1	0.3	0.5	1.4	0.2	2.9	0.1	14.2
	2.2	0.2				3.1	0.2	0.5	2.0	0.9	0.3	0.5	0.9	15.4	0.6	0.5	9.3	7.8	1.4	10.5
	0.4	0.2				0.5	0.6	0.3	0.3	6.5	4.8	0.6	1.1	8.1	0.3	0.5	1.2	6.2	3.1	3.0
	0.6	0.3				1.0	0.2	0.9	9.0	0.2	3.3	0.4	2.9	1.6	0.4	5.2	4.9	13.7	1.4	0.2
	1.1	13.8				4.4	5.3	0.1	1.7	31.6	5.6	0.1	3.1	2.9	3.8	1.4	0.2	0.8	0.5	0.2
	4.4					0.9	7.5	0.2	0.6	0.1	0.3	0.1	2.2	3.2	4.5	0.2	0.2	2.3	2.6	1.0
						0.4	0.2	1.4	6.1	0.1	6.0	3.8	4.5	0.1	19.5	0.2	1.2	2.0	3.9	3.0
						1.5	0.3	7.4	1.3		0.2	2.5	12.1		0.4	2.2	0.4	3.7	2.3	
						2.2	0.9	0.4	9.2		5.1	0.4	0.3		0.5	9.7	0.1	3.1	6.8	
						0.8	0.7	0.3	0.3		0.8	0.8	0.2		0.6	4.1	0.1	7.0	0.2	
						0.2	0.1	9.2	3.1		5.1	0.5	8.8		0.5	0.9		3.6		
						1.0	1.5	0.5	0.9		1.2	0.2	9.5		9.0	0.6				
						0.1	0.3	0.2	0.5		2.2	0.2			9.1	4.8				
						0.1	2.3	1.1	0.0		0.1				0.3	1.3				
						0.3	0.1	1.8	0.1		3.2					0.7				
							0.4				0.1					2.7				
							0.3				1.1					0.2				
											1.5									
											5.5									
											0.2									
											1.2									
Ave.1	2.9	5.7	4.8	8.8	2.9	1.2	1.2	1.6	2.0	5.1	2.1	1.1	3.8	3.2	4.0	2.4	2.6	3.9	2.7	4.6

(Continue on next page)

Table B.3. – continue

	Projected area of flocs (1000*μm^2)																			
	22 °C					4 °C					1 °C					0 °C				
	3 min	5 min	10 min	15 min	20 min	3 min	5 min	10 min	15 min	20 min	3 min	5 min	10 min	15 min	20 min	3 min	5 min	10 min	15 min	20 min
Test 2	7.3	14.2	8.5	12.1	0.1	0.3	3.3	10.4	2.4	0.5	2.1	0.1	12.3	3.7	0.4	0.1	0.4	9.8	1.9	1.1
	0.7	11.8	4.5	2.7	4.9	3.4	0.2	2.8	0.1	2.7	0.7	0.2	2.3	7.9	0.3	0.5	8.3	2.4	0.8	0.3
	5.1	9.4	3.4	3.7	11.7	1.8	1.1	0.7	0.4	0.8	1.8	0.6	7.2	0.1	3.1	2.8	0.9	0.1	3.7	2.4
	2.6	0.9	0.7	12.8	0.8	0.9	0.3	0.6	5.7	16.7	0.3	0.7	0.7	3.4	1.7	0.4	4.2	7.3	2.3	1.7
	7.8	4.1	12.4	1.7	0.5	1.1	0.3	1.6	0.6	0.4	1.4	2.8	1.5	0.7	0.6	3.2	0.7	2.7	0.8	4.6
	0.6	0.6	2.7	0.6	1.5	0.1	0.7	0.1	2.9	0.7	0.2	0.7	4.8	13.7	6.5	0.6	0.8	0.3	7.9	0.6
	0.4	0.8	0.1	23.1	0.2	0.4	7.3	1.1	1.6	3.4	4.3	0.2	1.6	0.2	0.7	4.7	1.9	1.3	2.6	1.9
	2.1	1.6	3.8			3.2	0.4	1.4	4.8	0.1	0.4	0.9	3.5	0.5	5.7	1.5	4.6	0.7	1.6	9.8
	3.2	12.9				1.7	1.2	0.5	0.8	18.6	0.6	0.9	6.6	2.3	10.6	1.8	0.3	2.4	5.8	2.1
	1.8	0.4				0.5	0.3	0.3	0.1	3.3	0.2	1.7	0.1	2.8	0.4	0.6	0.7	8.1	9.2	11.5
	0.5	0.5				3.1	0.8	0.3	1.3		6.1	4.1	0.8	0.8	1.3	3.4	1.8	5.2	1.1	2.8
	1.2					2.3	1.2	3.5	0.4		0.4	0.3	9.7	1.6	0.5	1.7	0.8	6.4	0.4	13.2
	0.2					0.2	1.4	0.2			1.3	0.5	0.5	0.4	17.8	0.8	0.7	0.8	0.1	2.3
						0.6	0.1	0.3			3.6	1.6	5.4			1.8	9.5	3.2		
						0.3					1.5	0.2				0.2	0.9	1.9		
						1.5					0.3					7.6	1.6			
											4.7					6.1	0.4			
											0.6					0.7				
											5.8					5.5				
Ave. 2	2.6	5.2	4.5	8.1	2.8	1.3	1.3	1.7	1.8	4.7	1.9	1.0	4.1	2.9	3.8	2.3	2.3	3.5	2.9	4.2
Ave.	2.8	5.5	4.7	8.5	2.9	1.2	1.3	1.6	1.9	4.9	2.0	1.1	3.9	3.0	3.9	2.3	2.4	3.7	2.8	4.4

Table B.4. Projected area of flocs with FS at 50 mg/L

| | Projected area of flocs ($1000*\mu m^2$) | | | | | | | | | | | | | | | | | | | |
| | 22 °C | | | | | 4 °C | | | | | 1 °C | | | | | 0 °C | | | | |
	3 min	5 min	10 min	15 min	20 min	3 min	5 min	10 min	15 min	20 min	3 min	5 min	10 min	15 min	20 min	3 min	5 min	10 min	15 min	20 min
Test1	18.0	48.3	49.6	81.9	167.8	25.2	45.8	80.0	100.0	139.1	1.5	20.7	81.4	115.0	68.3	4.1	9.5	9.2	37.6	27.2
	18.7	14.7	58.1	58.7	76.7	1.3	11.2	26.4	137.4	64.2	31.5	34.8	75.3	61.5	137.7	1.2	43.9	13.4	35.1	19.5
	17.3	32.6	73.0	112.8	219.9	1.9	41.2	108.0	61.1	22.7	3.9	12.3	39.2	32.0	33.0	3.7	17.6	13.7	16.6	22.3
	3.2	56.6	47.0	73.9	122.6	18.4	15.3	40.6	69.2	190.8	4.7	21.0	65.7	58.5	57.4	0.9	1.9	12.4	17.7	48.1
	7.4	43.1	47.3	116.3		26.1	13.2	15.1	53.5	112.6	8.6	32.8	76.4	18.9	93.5	0.7	40.0	19.2	13.4	32.1
	10.3	97.4	80.8			2.5	29.3	56.9	18.2		6.2	50.0	10.4	13.3	95.4	6.9	17.3	19.6	66.3	26.2
	21.2	21.2	65.4			3.6	6.9	23.1			10.4	15.1	41.4		42.4	5.6	12.0	28.7	26.2	14.8
	5.4	29.0	15.3			41.8	31.3	34.5			7.4	16.0			86.0	11.4	0.7	26.2	31.1	62.5
	41.4					7.6		31.9			2.9	36.7			75.5	13.2	8.6	26.8	16.9	37.5
	31.7					8.1		44.3			14.6	41.0				2.0	9.4	10.5	55.0	29.3
	55.7					8.9					6.1	23.6				2.1	33.1	43.8	17.6	38.1
	18.4					7.4					1.3	29.4				4.1	5.7	64.0	66.0	35.9
	25.6					15.3					6.8	14.7				8.7	14.8	51.0	31.0	
	26.2					0.9					9.1					19.7	3.8	20.5	12.0	
	2.4					0.7					19.3					7.0	21.7	23.2	43.5	
	5.1					18.2					13.0					23.7	6.4	10.8	19.9	
						8.9										10.3	8.0			
						7.6										4.6	1.7			
						14.1										5.5	1.9			
						9.9										19.9	41.7			
						1.6										6.8	0.9			
						10.0										5.9	8.5			
						13.2										17.5	31.8			
						11.4										7.7	17.9			
						2.6										19.2	6.0			
						11.7											2.0			
						9.1														
Ave.1	19.3	42.9	54.6	88.7	146.7	10.7	24.3	46.1	73.2	105.9	9.2	26.8	55.7	49.9	76.6	8.5	14.1	24.6	31.6	32.8

(Continue on next page)

Table B.4. – continue

| | Projected area of flocs (1000*μm^2) | | | | | | | | | | | | | | | | | | | |
| | 22 °C | | | | | 4 °C | | | | | 1 °C | | | | | 0 °C | | | | |
	3 min	5 min	10 min	15 min	20 min	3 min	5 min	10 min	15 min	20 min	3 min	5 min	10 min	15 min	20 min	3 min	5 min	10 min	15 min	20 min
Test 2	4.5	13.1	14.7	61.7	78.2	0.3	20.5	47.4	51.7	144.7	15.9	16.8	31.3	65.4	38.9	0.2	21.2	28.3	69.1	12.3
	11.6	24.5	21.7	97.3	187.1	0.8	37.8	34.3	54.3	74.2	2.1	47.2	84.2	22.7	51.1	5.5	0.8	11.6	48.4	17.1
	47.6	47.6	58.6	81.5	143.8	4.7	27.6	12.8	14.5	127.8	16.8	18.5	26.1	68.0	129.8	7.0	11.2	7.3	14.2	24.4
	12.3	43.7	67.1	108.8	124.7	12.5	37.1	31.7	88.6	49.3	2.2	24.6	17.3	15.4	81.6	24.2	38.1	45.4	12.2	21.6
	13.9	41.5	77.3	53.8	214.3	14.3	48.9	39.8	65.8	87.1	17.3	48.2	54.7	48.7	91.3	4.9	24.5	67.0	28.4	67.1
	3.3	36.6	71.4	99.6	71.8	0.3	8.1	97.3	131	27.3	0.6	28.1	78.0	94.6	98.7	10.4	3.2	23.5	51.7	43.8
	23.7	37.8	73.9			17.5	33.7	58.2		171.0	16.7	41.7	72.1	17.2		12.7	18.3	37.1	17.8	31.5
	58.7	51.8	87.5			9.9	14.0	72.8			6.2	34.0	46.6	85.1		16.6	7.6	12.5	62.3	24.3
	2.9	93.3				19.1	7.7				10.1	14.5				1.6	4.0	24.9	31.7	39.0
	9.6	15.2				29.5					2.4	13.3				9.2	36.2	27.8	13.3	24.7
	14.7	40.5				49.8					13.7					4.7	14.8	20.6	19.4	
	6.5					8.4					17.3					2.5	19.2	15.1	10.1	
	23.3					1.5					11.5					0.5	5.8	19.7	24.3	
	17.9					16.6					6.1					8.8	10.0	25.7	13.5	
						29.6					7.8					20.0	32.5	29.2		
						5.8					6.1					13.7	3.2	23.5		
						7.1					33.1					3.1	16.7			
						13.7					0.4					19.1	8.5			
						0.8					2.2					12.4	12.4			
						4.7										6.2	0.7			
						0.2										6.1	40.7			
						1.4											1.7			
Ave. 2	17.9	40.5	59.0	83.8	136.7	11.3	26.2	49.3	67.7	97.3	9.9	28.7	51.3	52.1	81.9	9.0	15.1	26.2	29.7	30.6
Ave.	18.6	41.7	56.8	86.3	141.7	11.0	25.2	47.7	70.5	101.6	9.6	27.7	53.5	51.0	79.2	8.8	14.6	25.4	30.7	31.7

Table B.5. Projected area of flocs with FS at 20 mg/L

	Projected area of flocs (1000*μm^2)																			
	22 °C					4 °C					1 °C					0 °C				
	3 min	5 min	10 min	15 min	20 min	3 min	5 min	10 min	15 min	20 min	3 min	5 min	10 min	15 min	20 min	3 min	5 min	10 min	15 min	20 min
Test1	1.0	3.2	30.0	65.6	96.2	0.2	0.3	26.6	54.7	25.7	5.2	8.7	9.4	72.8	47.8	4.0	4.3	6.0	29.0	9.3
	2.2	2.4	27.6	15.3	58.2	1.4	1.5	1.6	12.1	80.0	2.2	3.8	50.3	5.2	32.9	4.3	2.9	2.9	23.8	28.3
	3.4	4.6	14.9	48.9	78.0	1.1	0.3	6.8	20.8	50.4	3.1	5.4	21.3	20.2	76.0	2.0	0.8	5.7	16.6	37.7
	2.9	2.4	13.7	26.1		1.1	2.3	8.2		129.7	1.5	11.6	18.7	13.6	31.3	0.9	2.1	4.5	23.4	32.4
	2.4	9.0	50.7			7.1	7.3	15.5		28.0	0.3	1.9	25.8	18.9		0.3	2.9	12.3	7.6	16.0
	4.6	6.2	28.9			0.2	10.1	14.1			9.9	1.7	32.7	25.1		2.4	0.3	6.4	14.0	23.0
	3.8	3.2	27.6			0.2	4.4	23.5			0.6	33.9		92.2		10.0	0.5	2.5	9.5	
	5.6	7.4				0.2	29.6				2.1	1.4					4.8			
	4.8	7.2				20.4	0.3				0.2	11.3					8.5			
	4.2	4.1				0.5	0.5				6.0	1.7					0.2			
	4.2	34.8				0.8	0.6				0.4	1.9								
	0.7	6.5				0.6	0.2				5.8	7.7								
	5.4	20.6				1.3	4.7				3.2	26.7								
	6.8	1.4				0.3	0.1				3.3	5.0								
	0.9	24.4				0.4	2.6				0.3	12.5								
	8.1					0.1	0.4				0.6	12.2								
	6.2					3.3					8.5	5.4								
	1.0					2.2					5.4	5.1								
	0.2					0.9					7.6									
	4.3					0.2					2.3									
	5.4										2.4									
	0.6										2.4									
	0.6										0.4									
Ave.1	3.8	9.2	27.6	39.0	77.5	2.1	4.1	13.8	29.2	62.8	3.2	8.8	26.4	35.4	47.0	3.4	2.7	5.7	17.7	24.4

(Continue on next page)

Table B.5. – continue

| | Projected area of flocs (1000*μm^2) | | | | | | | | | | | | | | | | | | | |
| | 22 °C | | | | | 4 °C | | | | | 1 °C | | | | | 0 °C | | | | |
	3 min	5 min	10 min	15 min	20 min	3 min	5 min	10 min	15 min	20 min	3 min	5 min	10 min	15 min	20 min	3 min	5 min	10 min	15 min	20 min
Test 2	0.2	1.5	21.8	39.8	62.3	3.6	0.1	4.6	19.6	54.5	3.4	5.8	23.9	27.0	31.1	0.6	0.9	2.4	7.1	35.1
	2.4	23.4	27.1	47.1	94.7	0.7	5.0	18.7	48.1	21.0	6.0	1.7	15.7	19.1	44.3	3.7	3.7	7.0	16.2	31.4
	1.3	4.7	21.9	34.5	76.8	0.2	4.5	16.9	18.7	37.4	0.7	4.8	34.4	25.7	37.8	1.8	2.5	14.3	9.8	19.8
	0.1	6.6	24.8	74.6	81.6	0.6	3.8	21.2	27.4	46.1	0.5	3.0	17.8	87.3	57.0	2.4	1.3	5.7	24.8	6.8
	8.5	5.5	19.7	6.5	89.1	0.4	1.5	23.0	36.2	75.6	3.6	2.1	27.4	54.9	84.1	3.3	5.4	2.1	27.1	38.7
	2.3	11.3	28.7			1.1	0.3	9.1		108.3	2.7	3.7	6.7	13.4	52.3	3.2	1.5	4.7	6.5	24.0
	2.4	7.0	13.5			2.3	9.5	7.8			1.1	1.4	44.3	8.7		1.2	5.1	3.5	22.4	7.6
	1.8	4.7	48.8			1.9	0.4	1.9			1.8	5.1				4.7	0.6	9.1		16.9
	4.6	7.9				2.7	0.1				3.9	14.8				0.5				
	15.2	8.1				0.3	5.5				7.0	18.2				7.8				
	7.7	6.4				0.6	14.1				3.6	9.7				5.3				
	3.0	7.8				0.7	8.4				2.1	29.1								
	3.4	34.3				1.8					2.5	13.2								
	7.7					3.5					1.4	1.5								
	2.8					14.3					0.8	6.7								
	1.5					0.5					0.2									
	3.7					6.3					4.7									
	8.6					0.3					8.7									
	3.5										6.4									
											9.0									
Ave. 2	4.2	9.9	25.8	40.5	80.9	2.3	4.4	12.9	30.0	57.2	3.5	8.1	24.3	33.7	51.1	3.1	2.6	6.1	16.3	22.5
Ave.	4.0	9.6	26.7	39.8	79.2	2.2	4.2	13.3	29.6	60.0	3.3	8.4	25.3	34.6	49.0	3.2	2.7	5.9	17.0	23.5

Table B.6. Projected area of flocs with FS at 5 mg/L

	Projected area of flocs (1000*μm^2)																			
	22 °C					4 °C					1 °C					0 °C				
	3 min	5 min	10 min	15 min	20 min	3 min	5 min	10 min	15 min	20 min	3 min	5 min	10 min	15 min	20 min	3 min	5 min	10 min	15 min	20 min
Test1	0.7	0.2	46.4	1.9	6.5	1.2	0.5	4.8	1.5	7.2	2.2	1.2	6.1	0.3	12.7	0.7	2.3	4.0	1.1	6.1
	7.5	1.7	20.1	2.8	34.4	15.4	0.1	0.3	1.1	0.2	4.5	4.0	0.6	0.1	3.5	0.6	0.4	9.5	2.1	0.3
	25.2	0.3	9.7	31.9	2.7	0.4	7.8	10.0	1.3	4.6	1.3	4.9	0.3	1.6	10.1	1.3	1.1	4.5	1.0	0.9
	3.2	4.0	2.2	3.7		6.3	9.6	3.8	2.4	2.5	0.7	3.7	16.1	0.1	0.4	0.5	14.1	9.0	0.7	0.1
	6.5	1.7	12.2			2.8	0.1	0.6	7.2	0.6	3.0	1.8	3.1	7.1		4.0	1.1	8.9	3.1	0.3
	1.0	0.1	2.1			0.4	0.2	22.6	0.1	3.0	0.8	3.7	1.6	0.5		4.9	0.6	0.4	0.6	0.2
	0.4	6.4	2.0			0.1	0.6	28.6	0.8	18.4	4.2	0.2	0.2	39.1		0.3	1.3	19.7	0.2	39.6
	8.8	3.5	0.1			2.7	1.6	1.1	16.7	18.0	0.5	4.5	1.2	0.6		1.9	2.6	0.1	28.4	0.2
	28.2	0.4	4.9			2.4	0.2	1.2	0.2	0.1	0.6	14.4	0.4			4.1	2.3	0.9		0.5
	10.5	8.7	29.8			0.1	2.5	26.5	2.1	3.0	0.1	0.4	7.0			4.1	0.2	0.1		1.2
		6.1				0.5	8.1	0.3			4.2	1.1	0.3			0.7	2.2	16.5		13.0
						1.4	21.5				1.7	1.9	0.4			2.8	6.5	5.7		6.7
						0.2	0.9				0.3	1.7				1.5	1.2	4.0		3.5
							27.2				11.9	0.2				0.2	3.3	0.1		0.4
							0.1				0.6	1.5				0.2	2.3	0.1		0.4
							1.9				3.1	0.1						3.7		
							2.9				1.9	0.4								
Ave1	9.2	3.0	13.0	10.1	14.5	2.6	5.1	9.1	3.3	5.7	2.4	2.7	3.1	6.2	6.7	1.9	2.8	5.5	4.6	4.9

(Continue on next page)

Table B.6. – continue

	Projected area of flocs $(1000*\mu m^2)$																			
	22 ºC					4 ºC					1 ºC					0 ºC				
	3 min	5 min	10 min	15 min	20 min	3 min	5 min	10 min	15 min	20 min	3 min	5 min	10 min	15 min	20 min	3 min	5 min	10 min	15 min	20 min
Test2	3.7	1.8	3.9	3.8	6.9	1.4	0.5	5.9	1.3	4.4	4.0	0.8	1.3	1.2	2.0	1.5	2.3	6.5	2.6	0.2
	3.9	4.6	5.2	1.6	5.3	2.1	0.1	4.0	2.7	3.2	1.3	4.7	1.5	1.8	1.7	2.3	1.6	0.8	0.4	2.4
	3.0	1.7	14.1	2.7	29.1	1.3	0.1	0.8	1.2	4.8	0.2	1.4	0.7	0.4	14.1	3.7	2.9	0.1	0.8	2.1
	2.3	3.8	19.6	28.6	3.8	0.5	1.7	18.4	2.5	9.7	2.1	1.6	6.8	0.4	11.7	2.4	0.6	12.6	23.9	7.0
	4.2	0.8	4.2	2.7	31.5	1.7	2.6	4.7	22.1	15.2	1.8	0.6	10.7	47.7	4.8	0.4	0.7	8.4	3.8	2.9
	11.9	0.3	38.3	3.5	6.2	2.7	18.1	25.8	5.7	6.4	2.3	12.5	5.7	5.4	0.2	0.2	2.8	1.4	1.7	28.7
	22.4	7.7	28.5	20.7		1.6	9.4	4.1	0.3	0.5	2.7	1.9	1.8	1.2	8.1	1.8	1.2	0.5	3.5	1.6
	3.8	6.8	7.8			0.1	6.7	19.4	0.7	0.1	0.5	0.6	4.9	0.1		0.7	3.0	0.1	0.3	5.8
	0.5	2.4	4.7			0.8	14.8	13.2	1.6	4.1	0.6	0.1	1.1	0.4		4.0	2.5	4.6	1.8	4.7
	27.1	0.1	4.1			1.8	5.5	5.0	0.1	3.8	3.7	4.0	0.1			3.9	8.9	17.7		0.2
	10.7	5.4	0.2			2.3	1.4	1.2	1.4		6.9	3.8	2.0			0.5	0.1	7.4		2.5
	7.4					0.2	0.7	0.4			3.8	4.7				0.1	5.1	5.5		
						13.5	2.3				2.8	1.5				4.7	4.8	0.1		
						5.4	0.5				1.5	0.2				1.8	1.5			
						0.1					0.4	2.7				2.1	1.3			
												0.7				2.2				
												0.1								
												1.8								
Ave2	8.4	3.2	11.9	9.1	13.8	2.4	4.6	8.6	3.6	5.2	2.3	2.4	3.3	6.5	6.1	2.0	2.6	5.1	4.3	5.3
Ave.	8.8	3.1	12.4	9.6	14.2	2.5	4.8	8.8	3.5	5.5	2.4	2.5	3.2	6.3	6.4	1.9	2.7	5.3	4.5	5.1

Table B.7. Average floc projected area distribution (JC polymer)

t	Average projected area ($*1000$ μm^2)			
(sec)	0 ^{o}C	1 ^{o}C	4 ^{o}C	22 ^{o}C
0	2	2	2	2
20	4	106	75	78
40	4	129	101	159
60		225	176	199
80	5	254	430	652
100		459	480	
120	7	506		
140		576		
160	10	594	550	715
180	14		570	715
300		589	582	
600	72		639	714
900	107	648	615	719
1200	86	709	633	688

Appendix C – Flocculation Kinetics

Table C.1. Data of flocculation kinetics

Coagulant	Temp. (°C)	Particle count	t (sec)	$1/n_t$	$1/(1/t+K_BG^2)$ (sec)
AS 50mg/L	22	160	180	6.25E-03	1.69E+02
		120	300	8.33E-03	2.70E+02
		61	600	1.64E-02	4.89E+02
		48	900	2.08E-02	6.72E+02
		44	1200	2.27E-02	8.26E+02
	4	220	180	4.55E-03	1.60E+02
		182	300	5.49E-03	2.49E+02
		120	600	8.33E-03	4.26E+02
		96	900	1.04E-02	5.59E+02
		85	1200	1.18E-02	6.61E+02
	0	345	180	2.90E-03	1.61E+02
		196	300	5.10E-03	2.50E+02
		154	600	6.49E-03	4.30E+02
		138	900	7.25E-03	5.64E+02
		120	1200	8.33E-03	6.69E+02
FS 50 mg/L	22	172	180	5.81E-03	1.64E+02
		112	300	8.93E-03	2.59E+02
		78	600	1.28E-02	4.56E+02
		55	900	1.82E-02	6.10E+02
		50	1200	2.00E-02	7.35E+02
	4	240	180	4.17E-03	1.58E+02
		180	300	5.56E-03	2.44E+02
		128	600	7.81E-03	4.12E+02
		104	900	9.62E-03	5.33E+02
		92	1200	1.09E-02	6.26E+02
	0	350	180	2.86E-03	1.61E+02
		200	300	5.00E-03	2.49E+02
		168	600	5.95E-03	4.27E+02
		140	900	7.14E-03	5.60E+02
		124	1200	8.06E-03	6.63E+02

Table C.2. Relationship among K_B, K_A and R^2

22 °C				4 °C				0 °C			
K_B	K_A	R^2		K_B	K_A	R^2		K_B	K_A	R^2	
(sec)		AS	FS	(sec)		AS	FS	(sec)		AS	FS
5E-09	4.32E-04	0.92	0.93	5E-08	1.85E-04	0.92	0.90	1.5E-07	1.81E-04	0.85	0.87
1E-08	4.32E-04	0.93	0.93	6E-08	1.85E-04	0.92	0.90	2.1E-07	1.82E-04	0.86	0.88
2E-08	4.32E-04	0.93	0.93	7E-08	1.86E-04	0.92	0.90	2.3E-07	1.83E-04	0.87	0.89
3E-08	4.33E-04	0.93	0.94	8E-08	1.86E-04	0.93	0.91	2.5E-07	1.83E-04	0.87	0.89
4E-08	4.33E-04	0.93	0.94	9E-08	1.86E-04	0.93	0.91	2.7E-07	1.84E-04	0.87	0.89
5E-08	4.33E-04	0.94	0.94	1E-07	1.86E-04	0.93	0.91	3E-07	1.84E-04	0.88	0.90
6E-08	4.34E-04	0.94	0.95	1.5E-07	1.88E-04	0.94	0.92	3.2E-07	1.85E-04	0.88	0.90
7E-08	4.34E-04	0.94	0.95	2.1E-07	1.89E-04	0.95	0.94	3.4E-07	1.86E-04	0.88	0.90
8E-08	4.35E-04	0.95	0.95	2.3E-07	1.90E-04	0.96	0.94	4E-07	1.87E-04	0.89	0.91
9E-08	4.35E-04	0.95	0.95	2.5E-07	1.91E-04	0.96	0.95	4.2E-07	1.88E-04	0.90	0.91
1E-07	4.35E-04	0.95	0.96	2.7E-07	1.91E-04	0.96	0.95	5E-07	1.90E-04	0.91	0.92
1.5E-07	4.37E-04	0.96	0.97	3E-07	1.92E-04	0.97	0.95	5.5E-07	1.91E-04	0.91	0.93
2.1E-07	4.39E-04	0.97	0.98	3.2E-07	1.93E-04	0.97	0.96	6E-07	1.92E-04	0.92	0.93
2.3E-07	4.40E-04	0.98	0.98	3.4E-07	1.93E-04	0.97	0.96	7E-07	1.95E-04	0.92	0.94
2.5E-07	4.41E-04	0.98	0.98	4E-07	1.95E-04	0.98	0.97	8E-07	1.97E-04	0.93	0.94
2.7E-07	4.41E-04	0.98	0.98	4.2E-07	1.95E-04	0.98	0.97	8.5E-07	1.99E-04	0.93	0.94
3E-07	4.42E-04	0.98	0.98	5E-07	1.98E-04	0.99	0.98	8.8E-07	2.00E-04	0.94	0.94
3.2E-07	4.43E-04	0.98	0.99	5.5E-07	1.99E-04	0.99	0.98	9E-07	2.00E-04	0.94	0.94
3.4E-07	4.44E-04	0.98	0.99	6E-07	2.00E-04	0.99	0.99	9.5E-07	2.01E-04	0.94	0.95
4E-07	4.46E-04	0.98	0.99	7E-07	2.03E-04	1.00	0.99	9.7E-07	2.02E-04	0.94	0.95
4.2E-07	4.47E-04	0.98	0.99	8E-07	2.06E-04	1.00	1.00	9.8E-07	2.02E-04	0.94	0.95
5E-07	4.49E-04	0.98	0.99	8.5E-07	2.07E-04	1.00	1.00	9.9E-07	2.02E-04	0.94	0.95
5.5E-07	4.51E-04	0.98	0.99	8.8E-07	2.08E-04	1.00	1.00	1E-06	2.03E-04	0.94	0.95
6E-07	4.53E-04	0.97	0.99	9E-07	2.09E-04	1.00	1.00	1.1E-06	2.05E-04	0.94	0.95
7E-07	4.57E-04	0.97	0.98	9.5E-07	2.10E-04	1.00	1.00	1.5E-06	2.16E-04	0.94	0.94
8E-07	4.60E-04	0.96	0.97	9.9E-07	2.11E-04	1.00	1.00	2E-06	2.29E-04	0.93	0.93
9E-07	4.64E-04	0.95	0.96	1E-06	2.11E-04	1.00	1.00	3E-06	2.55E-04	0.89	0.89
1E-06	4.67E-04	0.94	0.95	1.5E-06	2.25E-04	0.98	0.99	4E-06	2.81E-04	0.84	0.84
1.5E-06	4.85E-04	0.88	0.90	2E-06	2.39E-04	0.95	0.97	5E-06	3.07E-04	0.80	0.79
2E-06	5.03E-04	0.83	0.84	3E-06	2.67E-04	0.89	0.91	6E-06	3.33E-04	0.75	0.74